

EN - For pricing and availability in your local country please visit one of the below links:

DE - Informationen zu Preisen und Verfügbarkeit in Ihrem Land erhalten Sie über die unten aufgeführten Links:

FR - Pour connaître les tarifs et la disponibilité dans votre pays, cliquez sur l'un des liens suivants:

[ISL95829CHRTZ](#)

[ISL95829CIRTZ](#)

EN

This Datasheet is presented by
the manufacturer

DE

Dieses Datenblatt wird vom
Hersteller bereitgestellt

FR

Cette fiche technique est
présentée par le fabricant

ISL95859C

1+2+1 Voltage Regulator With Expanded Iccmax Register Range Supporting Intel IMVP8 CFL/CNL CPUs

FN8973
Rev.0.00
Oct 6, 2017

The ISL95859C provides a complete power solution for Intel microprocessors supporting core, graphics, and system agent rails and is compliant with Intel IMVP8™. The controller provides control and protection for three Voltage Regulator (VR) outputs. The VR A and VR C outputs support 1-phase operation only, while VR B is configurable for 2- or 1-phase operation. The programmable address options for these three outputs allow for maximum flexibility in support of the IMVP8 CPU. All three VRs share a common serial control bus to communicate with the CPU and achieve lower cost and smaller board area compared with a two-chip approach.

Based on Intersil's Robust Ripple Regulator (R3™) technology, the R3 modulator has many advantages compared to traditional modulators, including faster transient settling time, variable switching frequency in response to load transients, and improved light-load efficiency due to Diode Emulation Mode (DEM) with load-dependent low switching frequency.

The controller provides PWM outputs, which support Intel DrMOS power stages (or similar) and discrete power stages using the Intersil ISL95808 high voltage synchronous rectified buck MOSFET driver. The controller complies with IMVP8 PS4 power requirements and supports power stages and drivers, which are compatible. The ISL95859C supports the system input power monitor (PSYS) option. The controller supports either DCR current sensing with a single NTC thermistor for DCR temperature compensation or more precision through resistor current sensing, if desired. All three outputs feature remote voltage sense, programmable I_{MAX} , adjustable switching frequency, OC protection, and a single VR_READY power-good indicator.

Features

- Supports the Intel serial data bus interface
 - Fully supports PS4 Power Domain entry/exit
- Supports system input power monitor (PSYS)
- Three output controller
 - VR A supports 1-phase VR design
 - VR B configurable for 2- or 1-phase VR design
 - VR C supports 1-phase VR design
- 0.5% system accuracy over temperature
- Low supply current in PS4 state
- Supports multiple current sensing methods
 - Lossless inductor DCR current sensing
 - Precision resistor current sensing
- Differential remote voltage sensing
- Programmable SVID address
- Programmable V_{BOOT} voltage at start-up
- Resistor programmable address selection, I_{MAX} , and switching frequency
- Adaptive body diode conduction time reduction

Applications

- IMVP8 compliant notebooks, desktops, Ultrabooks, and tablets

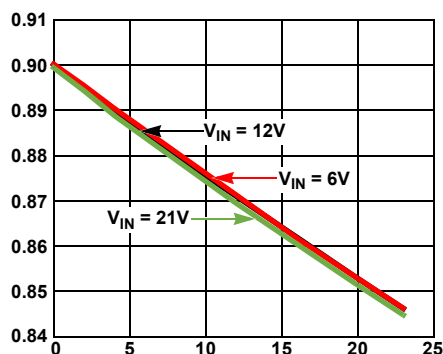


Figure 1. $V_{CORE}/VR A$ Load Line = 2.4mΩ

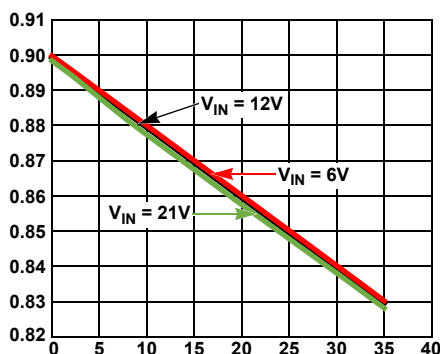


Figure 2. $V_{GT}/VR B$ Load Line = 2mΩ

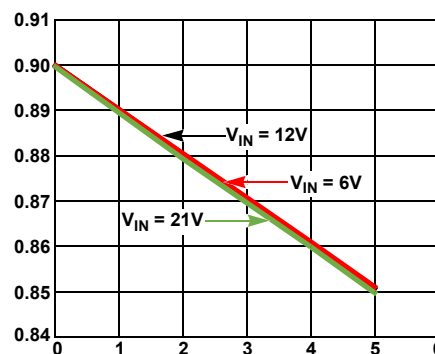


Figure 3. $V_{SA}/VR C$ Load Line = 10.3mΩ

Contents

1. Overview	4
1.1 Block Diagram	4
1.2 Simplified Application Circuits	5
1.3 Ordering Information	7
1.4 Pin Configuration	7
1.5 Pin Descriptions	8
2. Specifications	10
2.1 Absolute Maximum Ratings	10
2.2 Thermal Information	10
2.3 Recommended Operating Conditions	10
2.4 Electrical Specifications	11
3. Typical Performance Curves for VR A	14
4. Typical Performance Curves for VR B	17
5. Typical Performance Curves for VR C	20
6. Theory of Operation	23
6.1 R3 Modulator	23
6.2 Multiphase Power Conversion	23
6.3 Diode Emulation and Period Stretching	29
6.4 Adaptive Body Diode Conduction Time Reduction	30
6.5 Modes of Operation	30
6.6 Programming Resistors	32
6.7 PSYS System Power Monitoring	33
7. General Design Guide	34
7.1 Power Stages	34
7.2 Output Filter Design	36
7.3 Input Capacitor Selection	37
7.4 Inductor Current Sensing and Balancing	38
7.5 Inductor DCR Current-Sensing Network	38
7.6 Current Sense Circuit Adjustments	49
7.7 Voltage Regulation	53
8. Fault Protection	65
8.1 VR_HOT#/ALERT# Behavior	65

9. **Serial VID (SVID) Supported Data and Configuration Registers 67**

10. **Layout Guidelines 69**

11. **Revision History 72**

12. **Package Outline Drawing 73**

13. **About Intersil 74**

CONFIDENTIAL

1. Overview

1.1 Block Diagram

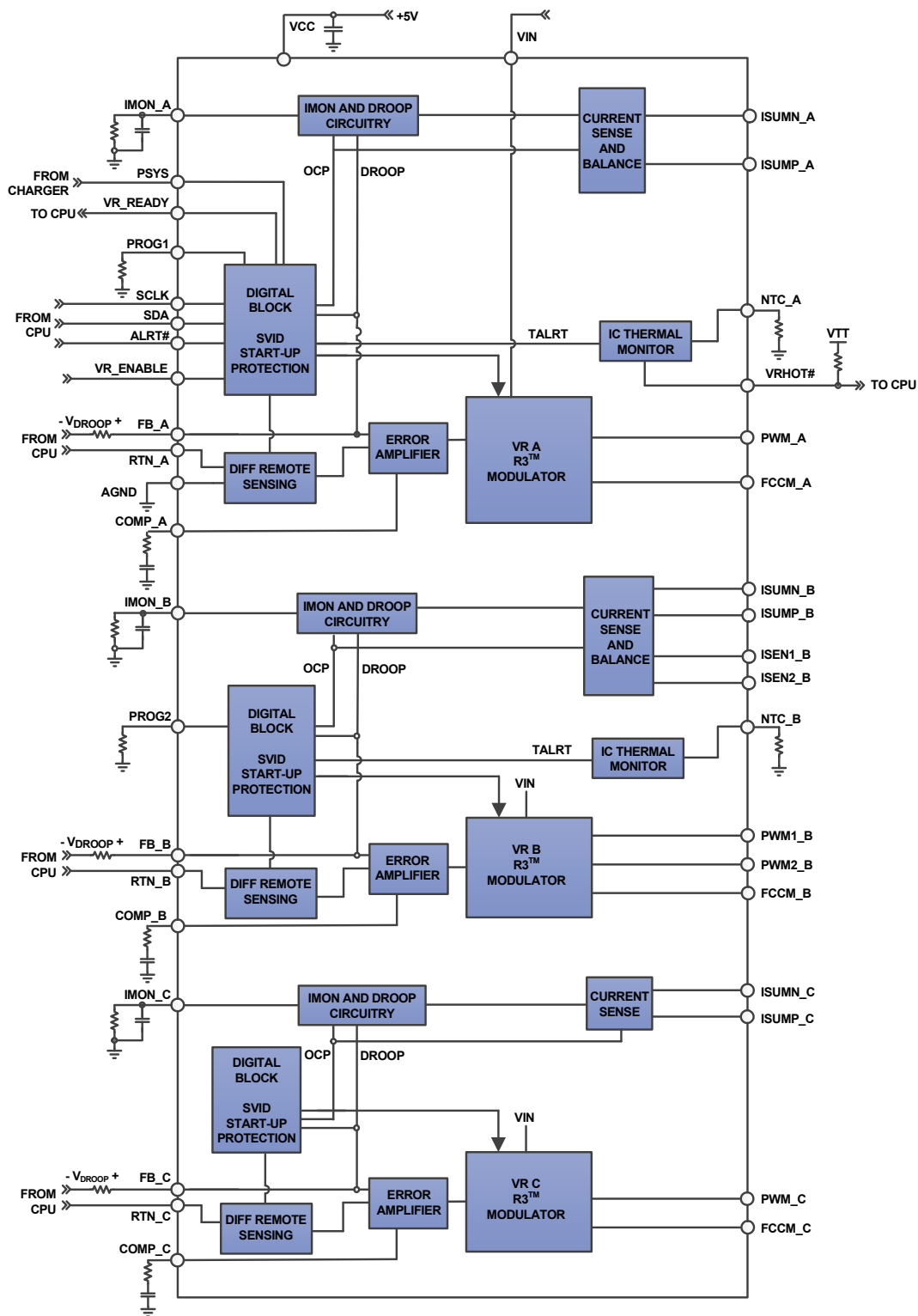


Figure 4. Block Diagram

1.2 Simplified Application Circuits

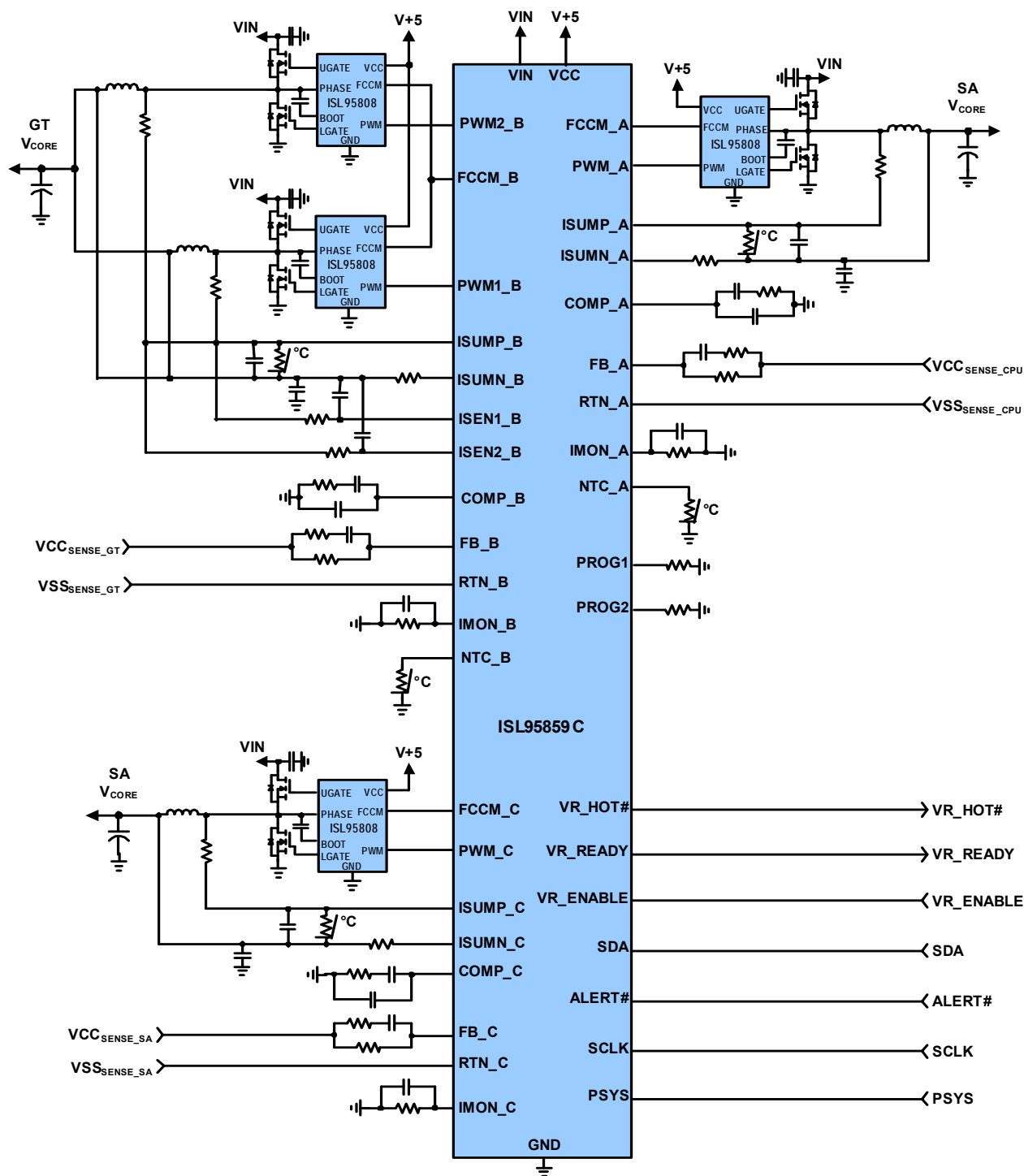


Figure 5. Typical ISL95859C Application Circuit Using Inductor DCR Current Sensing

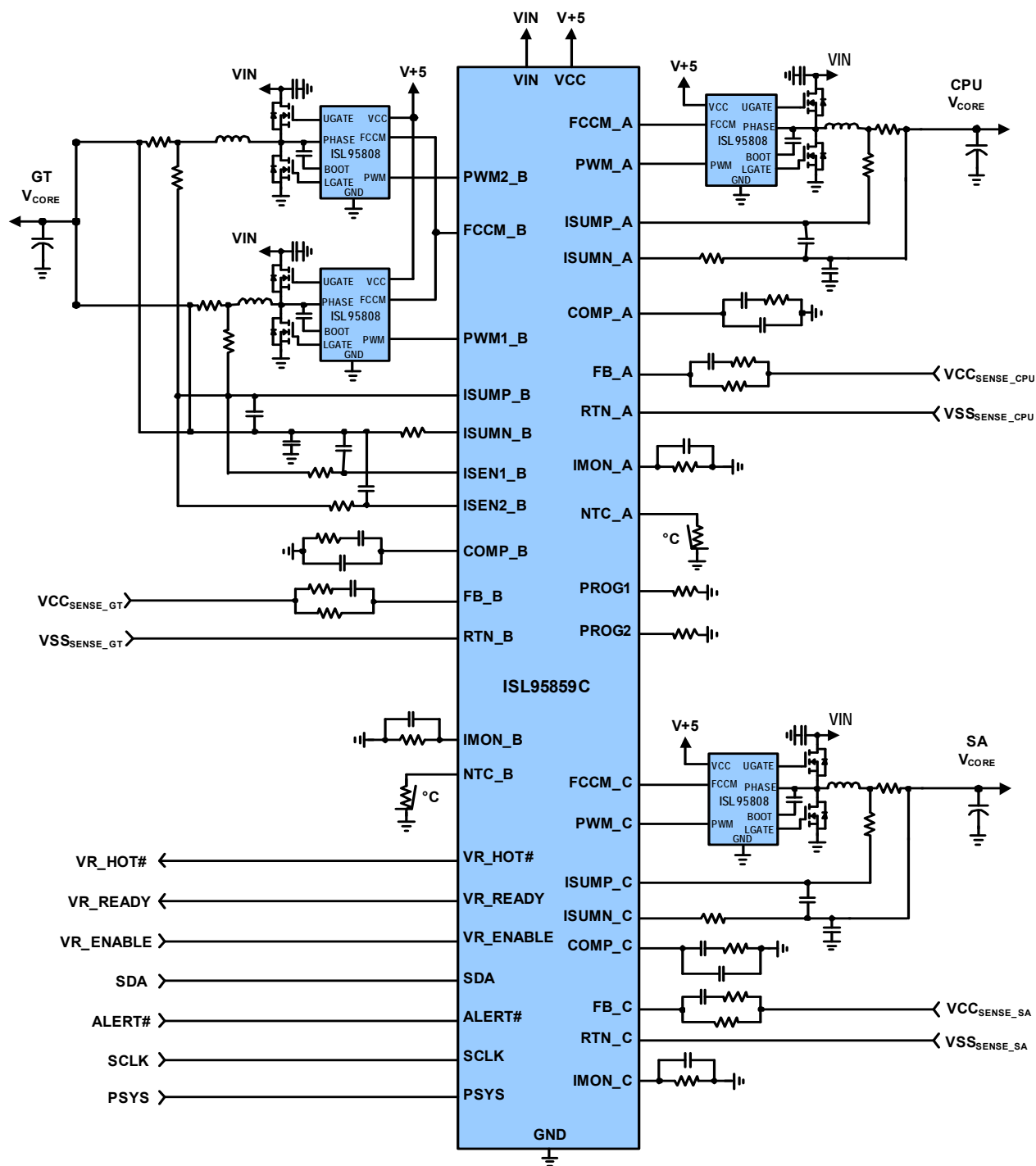


Figure 6. Typical ISL95859C Application Circuit Using Resistor Sensing

1.3 Ordering Information

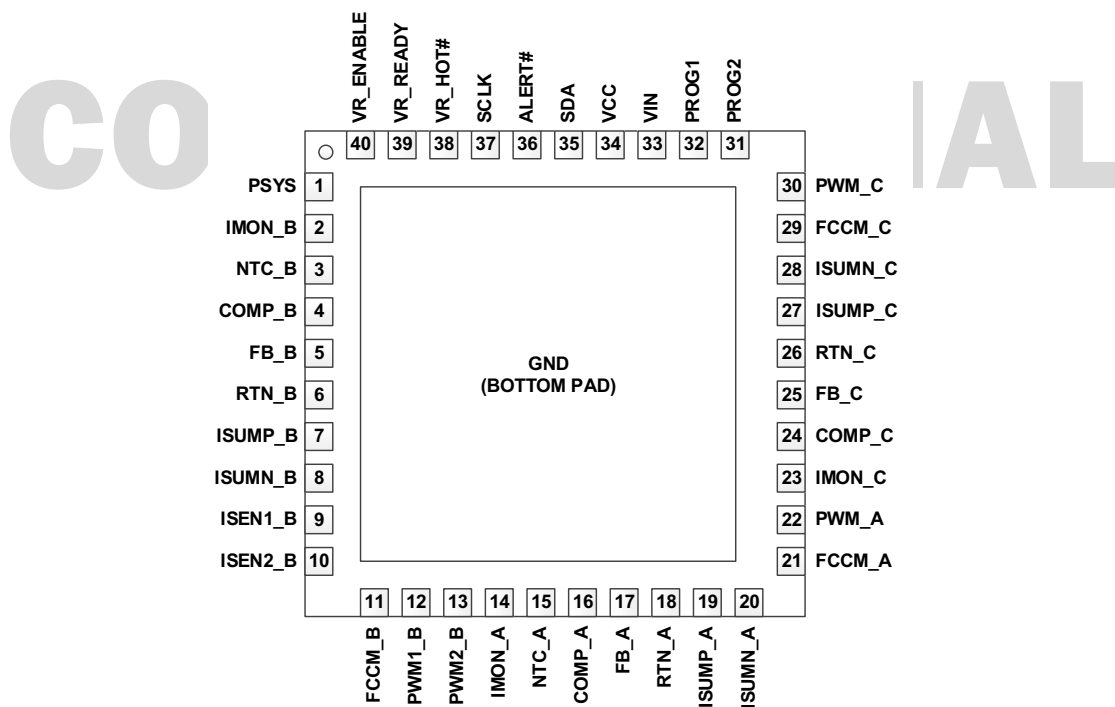
Part Number (Notes 1, 2, 3)	Part Marking	Temp Range (°C)	Package (RoHS Compliant)	Pkg. Dwg. #
ISL95859CHRTZ	95859C HRTZ	-10 to +100	40 Ld 5x5 TQFN	L40.5x5
ISL95859CIRTZ	95859C IRTZ	-40 to +100	40 Ld 5x5 TQFN	L40.5x5

Notes:

1. Add "-T" for 6k unit tape and reel options. Refer to [TB347](#) for details on reel specifications.
2. These Intersil Pb-free plastic packaged products employ special Pb-free material sets, molding compounds/die attach materials and 100% matte tin plate plus anneal (e3 termination finish, which is RoHS compliant and compatible with both SnPb and Pb-free soldering operations). Intersil Pb-free products are MSL classified at Pb-free peak reflow temperatures that meet or exceed the Pb-free requirements of IPC/JEDEC J STD-020.
3. For more information on MSL, refer to [TB363](#).

1.4 Pin Configuration

ISL95859C
(40 LD TQFN)
Top View



1.5 Pin Descriptions

Pin Number	Pin Name	Description
BOTTOM PAD	GND	Signal common to the IC. Unless otherwise stated, all signals are referenced to the GND pad. It is also the primary thermal conduction pad for heat removal. Connect this ground pad to the ground plane or planes through a low impedance path. Best performance is obtained with an uninterrupted ground plane under the ISL95859C and all associated components, signal sources, signal paths and extending from the controller to the load. Do not attempt to isolate signal and power grounds.
1	PSYS	Analog input from the platform battery charger that is proportional to real-time, total system power dissipation. Information is to be digitized and stored by the controller to be read by the CPU from SVID.
2	IMON_B	Regulator B current monitor. The IMON_B pin sources a current proportional to the regulator output current. A resistor connected from this pin to ground will set a voltage that is proportional to the load current. This voltage is sampled internally to produce a digital IMON signal that is read through the serial communication bus.
3	NTC_B	Thermistor input from VR B to the temperature monitor circuit of the IC controlling the VR_HOT# output. Connect this pin to a resistor network with a thermistor (NTC) to GND. A current is sourced from the pin and generates a voltage, which is monitored versus an internal threshold to determine when the VR is too hot.
4	COMP_B	Output of the transconductance error amplifier for VR B regulation and stability. Connect to ground through a type-II network to compensate the control loop.
5	FB_B	Output voltage feedback sensing input for regulation of Regulator B. Connect to the remote positive sense point on the CPU through a resistor. The resistor value is used to scale droop for VR B.
6	RTN_B	Ground return for differential remote output voltage sensing. Connect to the remote negative sense point on the CPU through a resistor.
7	ISUMP_B	VR B droop current sensing inputs.
8	ISUMN_B	Connecting ISUMN_B to VCC disables VR B.
9	ISEN1_B	Individual current sensing for VR B Phase 1. This signal monitors and corrects for phase current imbalance. In 1-phase configurations, connect ISEN1_B to VCC or leave it open.
10	ISEN2_B	Individual current sensing for VR B Phase 2. When ISEN2_B is pulled to VDD (+5V), the controller will disable VR Phase 2. This signal is used to monitor and correct for phase current imbalance.
11	FCCM_B	Driver control signal for Regulator B. When FCCM_B is high, continuous conduction mode is forced. When FCCM_B is low, diode emulation is allowed. FCCM_B is high impedance and interfaces with the ISL95808 or similar driver when entering a PS4 state.
12	PWM1_B	Regulator B, Channel 1 PWM output. See “Driver Selection” on page 35 for more information on interfacing with the ISL95808 driver or compatible power stages.
13	PWM2_B	Regulator B, Channel 2 PWM output. See “Driver Selection” on page 35 for more information on interfacing with the ISL95808 driver or compatible power stages.
14	IMON_A	Regulator A current monitor. The IMON_A pin sources a current proportional to the regulator output current. A resistor connected from this pin to ground will set a voltage that is proportional to the load current. This voltage is sampled internally to produce a digital IMON_A signal that is read through the serial communication bus.
15	NTC_A	Thermistor input from VR A to the temperature monitor circuit of the IC controlling the VR_HOT# output. Connect this pin to a resistor network with a thermistor (NTC) to GND. A current is sourced from the pin and generates a voltage, which is monitored versus an internal threshold to determine when the VR is too hot.
16	COMP_A	Output of the transconductance error amplifier for VR A regulation and stability. Connect to ground through a type-II network to compensate the control loop.
17	FB_A	Output voltage feedback sensing input for regulation of Regulator A. Connect to the remote positive sense point on the CPU through a resistor. The resistor value is used to scale droop for VR A.
18	RTN_A	Ground return for differential remote output voltage sensing. Connect to the remote negative sense point on the CPU through a resistor.

Pin Number	Pin Name	Description
19	ISUMP_A	VR A droop current sensing inputs. Connecting ISUMN_A to VCC disables VR A.
20	ISUMN_A	
21	FCCM_A	Driver control signal for Regulator A. When FCCM_A is high, Continuous Conduction Mode (CCM) is forced. When FCCM_A is low, diode emulation is allowed. FCCM_A is high impedance and interfaces with the ISL95808 or similar driver when entering a PS4 state.
22	PWM_A	Regulator A, PWM output. See "Driver Selection" on page 35 for more information on interfacing with the ISL95808 driver or compatible power stages.
23	IMON_C	Regulator C current monitor. The IMON_C pin sources a current proportional to the regulator output current. A resistor connected from this pin to ground will set a voltage that is proportional to the load current. This voltage is sampled internally to produce a digital IMON signal that is read through the serial communication bus.
24	COMP_C	Output of the transconductance error amplifier for VR C regulation and stability. Connect to ground through a type-II network to compensate the control loop.
25	FB_C	Output voltage feedback sensing input for regulation of Regulator C. Connect to the remote positive sense point on the CPU through a resistor. The resistor value is used to scale droop for VR C.
26	RTN_C	Ground return for differential remote output voltage sensing. Connect to the remote negative sense point on the CPU through a resistor.
27	ISUMP_C	VR C droop current sensing inputs. Connecting ISUMN_C to VCC disables VR C.
28	ISUMN_C	
29	FCCM_C	Driver control signal for Regulator C. When FCCM_C is high, Continuous Conduction Mode (CCM) is forced. When FCCM_C is low, diode emulation is allowed. FCCM_C is high impedance and interfaces with the ISL95808 or similar driver when entering a PS4 state.
30	PWM_C	Regulator C, PWM Output. See "Driver Selection" on page 35 for more information on interfacing with the ISL95808 driver or compatible power stages.
31	PROG2	Place a resistor from this pin to GND. The resistor value is selected based on programming options defined in the controller option tables.
32	PROG1	Place a resistor from this pin to GND. The resistor value is selected based on programming options defined in the controller option tables.
33	VIN	Input supply voltage used for input voltage feed-forward.
34	VCC	+5V bias supply input for the controller. Bypass to ground with a high quality 0.1µF ceramic capacitor. This pin establishes the voltage reference for all PWM and FCCM driver interface outputs. To ensure proper operation of drivers, especially during power-up and power-down sequencing, it is essential that this pin be powered with the same +5V power supply as the VCC or VCCP pins of the Intersil gate drivers.
35	SDA	Communication bus between the CPU and the VRs.
36	ALERT#	
37	SCLK	
38	VR_HOT#	Open-drain thermal overload output indicator. Considered part of the communication bus with the CPU.
39	VR_READY	Power-good open-drain output indicating when controller is able to supply regulated voltage on all outputs. Pull up externally with a 680Ω resistor to VCC or 1.9kΩ to 3.3V
40	VR_ENABLE	Controller enable input. A high level logic signal on this pin enables the controller.

2. Specifications

2.1 Absolute Maximum Ratings

Parameter	Minimum	Maximum	Unit
Supply Voltage, V_{CC}	-0.3	+6.5	V
Battery Voltage, V_{IN}		+28	V
All Other Pins	-0.3	$V_{CC} + 0.3$	V
Open-Drain Outputs, VR_READY, VR_HOT#, ALERT#	-0.3	+6.5	V
ESD Rating	Value		Unit
Human Body Model (Tested per JESD22-A114E)	2		kV
Charged Device Model (Tested per JESD22-C101A)	1		kV
Latch-Up (Tested per JESD78B; Class 2, Level A)	100		mA

CAUTION: Do not operate at or near the maximum ratings listed for extended periods of time. Exposure to such conditions may adversely impact product reliability and result in failures not covered by warranty.

2.2 Thermal Information

Thermal Resistance (Typical)	θ_{JA} (°C/W)	θ_{JC} (°C/W)
40 Ld TQFN Package (Notes 4, 5)	30	1.5

Notes:

- θ_{JA} is measured in free air with the component mounted on a high-effective thermal conductivity test board with "direct attach" features. Refer to [TB379](#).
- For θ_{JC} , the "case temp" location is the center of the exposed metal pad on the package underside.

Parameter	Minimum	Maximum	Unit
Maximum Junction Temperature		+150	°C
Maximum Storage Temperature Range	-65	+150	°C
Maximum Junction Temperature (Plastic Package)		+150	°C
Storage Temperature Range	-65	+150	°C
Pb-Free Reflow Profile	Refer to TB493		

2.3 Recommended Operating Conditions

Parameter	Minimum	Maximum	Unit
Supply Voltage, V_{CC}		+5V $\pm 5\%$	V
Input Voltage, V_{IN}	+4.5	25	V
Ambient Temperature			
HRTZ	-10	+100	°C
IRTZ	-40	+100	°C
Junction Temperature			
HRTZ	-10	+125	°C
IRTZ	-40	+125	°C

2.4 Electrical Specifications

$V_{CC} = 5V$, $V_{IN} = 15V$, $f_{SW} = 583kHz$, unless otherwise noted. **Boldface limits apply across the operating temperature range $T_A = -40^{\circ}C$ to $+100^{\circ}C$ for industrial (IRTZ) and $T_A = -10^{\circ}C$ to $+100^{\circ}C$ for high temperature commercial (HRTZ).**

Symbol	Parameter	Test Conditions	Min (Note 6)	Typ	Max (Note 6)	Unit
Input Power Supply						
I _{VCC}	+5V Supply Current	VR_ENABLE = 1V (PWMs are not switching)		16	18	mA
		VR_ENABLE = 0V			1	μA
		PS4 state for all VRs and input power domain		80	140	μA
I _{VIN}	V _{IN} Supply Current	VR_ENABLE = 0V			1	μA
R _{VIN}	V _{IN} Input Resistance	VR_ENABLE = 1V		700		kΩ
Power-on-Reset Thresholds						
VCCPOR _r	V _{CC} Power-On Reset Threshold	V _{CC} rising		4.40	4.50	V
VCCPOR _f		V _{CC} falling	4.00	4.15		V
VINPOR _r	V _{IN} Power-On Reset Threshold	V _{IN} rising		4.00	4.35	V
VINPOR _f		V _{IN} falling	2.90	3.40		V
System and References						
HRTZ	System Accuracy	VID = 0.75V to 1.52V	-0.5		0.5	%
		VID = 0.5V to 0.745V	-7		7	mV
		VID = 0.25V to 0.495V	-10		10	mV
IRTZ		VID = 0.75V to 1.52V	-0.8		0.8	%
		VID = 0.5V to 0.745V	-9		9	mV
		VID = 0.25V to 0.495V	-12		12	mV
HRTZ	SA Internal V _{BOOT}			1.05		V
IRTZ				1.05		V
HRTZ	IA, GT, GTUS Internal V _{BOOT}			0		V
IRTZ				0		V
V _{OUT(max)}	Maximum Programmed Output Voltage	VID = [11111111]		1.52		V
V _{OUT(min)}	Minimum Programmed Output Voltage	VID = [00000001]		0.25		V
Switching Frequency						
f _{SW_450k}	450kHz Configuration	Set by R_PROG1 and R_PROG2	415		500	kHz
f _{SW_583k}	583kHz Configuration		540		630	kHz
f _{SW_750k}	750kHz Configuration		685		795	kHz
Amplifiers						
HRTZ	Current-sense Amplifier Input Offset	I _{FB} = 0A	-0.2		0.2	mV
IRTZ			-0.3		0.3	mV
A _{v0}	Error Amplifier DC Gain (Note 7)			38		dB
GBW	Error Amplifier Gain-Bandwidth Product (Note 7)	C _L = 20pF		30		MHz

$V_{CC} = 5V$, $V_{IN} = 15V$, $f_{SW} = 583kHz$, unless otherwise noted. **Boldface limits apply across the operating temperature range $T_A = -40^{\circ}C$ to $+100^{\circ}C$ for industrial (IRTZ) and $T_A = -10^{\circ}C$ to $+100^{\circ}C$ for high temperature commercial (HRTZ).**

Symbol	Parameter	Test Conditions	Min (Note 6)	Typ	Max (Note 6)	Unit
ISEN						
	Imbalance Voltage	Maximum of ISENs - minimum of ISENs			1	mV
	Input Bias Current			20		nA
Power-Good and Protection Monitors						
V _{OL}	VR_READY Low Voltage	I _{VR_READY} = 4mA		0.15	0.40	V
I _{OH}	VR_READY Leakage Current	VR_READY = 3.3V			1	μA
	ALERT# Low Voltage (Note 7)			7	12	Ω
	VR_HOT# Low Voltage (Note 7)			7	12	Ω
	ALERT# Leakage Current				1	μA
	VR_HOT# Leakage Current				1	μA
PWM and FCCM						
V _{OL}	PWM Output Low	Sinking 5mA		0.6	0.9	V
	FCCM Output Low	Sinking 4mA		0.6	0.9	V
V _{OH}	PWM Output High (Note 7)	Sourcing 5mA	3.5	4.2		V
	FCCM Output High (Note 7)	Sourcing 4mA	3.3	3.6		V
	PWM Tri-State Voltage			2.5		V
	FCCM Mid-State Voltage			2.5		V
	PWM Tri-State and FCCM High Impedance Leakage	PWM and FCCM = 2.5V	-1		1	μA
t _{PS4EXIT}	PS4 Exit Latency	V _{CC} = 5V	50		100	μs
Protection						
OV _H	Overvoltage Threshold	ISUMN rising above setpoint for >1μs	240		360	mV
	Overcurrent Threshold (ISUMN Pin Current)	2-phase configuration PS0 state or 1-phase configuration covering all power states	56	60	64	μA
		2-phase configuration with 1-phase operation in PS1, PS2 and PS3 states	27	30	33	μA
Logic Thresholds						
V _{IL}	VR_ENABLE Input Low				0.3	V
V _{IH}	VR_ENABLE Input High	HRTZ	0.7			V
V _{IH}		IRTZ	0.75			V
Thermal Monitor						
	NTC Source Current	NTC = 1.3V	9.5	10	10.5	μA
	VR_HOT# Trip Voltage	Falling	0.187	0.198	0.209	V
	VR_HOT# Reset Voltage	Rising	0.209	0.220	0.231	V
	VR_HOT# Hysteresis			20		mV
	Thermal Alert Trip Voltage	Falling	0.203	0.214	0.225	V
	Thermal Alert Reset Voltage	Rising	0.225	0.236	0.247	V
	Thermal Alert Hysteresis			20		mV

$V_{CC} = 5V$, $V_{IN} = 15V$, $f_{SW} = 583kHz$, unless otherwise noted. **Boldface limits apply across the operating temperature range $T_A = -40^{\circ}C$ to $+100^{\circ}C$ for industrial (IRTZ) and $T_A = -10^{\circ}C$ to $+100^{\circ}C$ for high temperature commercial (HRTZ).**

Symbol	Parameter	Test Conditions	Min (Note 6)	Typ	Max (Note 6)	Unit
Current Monitor						
I _{IMON}	IMON Output Current	ISUM- pin current = 40μA	9.7	10	10.3	μA
		ISUM- pin current = 20μA	4.8	5	5.2	μA
		ISUM- pin current = 4μA	0.875	1	1.125	μA
V _{IMONr}	I _{CCMAX} Alert Trip Voltage	Rising	1.185	1.200	1.215	V
V _{IMONf}	I _{CCMAX} Alert Reset Voltage	Falling	1.115	1.130	1.145	V
Inputs						
I _{VR_ENABLE}	VR_ENABLE Leakage Current	VR_ENABLE = 0V	-1	0		μA
		VR_ENABLE = 1V		3	5	μA
	SCLK, SDA Leakage	VR_ENABLE = 0V, SCLK and SDA = 0V and 1V	-1		1	μA
		VR_ENABLE = 1V, SCLK and SDA = 1V	-5		1	μA
		VR_ENABLE = 1V, SCLK and SDA = 0V, SCLK Leakage		-42		μA
		VR_ENABLE = 1V, SCLK and SDA = 0V, SDA Leakage		-24		μA
Slew Rate (For VID Change)						
	Fast Slew Rate		30			mV/μs
	Slow Slew Rate		15			mV/μs
	SVID					
	SVID CLK Maximum Speed (Note 7)			42		MHz
	SVID CLK Minimum Speed (Note 7)			13		MHz

Notes:

- Parameters with MIN and/or MAX limits are 100% tested at $+25^{\circ}C$, unless otherwise specified. Temperature limits established by characterization and are not production tested.
- Limits established by characterization and are not production tested.

3. Typical Performance Curves for VR A

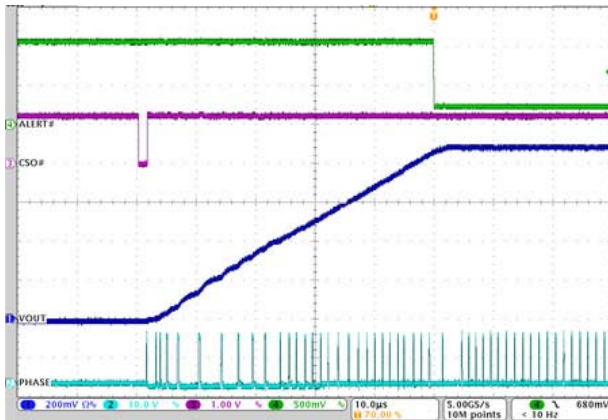


Figure 7. V_{CORE}/VR A Soft-Start, SetVID_fast 0V to 0.9V, $I_O = 0A$

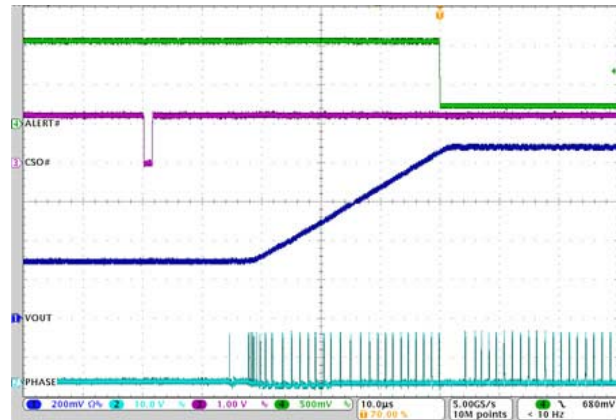


Figure 8. V_{CORE}/VR A Soft-Start with Precharged Output, SetVID_fast 0.9V, $I_O = 0A$

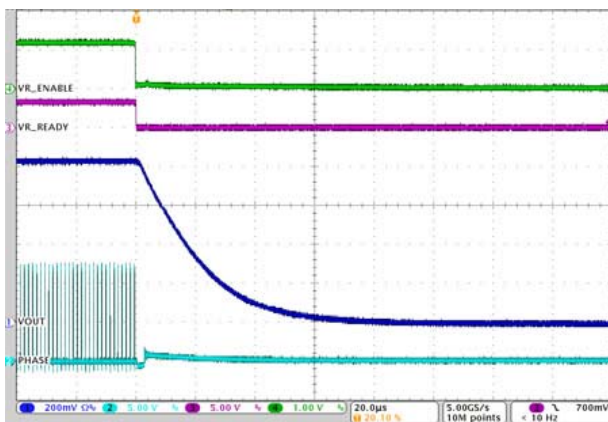


Figure 9. V_{CORE}/VR A Shutdown, $I_O = 23A$, VID = 0.9V

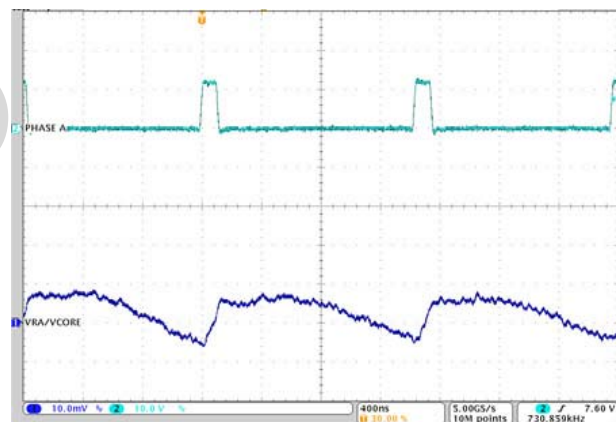


Figure 10. V_{CORE}/VR A PS0 Steady-State Phase and Ripple, $I_O = 23A$, VID = 0.9V

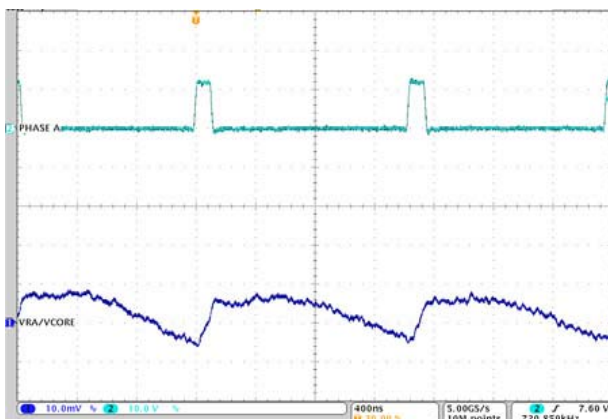


Figure 11. V_{CORE}/VR A PS1 Steady-State Phase and Ripple, $I_O = 23A$, VID = 0.9V

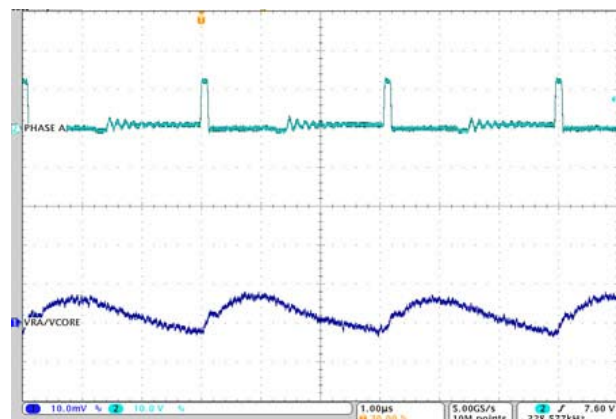


Figure 12. V_{CORE}/VR A PS2 Steady-State Phase and Ripple, $I_O = 2A$, VID = 0.9V

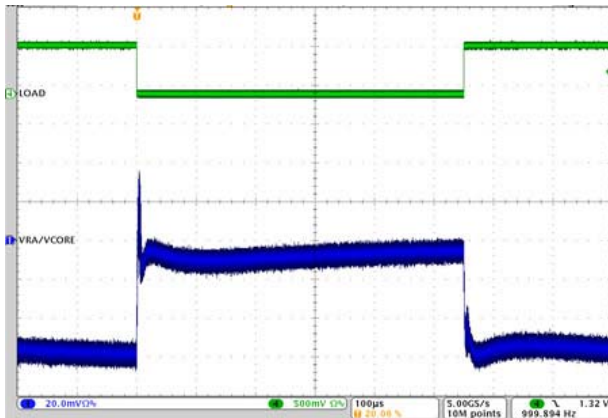


Figure 13. V_{CORE}/VR A PS0 Load Step, $I_O = 4A$ to $29A$,
 $VID = 0.9V$, $R_{LL} = 2.4m\Omega$

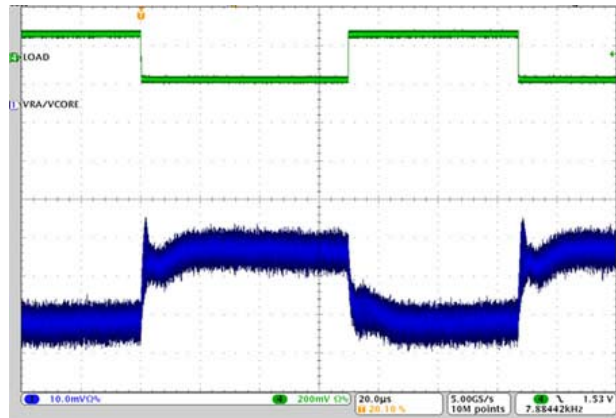


Figure 14. V_{CORE}/VR A PS0 Load Step, $I_O = 18A$ to $28A$,
 $VID = 0.9V$, $R_{LL} = 2.4m\Omega$

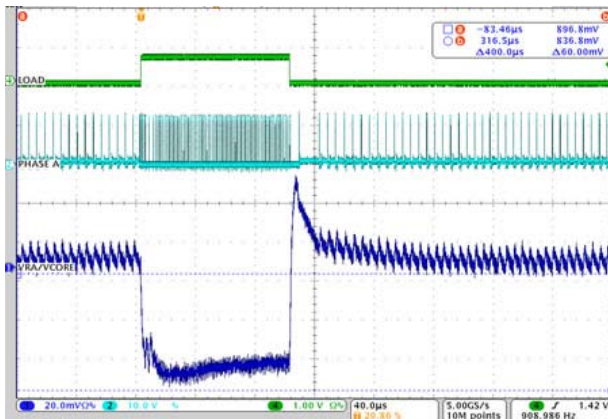


Figure 15. V_{CORE}/VR A Load Step, $I_O = 1A$ IN PS2 to $26A$
in PS0, $VID = 0.9V$, $R_{LL} = 2.4m\Omega$

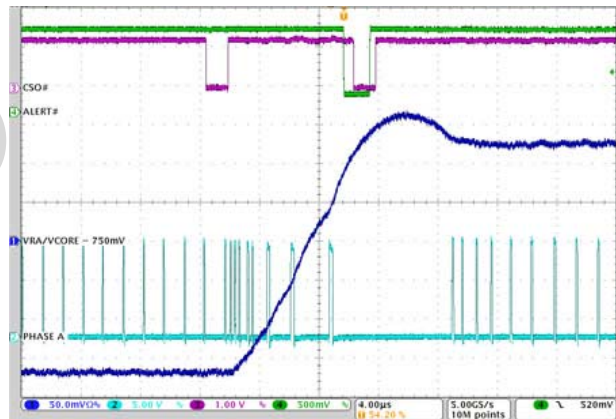


Figure 16. V_{CORE}/VR A SetVID_fast, $0.6V$ to $0.9V$, PS0,
 $I_O = 7A$, $R_{LL} = 2.4m\Omega$

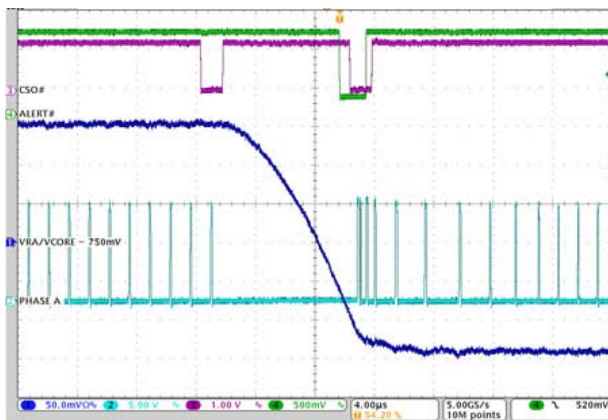


Figure 17. V_{CORE}/VR A SetVID_fast, $0.9V$ to $0.6V$, PS0,
 $I_O = 7A$, $R_{LL} = 2.4m\Omega$

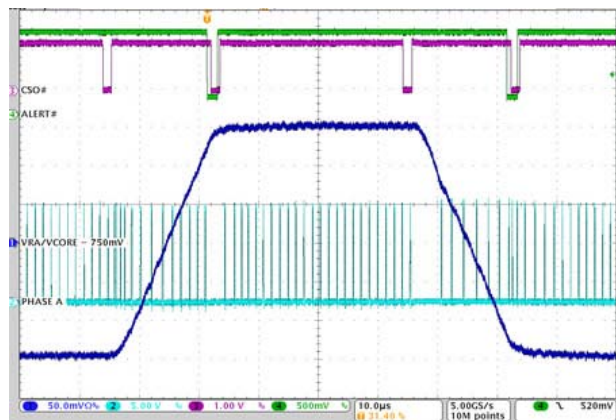


Figure 18. V_{CORE}/VR A SetVID_slow, $0.6V$ to $0.9V$ to $0.6V$,
PS0, $I_O = 7A$, $R_{LL} = 2.4m\Omega$



Figure 19. V_{CORE}/VR A SetVID_fast, 0.7V to 0.9V, PS0, SetVID_decay, 0.9V to 0.7V, $I_O = 1.5A$, $R_{LL} = 2.4m\Omega$

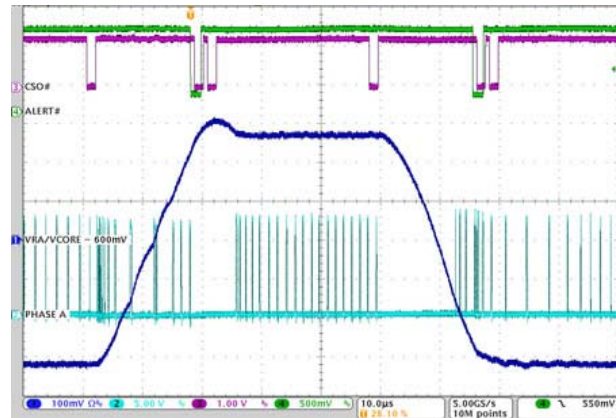


Figure 20. V_{CORE}/VR A SetVID_fast, 0.3V to 0.9V to 0.3V, PS1, $I_O = 7A$, $R_{LL} = 2.4m\Omega$

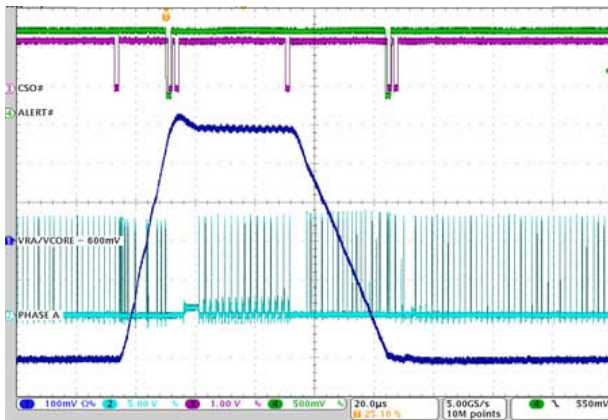


Figure 21. V_{CORE}/VR A SetVID_fast, 0.3V to 0.9V, SetVID_slow to 0.3V, PS2, $I_O = 1A$, $R_{LL} = 2.4m\Omega$

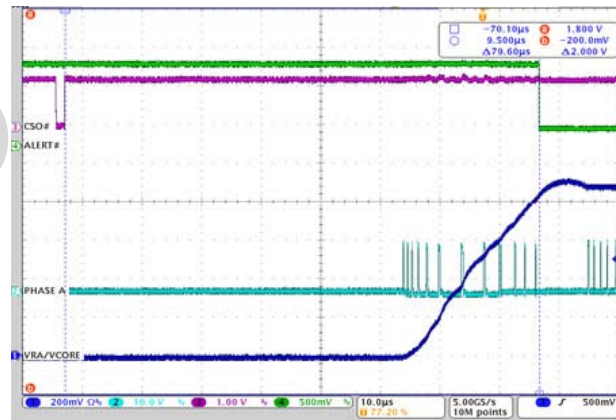


Figure 22. V_{CORE}/VR A PS4 EXIT, SetVID_fast 0.9V, PS0, $I_O = 0A$, $R_{LL} = 2.4m\Omega$

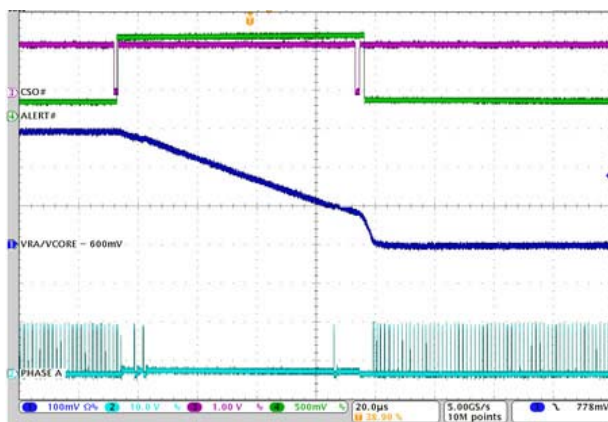


Figure 23. V_{CORE}/VR A SetVID_decay 0.9V to 0.3V, Pre-Empted Downward by SetVID_fast 0.6V, $I_O = 2.1A$, $R_{LL} = 2.4m\Omega$

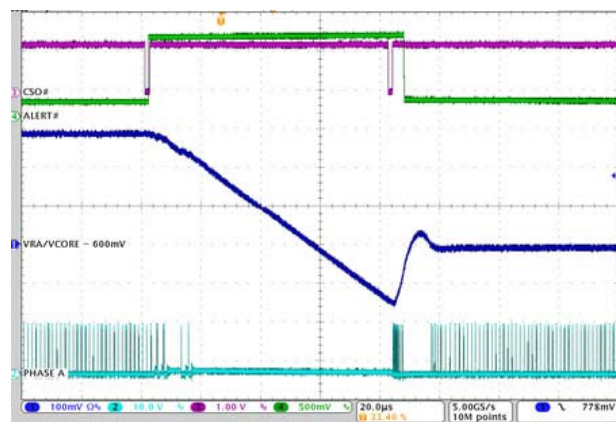


Figure 24. V_{CORE}/VR A SetVID_decay 0.9V to 0.3V, Pre-Empted Upward by SetVID_fast 0.6V, $I_O = 4.4A$, $R_{LL} = 2.4m\Omega$

4. Typical Performance Curves for VR B

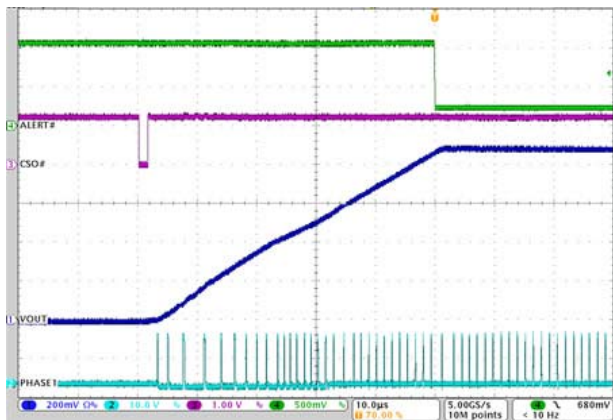


Figure 25. VGT/VR B Soft-Start, SetVID_fast 0V to 0.9V, $I_O = 0A$

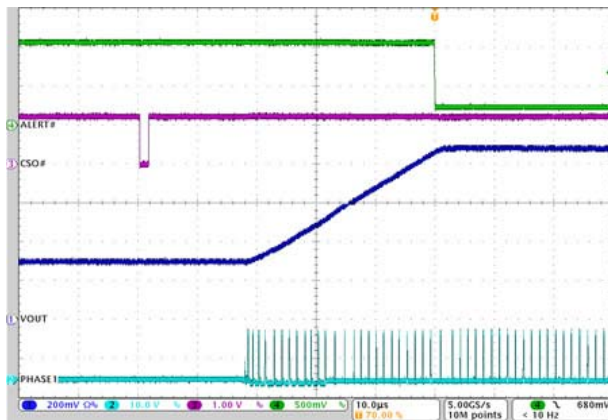


Figure 26. VGT/VR B Soft-Start with Precharged Output, SetVID_fast 0.9V, $I_O = 0A$

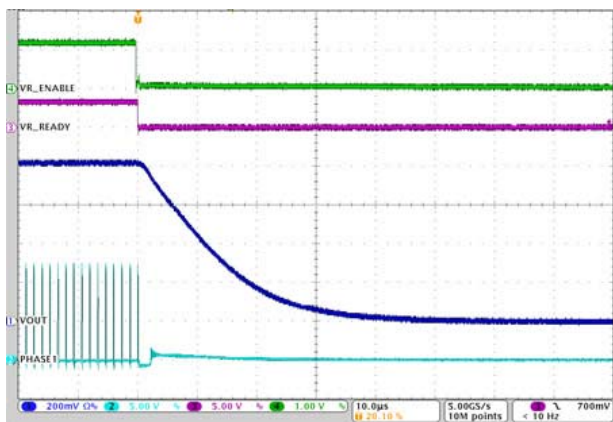


Figure 27. VGT/VR B Shutdown, $I_O = 35A$, VID = 0.9V

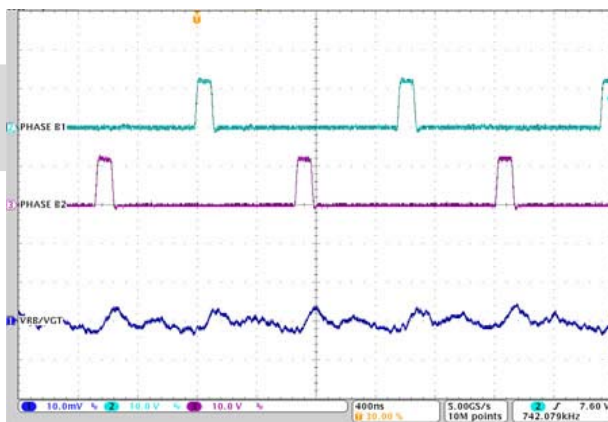


Figure 28. VGT/VR B PS0 Steady-State Phase and Ripple, $I_O = 35A$, VID = 0.9V

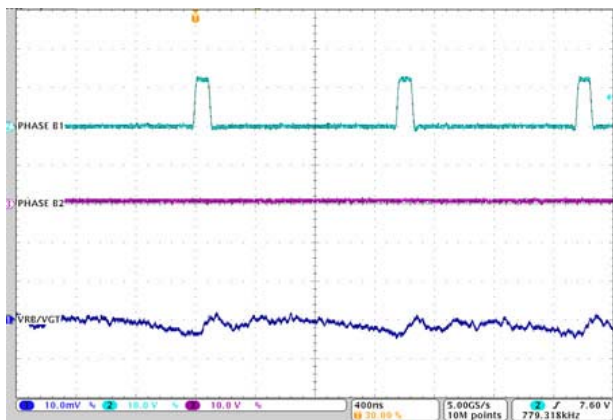


Figure 29. VGT/VR B PS1 Steady-State Phase and Ripple, $I_O = 10A$, VID = 0.9V

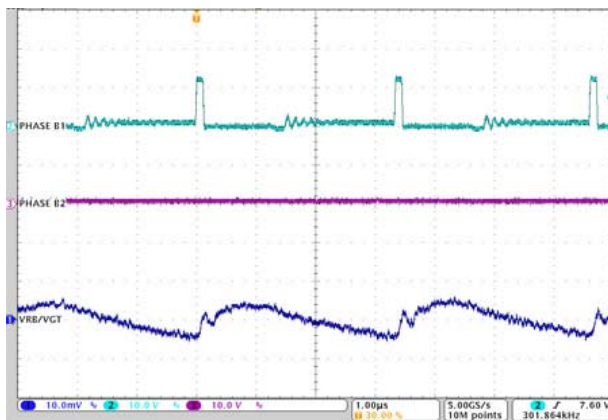


Figure 30. VGT/VR B PS2 Steady-State Phase and Ripple, $I_O = 2A$, VID = 0.9V

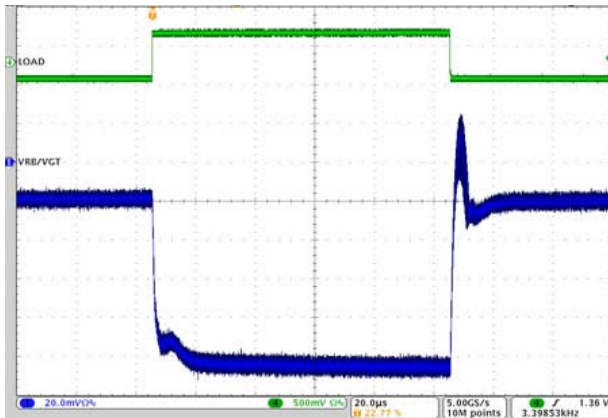


Figure 31. VGT/VR B PS0 Load Step, $I_O = 11A$ to $57A$, $VID = 0.9V$, $R_{LL} = 2.0m\Omega$

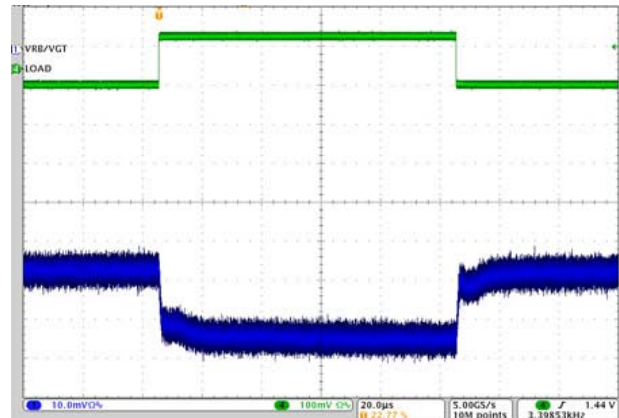


Figure 32. IVGT/VR B PS0 Load Step, $I_O = 30A$ to $40A$, $VID = 0.9V$, $R_{LL} = 2.0m\Omega$

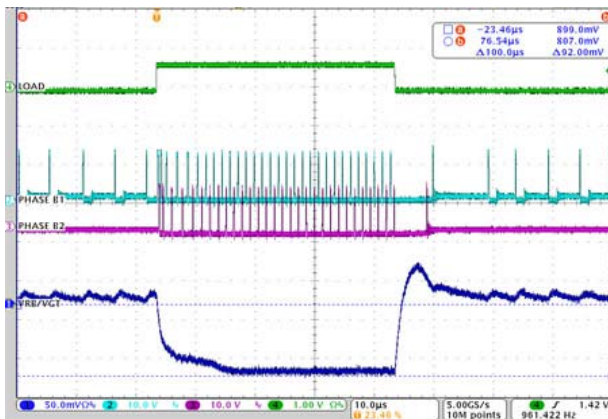


Figure 33. VGT/VR B Load Step, $I_O = 1A$ in PS2 to $47A$ in PS0, $VID = 0.9V$, $R_{LL} = 2.0m\Omega$

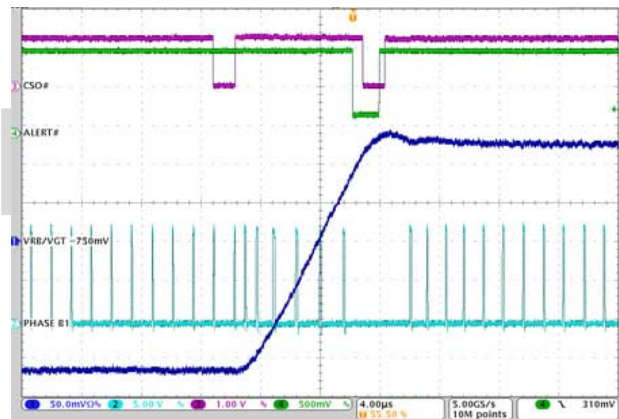


Figure 34. VGT/VR B SetVID_fast, $0.6V$ to $0.9V$, PS0, $I_O = 11A$, $R_{LL} = 2.0m\Omega$

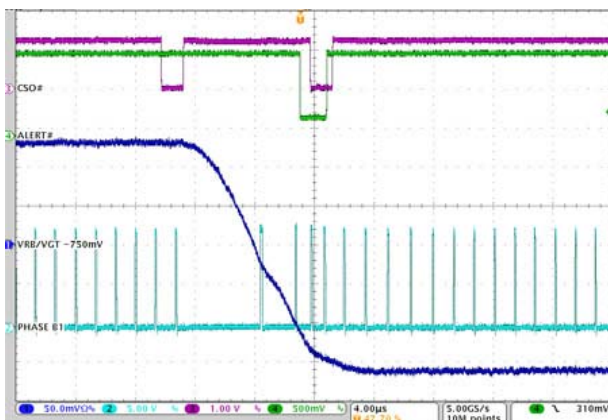


Figure 35. IVGT/VR B SetVID_fast, $0.9V$ to $0.6V$, PS0, $I_O = 11A$, $R_{LL} = 2.0m\Omega$

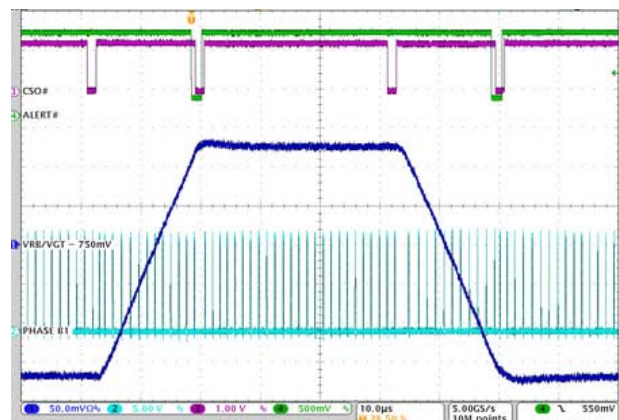


Figure 36. VGT/VR B SetVID_slow, $0.6V$ to $0.9V$ to $0.6V$, PS0, $I_O = 11A$, $R_{LL} = 2.0m\Omega$

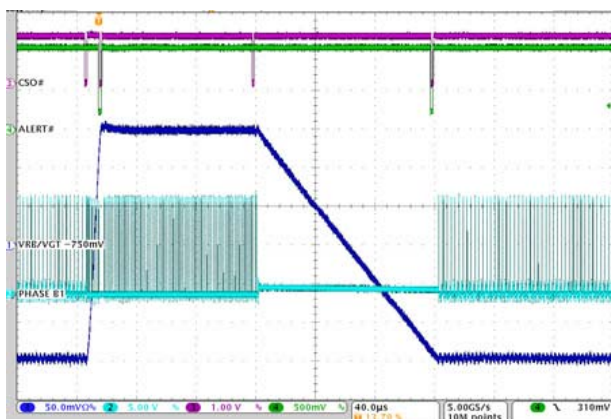


Figure 37. VGT/VR B SetVID_fast, 0.6V to 0.9V, PS0, SetVID_decay, 0.9V to 0.6V, $I_O = 2A$, $R_{LL} = 2.0m\Omega$

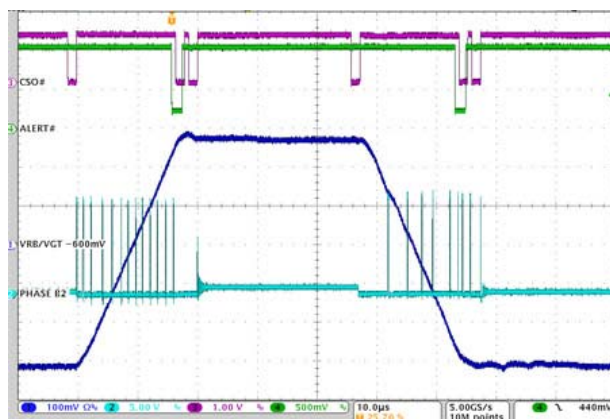


Figure 38. VGT/VR B SetVID_fast, 0.3V to 0.9V to 0.3V, PS1, $I_O = 10A$, $R_{LL} = 2.0m\Omega$

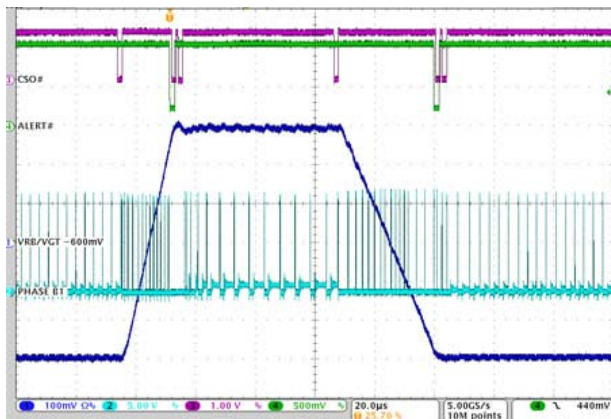


Figure 39. VGT/VR B SetVID_fast, 0.3V to 0.9V, SetVID_slow to 0.3V, PS2, $I_O = 1A$, $R_{LL} = 2.0m\Omega$

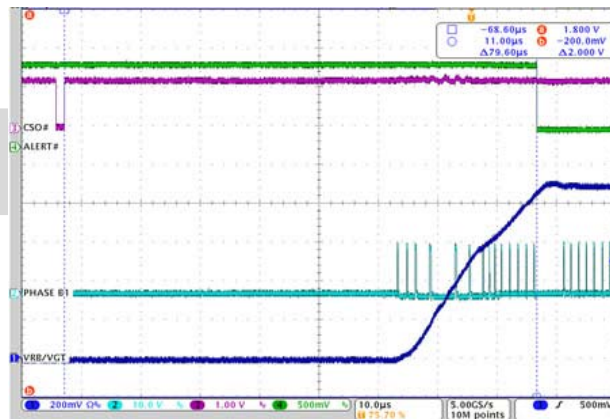


Figure 40. VGT/VR B PS4 Exit, SetVID_fast 0.9V, PS0, $I_O = 0A$, $R_{LL} = 2.0m\Omega$

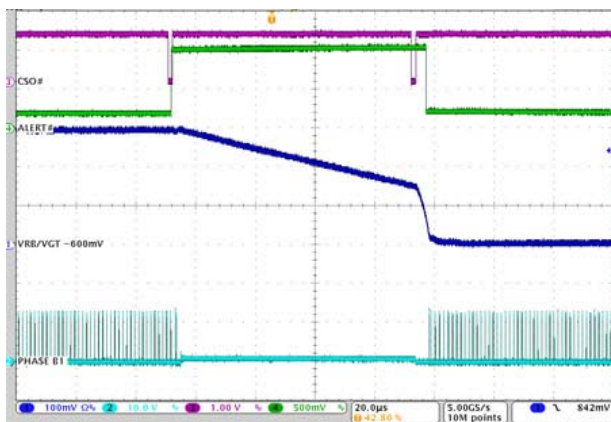


Figure 41. VGT/VR B SetVID_decay 0.9V to 0.3V, Pre-Empted Downward by SetVID_fast 0.6V, $I_O = 1.5A$, $R_{LL} = 2.0m\Omega$

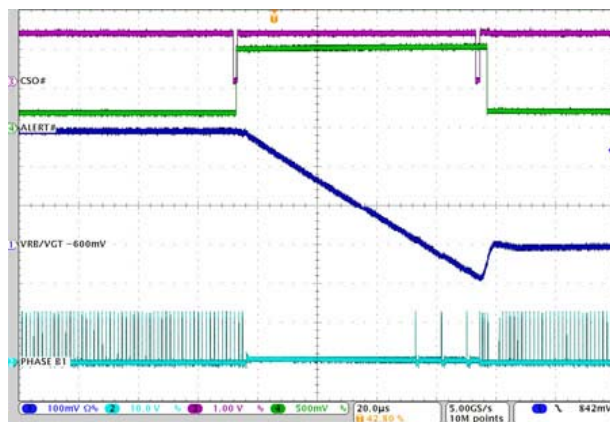


Figure 42. VGT/VR B SetVID_decay 0.9V to 0.3V, Pre-Empted Upward by SetVID_fast 0.6V, $I_O = 4A$, $R_{LL} = 2.0m\Omega$

5. Typical Performance Curves for VR C

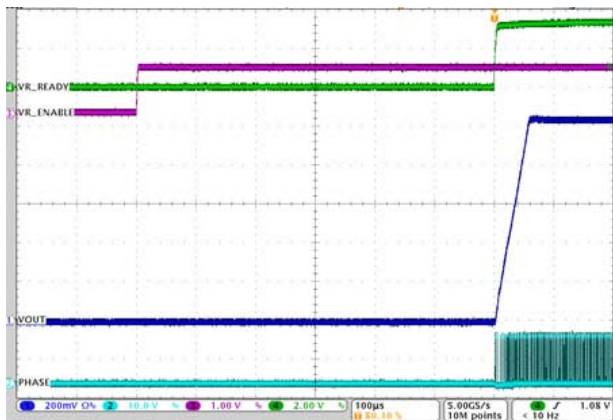


Figure 43. VSA/VR C Soft-Start, 0V to $V_{BOOT} = 1.05V$, $I_O = 0A$

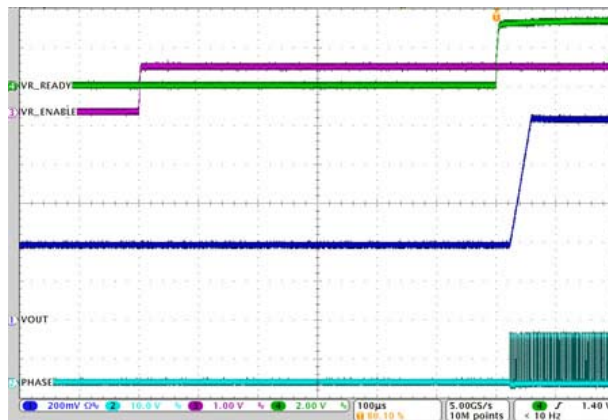


Figure 44. VSA/VR C Soft-Start with Precharged Output, $V_{BOOT} = 1.05V$, $I_O = 0A$

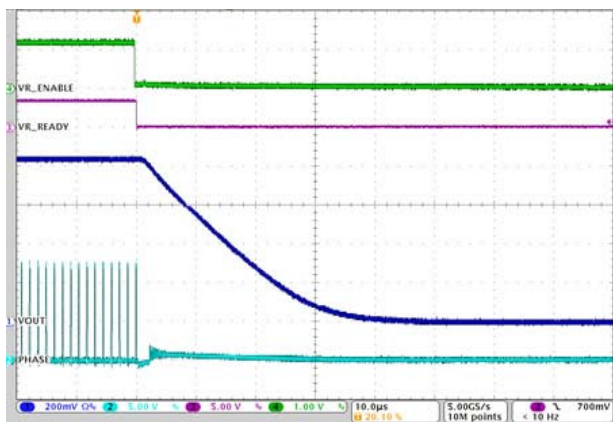


Figure 45. VSA/VR C Shutdown, $I_O = 5A$, $VID = 0.9V$

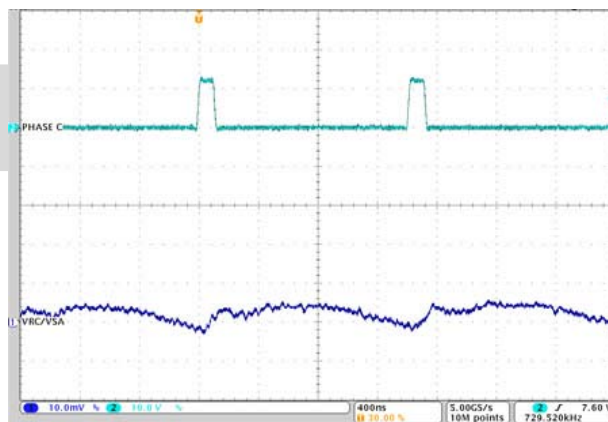


Figure 46. VSA/VR C PS0 Steady-State Phase and Ripple, $I_O = 5A$, $VID = 0.9V$

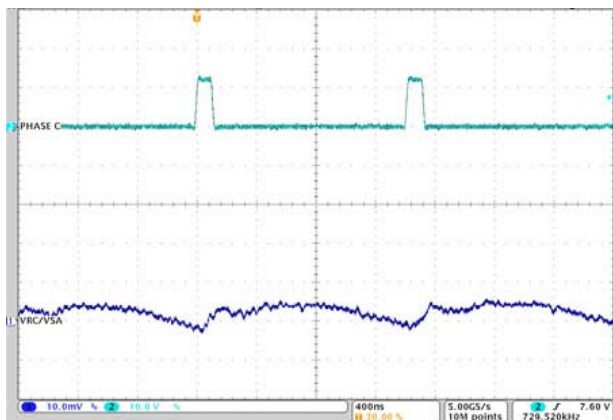


Figure 47. VSA/VR C PS1 Steady-State Phase and Ripple, $I_O = 5A$, $VID = 0.9V$

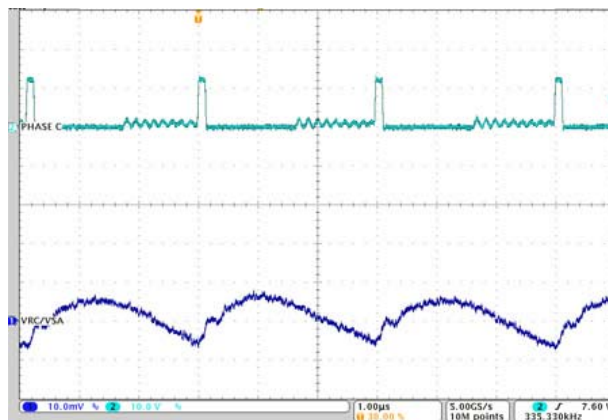


Figure 48. VSA/VR C PS0 Steady-State Phase and Ripple, $I_O = 1A$, $VID = 0.9V$

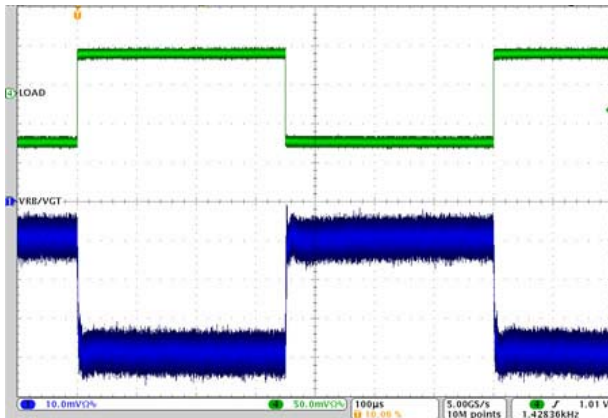


Figure 49. VSA/VR C PS0 Load Step, $I_O = 2A$ to $5A$, $VID = 0.9V$, $R_{LL} = 10.3m\Omega$

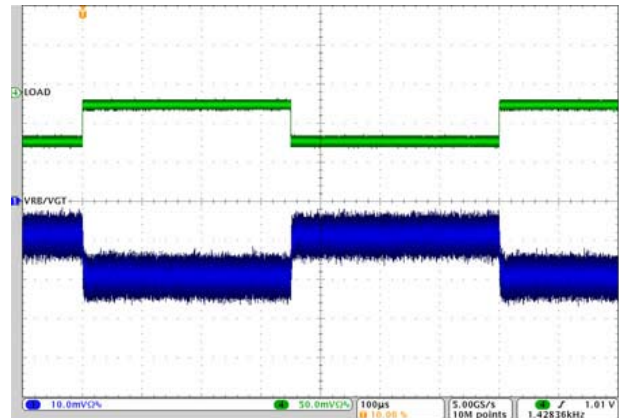


Figure 50. VSA/VR C PS0 Load Step, $I_O = 2A$ to $3A$, $VID = 0.9V$, $R_{LL} = 10.3m\Omega$

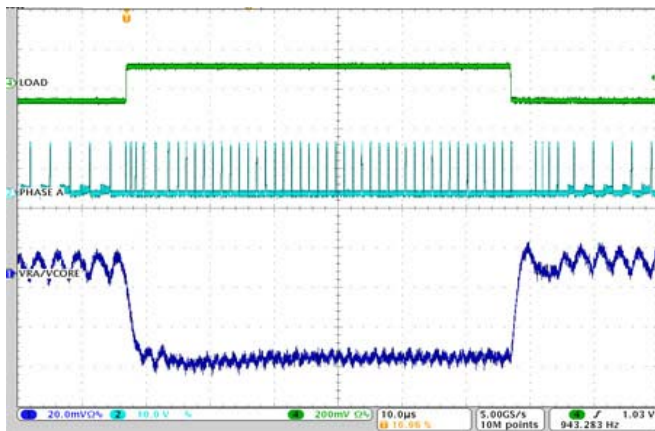


Figure 51. VSA/VR C Load Step, $I_O = 1A$ in PS2 to $5A$ in PS0, $VID = 0.9V$, $R_{LL} = 10.3m\Omega$

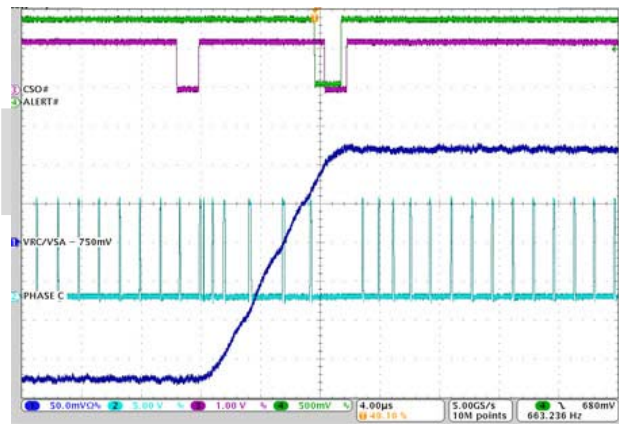


Figure 52. VSA/VR C SetVID_fast, $0.6V$ to $0.9V$, PS0, $I_O = 3A$, $R_{LL} = 10.3m\Omega$

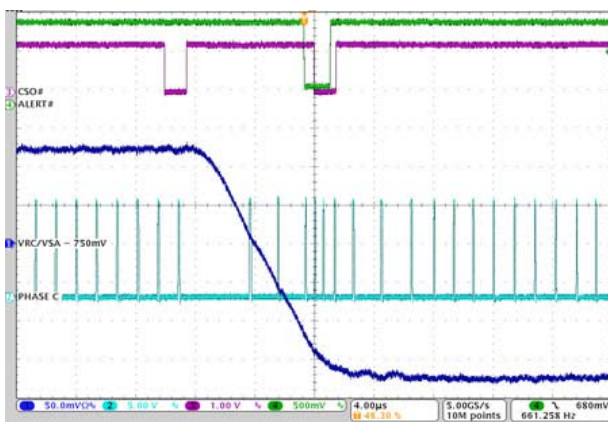


Figure 53. VSA/VR C SetVID_fast, $0.9V$ to $0.6V$, PS0, $I_O = 3A$, $R_{LL} = 10.3m\Omega$

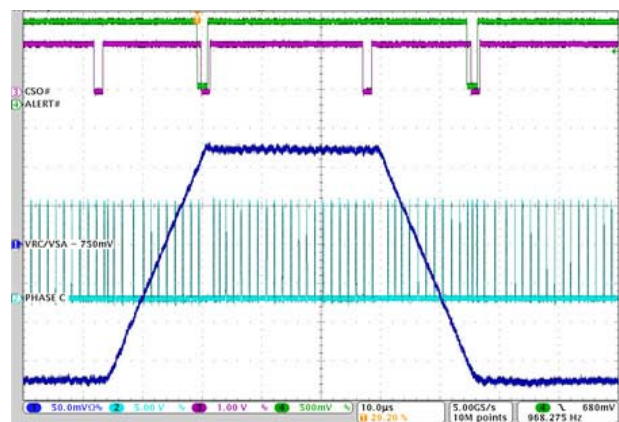


Figure 54. VSA/VR C SetVID_slow, $0.6V$ to $0.9V$ to $0.6V$, PS0, $I_O = 3A$, $R_{LL} = 10.3m\Omega$

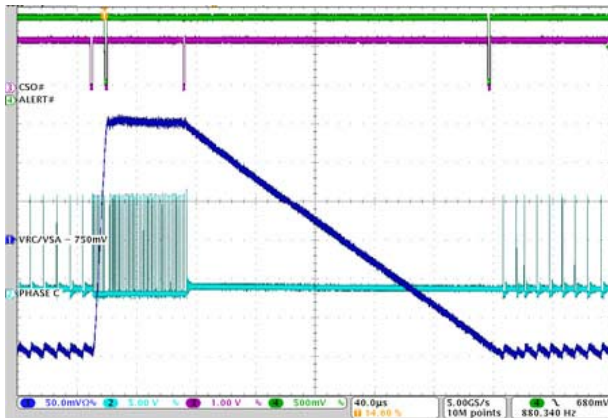


Figure 55. VSA/VR C SetVID_fast, 0.6V to 0.9V, PS0, SetVID_decay, 0.9V to 0.6V, $I_O = 200\text{mA}$, $R_{LL} = 10.3\text{m}\Omega$

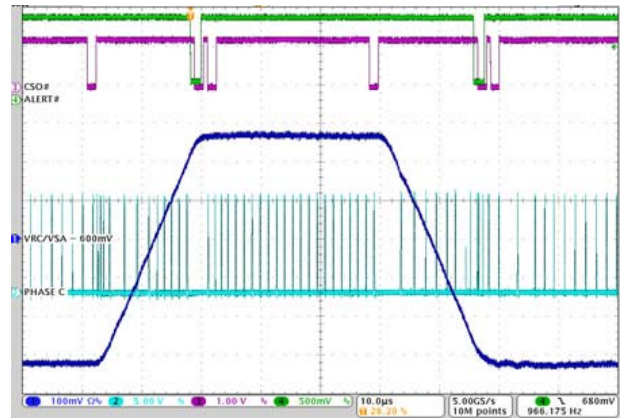


Figure 56. VSA/VR C SetVID_fast, 0.3V to 0.9V to 0.3V, PS1, $I_O = 3\text{A}$, $R_{LL} = 10.3\text{m}\Omega$

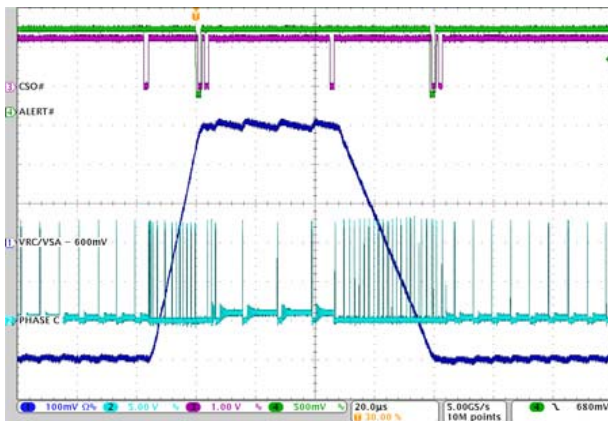


Figure 57. VSA/VR C SetVID_fast, 0.3V to 0.9V, SetVID_slow to 0.3V, PS2, $I_O = 200\text{mA}$, $R_{LL} = 10.3\text{m}\Omega$

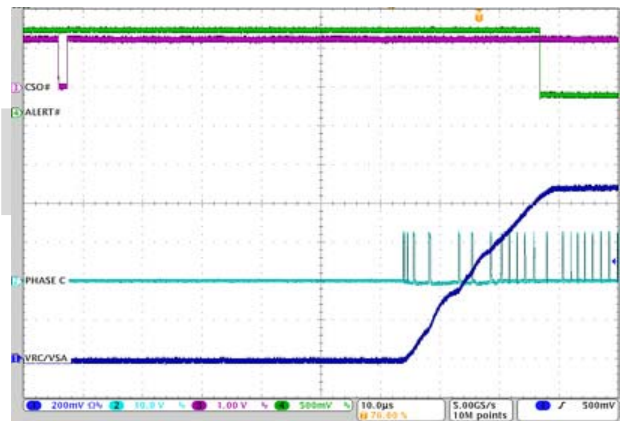


Figure 58. VSA/VR C PS4 Exit, SetVID_fast 0.9V, PS0, $I_O = 0\text{A}$, $R_{LL} = 10.3\text{m}\Omega$

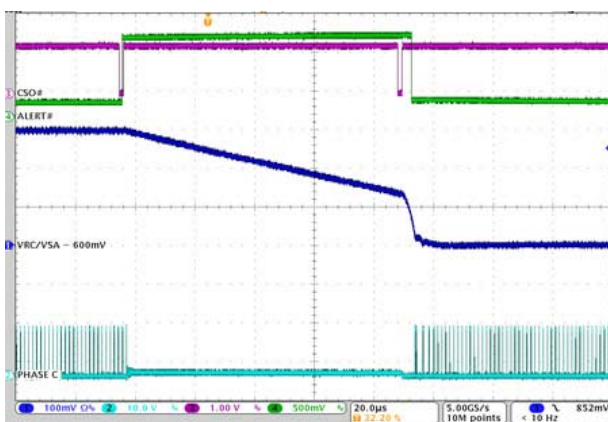


Figure 59. VSA/VR C SetVID_decay 0.9V to 0.3V, Pre-Empted Downward by SetVID_fast 0.6V, $I_O = 250\text{mA}$, $R_{LL} = 10.3\text{m}\Omega$

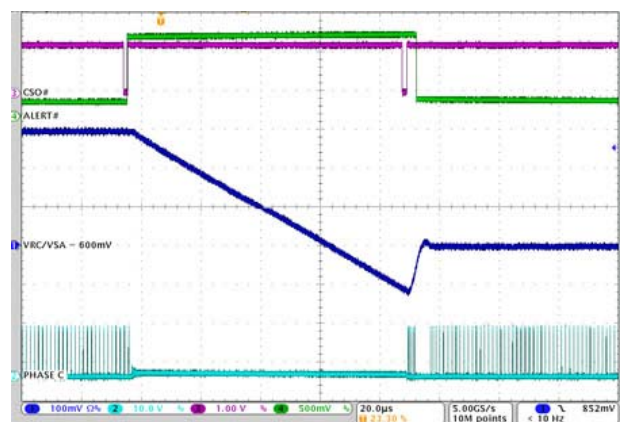


Figure 60. VSA/VR C SetVID_decay 0.9V to 0.3V, Pre-Empted Upward by SetVID_fast 0.6V, $I_O = 650\text{mA}$, $R_{LL} = 10.3\text{m}\Omega$

6. Theory of Operation

The ISL95859C is a three output, multiphase controller supporting Intel IMVP8 microprocessor Core (IA), Graphics (GT), and System Agent (SA), or GTUS rails. The controller supports single-phase operation on outputs VR A and VR C. Voltage regulator VR B supports 1- or 2-phase operation. The ISL95859C is compliant to Intel IMVP8 specifications with SerialVID features. The system parameters and SVID required registers are programmable through 2 dedicated programming pins. This greatly simplifies the system design for various platforms and lowers inventory complexity and cost by using a single device. The “Typical Application Circuits” section beginning on [page 14](#) provides a top level view of configuring all three outputs using the ISL95859C controller.

6.1 R3 Modulator

The R3 modulator is Intersil’s proprietary synthetic current-mode hysteretic controller which blends both fixed frequency PWM and variable frequency hysteretic control technologies. This modulator topology offers high noise immunity and a rapid transient response to dynamic load scenarios. Under static conditions the desired switching frequency is maintained within the entire specified range of input voltages, output voltages and load currents. During load transients the controller will increase or decrease the PWM pulses and switching frequency to maintain output voltage regulation. [Figure 61](#) illustrates this effect during a load insertion. As the window voltage starts to climb from a load step, the time between PWM pulses decreases as f_{SW} increases to keep the output within regulation.

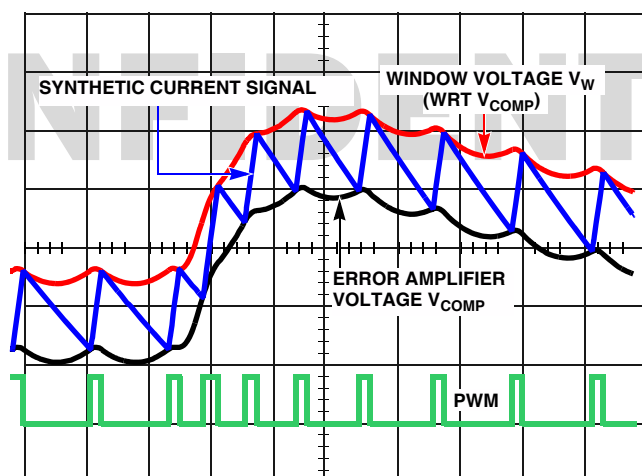


Figure 61. Modulator Waveforms During Load Transient

6.2 Multiphase Power Conversion

Microprocessor load current profiles have changed to the point that the advantages of multiphase power conversion are impossible to ignore. Multiphase converters overcome the daunting technical challenges in producing a cost-effective and thermally viable single-phase converter at the high Thermal Design Current (TDC) levels. The ISL95859C controller VR B output reduces the complexity of multiphase implementation by integrating vital functions and requiring minimal output components.

6.2.1 Interleaving

The switching of each channel in a multiphase converter is timed to be symmetrically out-of-phase with the other channels. For the example of a 3-phase converter, each channel switches 1/3 cycle after the previous channel and 1/3 cycle before the following channel. As a result, the 3-phase converter has a combined ripple frequency 3x that of the ripple frequency of any one phase, as illustrated in [Figure 62](#). The three channel currents (I_{L1} , I_{L2} , and I_{L3}) combine to form the AC ripple current and to supply the DC load current.

The ripple current of a multiphase converter is less than that of a single-phase converter supplying the same load. To understand why, examine [Equation 1](#), which represents an individual channel's peak-to-peak inductor current.

$$(EQ. 1) \quad I_{P-P} = \frac{(V_{IN} - V_{OUT}) \cdot V_{OUT}}{L \cdot f_{SW} \cdot V_{IN}}$$

In [Equation 1](#), V_{IN} and V_{OUT} are the input and output voltages respectively, L is the single-channel inductor value, and f_{SW} is the switching frequency.

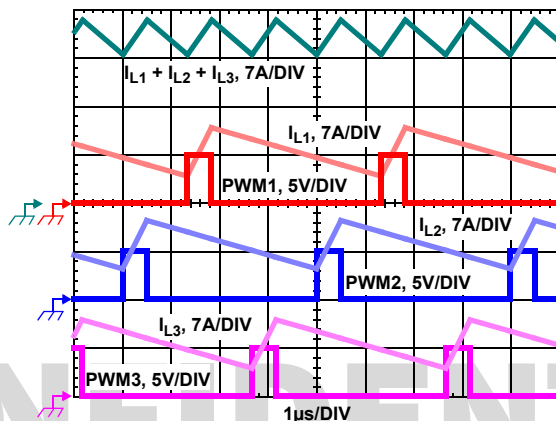


Figure 62. PWM and Inductor-Current Waveforms for 3-Phase Converter

In a multiphase converter, the output capacitor current is the superposition of the ripple currents from each of the individual phases. Compare [Equation 1](#) to the expression for the peak-to-peak current after the summation of N (symmetrically phase-shifted inductor currents) in [Equation 2](#). The peak-to-peak overall ripple current ($I_{C(P-P)}$) decreases with the increase in the number of channels, as shown in [Figure 63](#), which introduces the concept of the Ripple Current Multiplier (K_{RCM}). At the steady state duty cycles for which the ripple current and thus the K_{RCM} is zero, the turn-off of one phase corresponds exactly with the turn-on of another phase, resulting in the sum of all phase currents being always the (constant) load current and therefore there is no ripple current in this case.

The output voltage ripple is a function of capacitance, capacitor Equivalent Series Resistance (ESR), and the summed inductor ripple current. Increased ripple frequency and lower ripple amplitude allow the designer to use lower saturation-current inductors and fewer or less costly output capacitors for any performance specification.

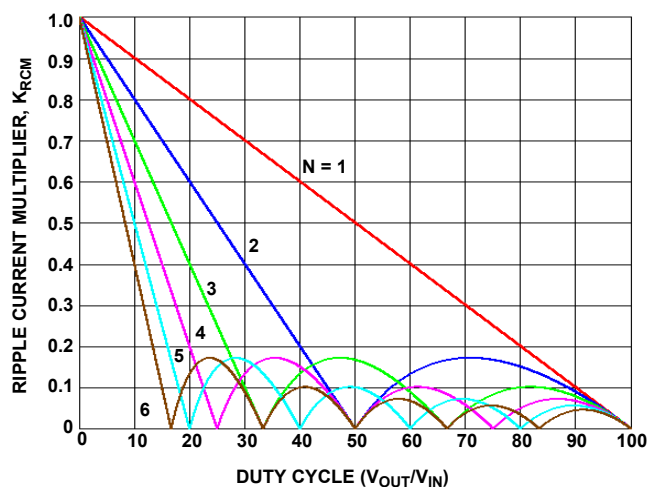


Figure 63. Ripple Current Multiplier vs Duty Cycle

$$I_{C(P-P)} = \frac{V_{OUT}}{L \cdot f_{SW}} K_{RCM}$$

(EQ. 2)

$$K_{RCM} = \frac{(N \cdot D - m + 1) \cdot (m - (N \cdot D))}{N \cdot D}$$

for

$$m - 1 \leq N \cdot D \leq m$$

$$m = \text{ROUNDUP}(N \cdot D, 0)$$

Another benefit of interleaving is to reduce the input ripple current. Input capacitance is determined in part by the maximum input ripple current. Multiphase topologies can improve overall system cost and size by lowering input ripple current and allowing the designer to reduce the cost of input capacitors. Figure 64 illustrates input currents from a 3-phase converter combining to reduce the total input ripple current.

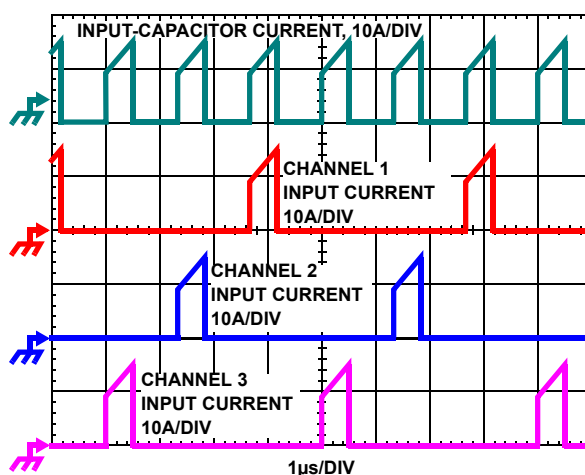


Figure 64. Channel Input Currents and Input-Capacitor RMS Current for 3-phase Converter

The converter depicted in Figure 64 delivers 36A to a 1.5V load from a 12V input. The RMS input capacitor current is 5.9A. Compare this to a single-phase converter also stepping down 12V to 1.5V at 36A. The single-phase converter has 11.9A_{RMS} input capacitor current. The single-phase converter must use an input capacitor bank with twice the RMS current capacity as the equivalent 3-phase converter.

A more detailed explanation of input capacitor design is provided in [“Input Capacitor Selection” on page 37](#).

6.2.2 Multiphase R3 Modulator

The Intersil ISL95859C VR B output uses the patented R3 (Robust Ripple Regulator) modulator. The R3 modulator combines the best features of fixed frequency PWM and hysteretic PWM while eliminating many of their shortcomings. [Figure 65](#) shows the conceptual multiphase R3 modulator circuit and [Figure 66 on page 27](#) illustrates the operational principles.

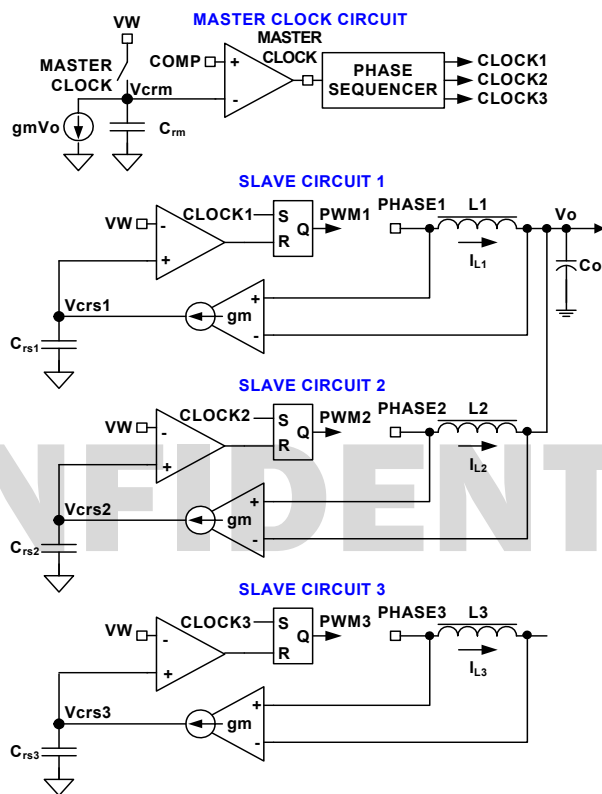


Figure 65. R3 Modulator Circuit

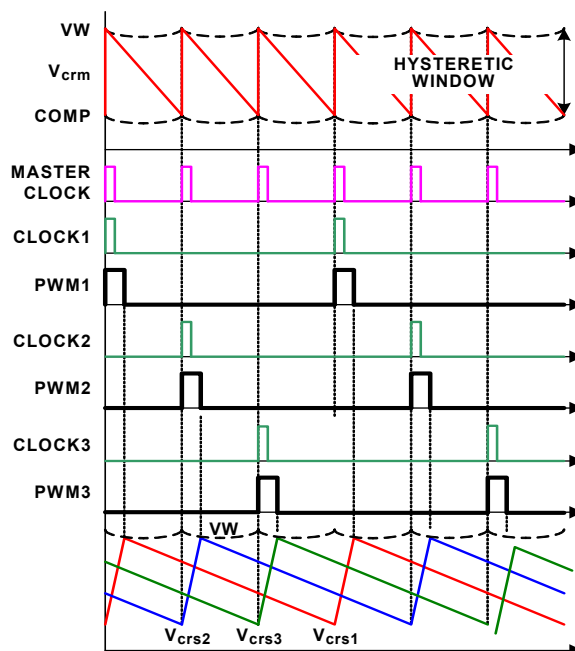


Figure 66. R3 Modulator Operation Principles in Steady State

The internal modulator uses a master clock circuit to generate the clocks for the slave circuits, one per phase. The R3™ modulator master oscillator slews between two voltage signals; the COMP voltage (the output of the voltage sense error amplifier, assuming the topology of [Figure 76 on page 43](#)) and VW (Voltage Window), a voltage positively offset from COMP by an offset voltage that is dependent on the nominal switching frequency. The modulator discharges the master clock ripple capacitor C_{rm} with a current source equal to $g_m V_o$, where g_m is a gain factor, dependent on the nominal switching frequency and also on the number of active phases. The C_{rm} voltage V_{erm} is a sawtooth waveform traversing between the VW and COMP voltages. It resets (charges quickly) to VW when it discharges (with discharge current $g_m V_o$) to COMP and generates a one-shot master clock signal. A phase sequencer distributes the master clock signal to the active slave circuits. For example, if the conceptual VR is in 4-phase mode, the master clock signal is distributed to the four phases 90° out-of-phase, in 3-phase mode distributed to the three phases 120° out-of-phase, and in 2-phase mode distributed to Phases 1 and 2 180° out-of-phase. If VR is in 1-phase mode, the master clock signal is distributed to Phase 1 only and is the Clock1 signal.

Each slave circuit has its own ripple capacitor C_{rsn} , whose voltage mimics the inductor ripple current. A g_m amplifier converts the inductor voltage (or alternatively, series sense resistor voltage, indicative of that phase's inductor current) into a current source to charge and discharge C_{rsn} . The slave circuit turns on its PWM pulse upon receiving its respective clock signal $Clock_n$ and the current source charges C_{rsn} with a current proportional to its respective positive inductor voltage. When the C_{rsn} voltage (V_{Crsn}) rises to VW, the slave circuit turns off the PWM pulse and the current source then discharges C_{rsn} , with a current proportional to its respective now-negative inductor voltage. C_{rsn} discharges until the next $Clock_n$ pulse and the cycle repeats.

Because the modulator works with the V_{crsn} , which are large-amplitude and noise-free synthesized signals, it achieves lower phase jitter than conventional hysteretic mode and fixed PWM mode controllers. Unlike conventional hysteretic mode converters, the ISL95859C uses an error amplifier that allows the controller outputs to maintain a 0.5% output voltage accuracy.

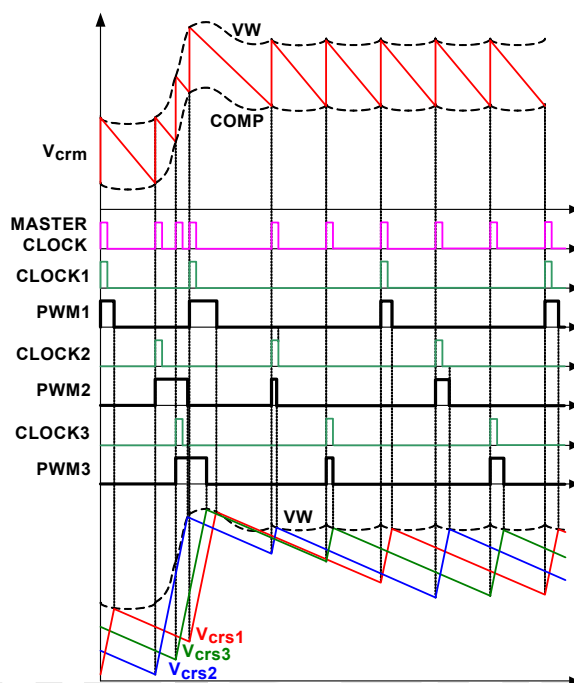


Figure 67. R3 Modulator Operation Principles in Load Insertion Response

Figure 67 illustrates the operational principles during load insertion response. The COMP voltage rises during load insertion (due to the sudden discharge of the output capacitor driving the inverting input of the error amplifier), generating the master clock signal more quickly. Thus, the PWM pulses turn on earlier, increasing the effective switching frequency. This phenomenon allows for higher control loop bandwidth than conventional fixed frequency PWM controllers. The VW voltage rises with the COMP voltage, making the PWM on-time pulses wider. During load release response, the COMP voltage falls. It takes the master clock circuit longer to generate the next master clock signal so the PWM pulse is held off until needed. The VW voltage falls with the COMP voltage, reducing the current PWM pulse width. The inherent pulse frequency and width increase due to an increasing load transient. Likewise, the pulse frequency and width reductions due to a decreasing load transient produce the excellent load transient response of the R3 modulator.

Because all phases share the same VW window (master clock frequency generator) and threshold (slave pulse width generator) voltage, dynamic current balance among phases is inherently ensured for the duration of any load transient event.

The R3 modulator intrinsically has input voltage feed-forward control, due to the proportional dependence of the clock generator slave transconductance gains on the input voltage. This dependence decreases the on-time pulse-width of each phase in proportion to an increase in input voltage, making the output voltage insensitive to a fast slew rate input voltage change.

6.3 Diode Emulation and Period Stretching

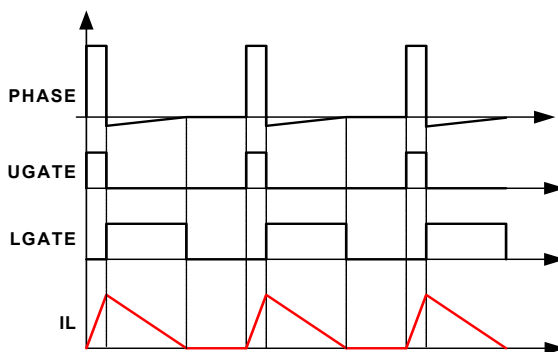


Figure 68. Diode Emulation

The ISL95859C can operate each of its three rails in Diode Emulation Mode (DEM) to improve light-load efficiency. Diode emulation is enabled in PS2 and PS3 power states. In DEM, the low-side MOSFET conducts while the current is flowing from source-to-drain and blocks reverse current, emulating a diode. [Figure 68](#) illustrates that, when LGATE is on, the low-side MOSFET carries current, creating negative voltage on the phase node due to the voltage drop across the ON-resistance. The controller monitors the inductor current by monitoring the phase node voltage. It turns off LGATE when the phase node voltage reaches zero to prevent the inductor current from reversing the direction and creating unnecessary power loss.

If the load current is light enough, as [Figure 68](#) illustrates, the inductor current will reach and stay at zero before the next phase node pulse and the regulator is in Discontinuous Conduction Mode (DCM). If the load current is heavy enough, the inductor current will never reach 0A and the regulator will appear to operate in Continuous Conduction Mode (CCM), although the controller is nevertheless configured for DEM.

[Figure 69](#) shows the operation principle in DEM at light load. The load gets incrementally lighter in the three cases from top to bottom. The PWM on-time is determined by the VW window size, making the inductor current triangle the same in the three cases (only the time between inductor current triangles changes). The controller clamps the ripple capacitor voltage V_{crs} in DEM to make it mimic the inductor current. It takes the COMP voltage longer to hit V_{crm} , which produces master clock pulses, naturally stretching the switching period. The inductor current triangles move further apart from each other such that the inductor current average value is equal to the load current. The reduced switching frequency improves light-load efficiency.

Because the next clock pulse occurs when V_{COMP} (which tracks output voltage error) rises above V_{CRM} , DEM switching pulse frequency is responsive to load transient events in a manner similar to that of the multiphase CCM operation.

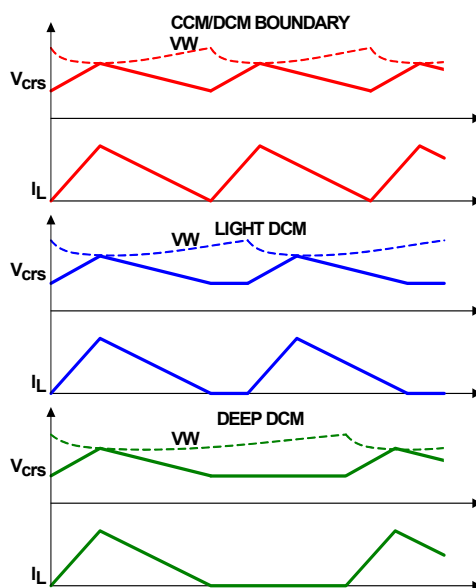


Figure 69. Period Stretching

6.4 Adaptive Body Diode Conduction Time Reduction

When in DCM, the controller ideally turns off the low-side MOSFET when the inductor current approaches zero. During on-time of the low-side MOSFET, phase voltage is negative, due to the product of the (negative) inductor current and the low-side MOSFET $r_{DS(ON)}$, producing a voltage drop that is proportional to the inductor current. A phase comparator inside the controller monitors the phase voltage during on-time of the low-side MOSFET and compares it with a threshold to determine the zero-crossing point of the inductor current. If the inductor current has not reached zero when the low-side MOSFET turns off, it will flow through the low-side MOSFET body diode, causing the phase node to have a larger voltage drop until it decays to zero. If the inductor current has crossed zero and reversed the direction when the low-side MOSFET turns off, it will flow through the high-side MOSFET body diode, causing the phase node to have a positive voltage spike (to V_{IN} plus a PN diode voltage drop) until the current decays to zero. The controller continues monitoring the phase voltage after turning off the low-side MOSFET and adjusts the phase comparator threshold voltage accordingly in iterative steps such that the low-side MOSFET body diode conducts for approximately 40ns (turning off 40ns before the inductor current zero-crossing) to minimize the body diode-related loss.

6.5 Modes of Operation

The ISL95859C controller supports three voltage regulator outputs and each output is configured independently. VR A and VR C are single-phase only regulators while VR B can support 2-phase or single-phase operation.

6.5.1 VR A Configuration and operation

Voltage Regulator A (VR A) operates only as a single-phase regulator. It operates in 1-phase CCM in PS0 and PS1 and enters 1-phase DEM in PS2 and PS3. The overcurrent protection level is the same for all power states as shown in [Table 1](#).

Table 1. VR Modes of Operation VR C

Power States	Mode	OCP Threshold (μA)
0	1-phase CCM	60
1		
2	1-phase DE	
3		

6.5.2 VR B Configuration and operation

Voltage Regulator B (VR B) can be configured for 2- or 1-phase operation. [Table 2](#) shows the VR B configurations and operational modes, programmed by the ISEN2_B and ISEN1_B pin connections and by the Power State (PS) command (SVID Register 32h). When configured for a 2-phase operation, the ISEN pins must be connected through a low-pass filter to their respective PHASE node at the output inductor. For a 1-phase configuration, tie both ISEN1_B and ISEN2_B to VCC. Phases are disabled in order, starting with the highest numbered phase, as follows.

Table 2. VR Modes of Operation VR B

ISEN2_B	Configuration	PS	Mode	OCP Threshold (μA)
To Power Stage	2-phase VR B Configuration	0	2-phase CCM	60
		1	1-phase CCM	30
		2	1-phase DE	
		3		
Tied to VCC (+5V)	1-phase VR B Configuration	0	1-phase CCM	60
	ISEN1_B open or tied to VCC (+5V)	1	1-phase DE	
		2		
		3		

In a 2-phase configuration, all phases are active and the ISEN2_B and ISEN1_B pins are connected to their associated PHASE nodes. For a 1-phase configuration, tie the ISEN2_B pin to VCC (+5V) and connect ISEN1_B to VCC (+5V) or leave it open.

In a 2-phase configuration, VR B operates in 2-phase CCM in PS0. It enters 1-phase mode in PS1, PS2, and PS3 by dropping Phase 2 and reducing the overcurrent protection level to 1/2 of the initial value. PS1 operates in CCM and PS2 and PS3 operate in DEM.

In a 1-phase configuration, VR A operates in 1-phase CCM in PS0 and PS1, and enters 1-phase DEM in PS2 and PS3. The overcurrent protection level is the same for all power states.

6.5.3 VR C Operation

Voltage Regulator C (VR C) supports 1-phase operation only. It operates in 1-phase CCM in PS0 and PS1 and enters 1-phase DEM in PS2 and PS3. The overcurrent protection level is the same for all power states as shown in [Table 3](#).

Table 3. VR Modes of Operation VR C

Power States	Mode	OCP Threshold (μA)
0	1-phase CCM	60
1		
2	1-phase DE	
3		

6.5.4 Disabling outputs

Each of the ISL95859C outputs is disabled by connecting the ISUMN_x pin of the voltage regulator to +5V. The controller will not acknowledge SVID communication to a disabled channel.

6.6 Programming Resistors

Two programming resistors (R_{PROG1} and R_{PROG2}) configure the ISL95859C. [Table 4](#) shows how to select R_{PROG1} to set the common switching frequency for the VR A and VR B outputs. The switching frequency options are 450kHz, 583kHz, and 750kHz. This provides flexibility in optimizing the regulators for a wide array of solutions.

R_{PROG1} also sets the $I_{\text{CC(MAX)}}$ register value for all three VRs. The $I_{\text{CC(MAX)}}$ register value determines the maximum current each VR can support. The CPU will read the individual VR $I_{\text{CC(MAX)}}$ register value and ensure that the VR current does not exceed the value specified.

Table 4. PROG1 Pin

Typical PROG1 Resistor ($\pm 1\%$, K Ω)	VR A and VR B Switching Frequency f_{sw} (kHz)	IMAX				
		VR A	VR B			VR C
		IA/GT 1-ph (A)	IA/GT 1-ph (A)	IA/GT 2-ph (A)	GTUS (A)	SA or GTUS (A)
1.87	450	21	24	40	18	18
5.62	450	30	30	60	20	20
9.31	450	33	35	40	18	18
13.3	450	34	35	67	18	18
16.9	450	35	40	70	20	20
20.5	450	40	40	75	25	25
24.3	583	21	24	40	18	18
28.0	583	30	30	60	20	20
34.0	583	33	35	40	18	18
41.2	583	34	35	67	18	18
48.7	583	35	40	70	20	20
56.2	583	40	40	75	25	25
63.4	750	21	24	40	18	18
71.5	750	30	30	60	20	20
78.7	750	33	35	40	18	18
88.7	750	34	35	67	18	18
100	750	35	40	70	20	20
110	750	40	40	75	25	25

R_{PROG2} sets the address registers for all three VRs (VR A, VR B, and VR C) on the ISL95859C. The three controller outputs can be configured to support three of the four potential processor rails required. The address selections include Core (IA), Graphics slice (GT), Graphics Unslice (GTUS), and System Agent (SA) rails of the Intel IMVP8™ processor. The selection should be based on the TDC requirements of the rail and the number of phases required to support the overall current. Processor SKUs require support for all four processor rails, and the ISL95859C can be used with the ISL95853 to support them all (see [Table 5](#)).

R_{PROG2} also selects the switching frequency for VR C. The switching frequency options are 450kHz, 583kHz, and 750kHz. This provides flexibility in optimizing the regulators for a wide array of solutions.

Table 5. PROG2 Pin

Typical PROG2 Resistor ($\pm 1\%$, k Ω)	Address Selection			VR C Switching Frequency f_{sw} (kHz)
	VR A	VR B	VR C	
1.87	GT[01h]	IA [00h]	SA [02h]	450
5.62	GT[01h]	IA [00h]	SA [02h]	583
9.31	GT[01h]	IA [00h]	SA [02h]	750
20.5	GT[01h]	IA [00h]	GTUS [03h]	450

Table 5. PROG2 Pin (Continued)

Typical PROG2 Resistor ($\pm 1\%$, k Ω)	Address Selection			VR C Switching Frequency f_{sw} (kHz)
	VR A	VR B	VR C	
24.3	GT[01h]	IA [00h]	GTUS [03h]	583
28.0	GT[01h]	IA [00h]	GTUS [03h]	750
48.7	IA [00h]	GT[01h]	SA [02h]	450
56.2	IA [00h]	GT[01h]	SA [02h]	583
63.4	IA [00h]	GT[01h]	SA [02h]	750
88.7	IA [00h]	GT[01h]	GTUS [03h]	450
100	IA [00h]	GT[01h]	GTUS [03h]	583
110	IA [00h]	GT[01h]	GTUS [03h]	750
150	IA [00h]	GTUS [03h]]	SA [02h]	450
165	IA [00h]	GTUS [03h]]	SA [02h]	583
182	IA [00h]	GTUS [03h]]	SA [02h]	750

6.6.1 Switching Frequency Selection

There are a number of variables to consider when choosing switching frequency, as there are considerable effects on the upper MOSFET loss calculation. These effects are outlined in [“MOSFETs” on page 34](#) and they establish the upper limit for the switching frequency. The lower limit is established by the requirement for fast transient response and small output voltage ripple as outlined in [“Output Filter Design” on page 36](#). Choose the lowest switching frequency that allows the regulator to meet the transient-response and output voltage ripple requirements.

The resistors from PROG1 and PROG2 to GND select one of three available switching frequencies: 450kHz, 583kHz, and 750kHz. Note that when the ISL95859C is in Continuous Conduction Mode (CCM), the switching frequency is not strictly constant due to the nature of the R3 modulator. As explained in [“Multiphase R3 Modulator” on page 26](#), the effective switching frequency will increase during load insertion and will decrease during load release to achieve fast response. However, the switching frequency is nearly constant at constant load. Variation is expected when the power stage condition, such as input voltage, output voltage, load, etc. changes. The variation is usually less than 15% and does not have any significant effect on output voltage ripple magnitude.

6.7 PSYS System Power Monitoring

In an IMVP8 system the PSYS signal monitors the total system input power from either the battery or adapter. When implemented according to Intel's specifications, the PSYS voltage is a 1.2V full-scale analog signal sent into the PSYS pin of the ISL95859C. The PSYS signal is then digitized and sent to the CPU over the SVID Bus.

This pin is designed to be used in conjunction with Intersil battery chargers. The full-scale current sent to the ISL95859C PSYS pin from the charger IC should be scaled to a 1.2V full-scale voltage using the appropriate resistor from the PSYS pin to GND.

7. General Design Guide

This design guide provides a high-level explanation of the steps necessary to design a multiphase power converter. It is assumed that the reader is familiar with many of the basic skills and techniques referenced in the following. In addition to this guide, Intersil provides complete reference designs, which include schematics, bills of materials, and example board layouts for common microprocessor applications.

7.1 Power Stages

The first step in designing a multiphase converter is to determine the number of phases. This determination depends heavily upon the cost analysis, which in turn depends on system constraints that differ from one design to the next. Principally, the designer is concerned with whether components can be mounted on both sides of the circuit board, whether through-hole components are permitted, and the total board space available for power supply circuitry. Generally speaking, the most economical solutions are those in which each phase handles between 15A and 25A. In cases where board space is the limiting constraint, current can be pushed as high as 40A per phase, but these designs require heatsinks and forced air to cool the MOSFETs, inductors, and heat-dissipating surfaces.

7.1.1 MOSFETs

MOSFET choice depends on the current each MOSFET is required to conduct, the switching frequency, the capability of the MOSFETs to dissipate heat and the availability and nature of heatsinking and air flow.

7.1.1.1 Lower MOSFET Power Calculation

The calculation for heat dissipated in the lower (alternatively called low-side) MOSFET of each phase is simple, because virtually all of the heat loss in the lower MOSFET is due to current conducted through the channel resistance ($r_{DS(ON)}$). In [Equation 3](#), I_M is the maximum continuous output current; I_{P-P} is the peak-to-peak inductor current per phase (see [Equation 1 on page 24](#)); d is the duty cycle (V_{OUT}/V_{IN}); and L is the per-channel inductance. [Equation 3](#) shows the approximation.

$$(EQ. 3) \quad P_{LOW,1} = r_{DS(ON)} \left[\frac{I_M^2}{N} + \frac{I_{P-P}^2}{12} \right] \cdot (1 - d)$$

A term can be added to the lower MOSFET loss equation to account for the loss during the dead time when inductor current is flowing through the lower MOSFET body diode. This term is dependent on the diode forward voltage at I_M , $V_{D(ON)}$; the switching frequency, f_{SW} ; and the length of dead times (t_{d1} and t_{d2}) at the beginning and end of the lower MOSFET conduction interval, respectively.

$$(EQ. 4) \quad P_{LOW,2} = V_{D(ON)} f_{SW} \left[\left(\frac{I_M}{N} - \frac{I_{P-P}}{2} \right) t_{d1} + \left(\frac{I_M}{N} - \frac{I_{P-P}}{2} \right) t_{d2} \right]$$

Finally, the power loss of output capacitance of the lower MOSFET is approximated in [Equation 5](#):

$$(EQ. 5) \quad P_{LOW,3} \approx \frac{2}{3} \cdot V_{IN}^{1.5} \cdot C_{OSS_LOW} \cdot \sqrt{V_{DS_LOW}} \cdot f_{SW}$$

where C_{OSS_LOW} is the output capacitance of the lower MOSFET at the test voltage of V_{DS_LOW} . Depending on the amount of ringing, the actual power dissipation is slightly higher than this.

Thus, the total maximum power dissipated in each lower MOSFET is approximated by the summation of $P_{LOW,1}$, $P_{LOW,2}$ and $P_{LOW,3}$.

7.1.1.2 Upper MOSFET Power Calculation

In addition to $r_{DS(ON)}$ losses, a large portion of the upper MOSFET losses are due to currents conducted across the input voltage (V_{IN}) during switching. Because a substantially higher portion of the upper MOSFET losses are dependent on switching frequency, the power calculation is more complex. Upper MOSFET losses are divided

into separate components involving the upper MOSFET switching times, the lower MOSFET body-diode reverse-recovery charge Q_{rr} , and the upper MOSFET $r_{DS(ON)}$ conduction loss.

When the upper MOSFET turns off, the lower MOSFET does not conduct any portion of the inductor current until the voltage at the phase node falls below ground. When the lower MOSFET begins conducting, the current in the upper MOSFET falls to zero as the current in the lower MOSFET ramps up to assume the full inductor current. In [Equation 6](#), the required time for this commutation is t_1 and the approximated associated power loss is $P_{UP(1)}$.

$$(EQ. 6) \quad P_{UP(1)} \approx V_{IN} \left(\frac{I_M}{N} + \frac{I_{P-P}}{2} \right) \left(\frac{t_1}{2} \right) f_{SW}$$

At turn on, the upper MOSFET begins to conduct and this transition occurs over a time (t_2). In [Equation 7](#), the approximate power loss is $P_{UP(2)}$.

$$(EQ. 7) \quad P_{UP(2)} \approx V_{IN} \left(\frac{I_M}{N} - \frac{I_{P-P}}{2} \right) \left(\frac{t_2}{2} \right) f_{SW}$$

A third component involves the lower MOSFET's reverse-recovery charge, Q_{rr} . Because the inductor current has fully commutated to the upper MOSFET before the lower MOSFET's body diode can draw all of Q_{rr} , it is conducted through the upper MOSFET across V_{IN} . The power dissipated as a result is $P_{UP(3)}$ and is approximated in [Equation 8](#).

$$(EQ. 8) \quad P_{UP(3)} = V_{IN} Q_{rr} f_{SW}$$

The resistive part of the upper MOSFET is given in [Equation 9](#) as $P_{UP(4)}$.

$$(EQ. 9) \quad P_{UP(4)} \approx r_{DS(ON)} \left[\left(\frac{I_M}{N} \right)^2 + \frac{I_{P-P}^2}{12} \right] \cdot d$$

[Equation 10](#) accounts for some power loss due to the drain-to-source parasitic inductance (L_{DS} , including PCB parasitic inductance) of the upper MOSFET, although it is not exact:

$$(EQ. 10) \quad P_{UP(5)} \approx L_{DS} \left(\frac{I_M}{N} + \frac{I_{P-P}}{2} \right)^2 f_{SW}$$

Finally, the power loss of output capacitance of the upper MOSFET is approximated in [Equation 11](#):

$$(EQ. 11) \quad P_{UP(6)} \approx \frac{2}{3} \cdot V_{IN}^{1.5} \cdot C_{OSS_UP} \cdot \sqrt{V_{DS_UP}} \cdot f_{SW}$$

where C_{OSS_UP} is the output capacitance of the lower MOSFET at the V_{DS_UP} test voltage. Depending on the amount of ringing, the actual power dissipation is slightly higher than this.

The total power dissipated by the upper MOSFET at full load can now be approximated as the summation of the results from [Equations 6](#) through [11](#). Because the power equations depend on MOSFET parameters, choosing the correct MOSFET is an iterative process involving repetitive solutions to the loss equations for different MOSFETs and different switching frequencies.

7.1.2 Driver Selection

The three voltage regulator outputs of the ISL95859C all feature PWM signals to drive external MOSFET drivers. Based on the PS4 low quiescent current requirements of the Intel IMVP8 system, only the Intersil ISL95808 driver or similar device is supported by the controller.

7.2 Output Filter Design

The output inductors and the output capacitor bank together to form a low-pass filter that smooths the pulsating voltage at the phase nodes. The output filter also must provide the transient energy until the regulator can respond. Because it has a low bandwidth compared to the switching frequency, the output filter necessarily limits the system transient response. The output capacitor must supply or sink load current while the current in the output inductors increases or decreases to meet the demand.

In high-speed converters, the output capacitor bank is usually the most costly (and often the largest) part of the circuit. Output filter design begins with minimizing the cost of this part of the circuit. The critical load parameters in choosing the output capacitors are the maximum size of the load step, ΔI ; the load-current slew rate, di/dt and the maximum allowable output voltage deviation under transient loading, ΔV_{MAX} . Capacitors are characterized according to their capacitance, Equivalent Series Resistance (ESR) and Equivalent Series Inductance (ESL).

At the beginning of the load transient, the output capacitors supply all of the transient current. The output voltage will initially deviate by an amount approximated by the voltage drop across the ESL. As the load current increases, the voltage drop across the ESR increases linearly until the load current reaches its final value. The capacitors selected must have sufficiently low ESL and ESR so that the total output voltage deviation is less than the allowable maximum. Neglecting the contribution of inductor current and regulator response, the output voltage initially deviates by an amount, as shown in [Equation 12](#):

$$(EQ. 12) \quad \Delta V \approx (ESL) \frac{di}{dt} + (ESR) \Delta I$$

The filter capacitor must have sufficiently low ESL and ESR so that $\Delta V < \Delta V_{MAX}$.

Most capacitor solutions rely on a mixture of high-frequency capacitors with relatively low capacitance in combination with bulk capacitors having high capacitance but limited high-frequency performance. Minimizing the ESL of the high-frequency capacitors allows them to support the output voltage as the current increases.

Minimizing the ESR of the bulk capacitors allows them to supply the increased current with less output voltage deviation.

The ESR of the bulk capacitors also creates the majority of the output voltage ripple. As the bulk capacitors sink and source the inductor AC ripple current (see [“Interleaving” on page 23](#) and [Equation 2 on page 25](#)), a voltage develops across the bulk-capacitor ESR equal to $I_{C(P-P)} (ESR)$. Thus, when the output capacitors are selected, the maximum allowable ripple voltage, $V_{P-P(MAX)}$, determines a lower limit on the inductance as shown in [Equation 13](#).

$$(EQ. 13) \quad L \geq ESR \cdot \frac{V_{OUT} \cdot K_{RCM}}{f_{SW} \cdot V_{IN} \cdot V_{P-P(MAX)}}$$

Because the capacitors are supplying a decreasing portion of the load current while the regulator recovers from the transient, the capacitor voltage becomes slightly depleted. The output inductors must be capable of assuming the entire load current before the output voltage decreases more than ΔV_{MAX} . This places an upper limit on inductance.

[Equation 14](#) gives the upper limit on L for the cases when the trailing edge of the current transient causes a greater output-voltage deviation than the leading edge. [Equation 15](#) addresses the leading edge. Normally, the trailing edge dictates the selection of L because duty cycles are usually less than 50%. Nevertheless, both inequalities should be evaluated and L should be selected based on the lower of the two results. In each equation, L is the per-channel inductance, C is the total output capacitance, and N is the number of active channels.

$$(EQ. 14) \quad L \leq \frac{2 \cdot N \cdot C \cdot V_{OUT}}{(\Delta I)^2} [\Delta V_{MAX} - \Delta I \cdot ESR]$$

$$(EQ. 15) \quad L \leq \frac{1.25 \cdot N \cdot C}{(\Delta I)^2} [\Delta V_{MAX} - \Delta I \cdot ESR] (V_{IN} - V_{OUT})$$

7.3 Input Capacitor Selection

The input capacitors are responsible for sourcing the AC component of the input current flowing into the upper MOSFETs. Their RMS current capacity must be sufficient to handle the AC component of the current drawn by the upper MOSFETs, which is related to duty cycle and the number of active phases. The input RMS current is calculated with [Equation 16](#).

$$(EQ. 16) \quad I_{IN(RMS)} = \sqrt{K_{IN(CM)}^2 \cdot I_O^2 + K_{RAMP(CM)}^2 \cdot I_{Lo(P-P)}^2}$$

$$(EQ. 17) \quad K_{IN(CM)} = \sqrt{\frac{(N \cdot D - m + 1) \cdot (m - N \cdot D)}{N^2}}$$

$$(EQ. 18) \quad K_{RAMP(CM)} = \sqrt{\frac{m^2(N \cdot D - m + 1)^3 + (m - 1)^2(m - N \cdot D)^3}{12N^2D^2}}$$

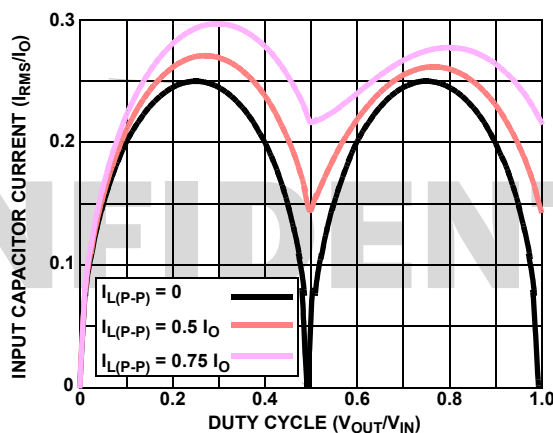


Figure 70. Normalized Input Capacitor RMS Current Vs Duty Cycle for 2-Phase Converter

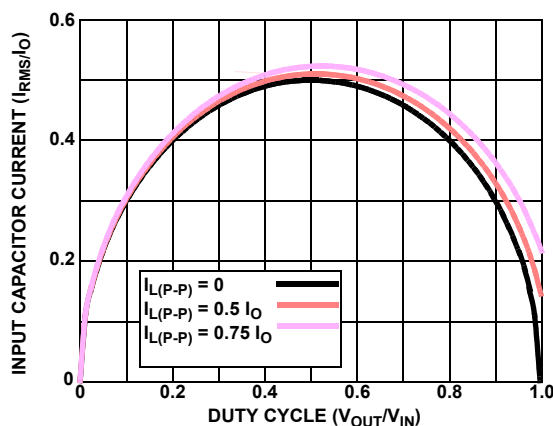


Figure 71. Normalized Input Capacitor RMS Current vs Duty Cycle for Single-Phase Converter

For a 2-phase design, use [Figure 70 on page 37](#) to determine the input capacitor RMS current requirement given the duty cycle, maximum sustained output current (I_O), and the ratio of the per-phase peak-to-peak inductor current ($I_{L(P-P)}$) to I_O . Select a bulk capacitor with a ripple current rating that will minimize the total number of input capacitors required to support the RMS current calculated. The voltage rating of the capacitors should also be at least 1.25x greater than the maximum input voltage.

For 1-phase designs, use [Figure 71 on page 37](#). Use the same approach to selecting the bulk capacitor type and number as previously described.

Low capacitance, high-frequency ceramic capacitors are needed in addition to the bulk capacitors to suppress leading and falling edge voltage spikes resulting from the high current slew rates produced by the upper MOSFETs turning on and off. Select low ESL ceramic capacitors and place one as close as possible to each upper MOSFET drain to minimize board parasitic impedances and maximize noise suppression.

7.3.1 Multiphase RMS Improvement

[Figure 71 on page 37](#) demonstrates the dramatic reductions in input-capacitor RMS current upon the implementation of the multiphase topology. For example, compare the input RMS current requirements of a 2-phase converter versus that of a single-phase. Assume both converters have a duty cycle of 0.25, maximum sustained output current of 40A, and a ratio of $I_{L(P-P)}$ to I_O of 0.5. The single-phase converter would require 17.3A_{RMS} current capacity, while the 2-phase converter would require only 10.9A_{RMS}. The advantages become even more pronounced when the output current is increased and additional phases are added to keep the component cost down relative to the single-phase approach.

7.4 Inductor Current Sensing and Balancing

The three VR outputs of the ISL95859C each support a different number of active channels. VR A of the controller can support up to 3-phase operation, VR B up to 2-phase operation, and VR C is only single phase. [Figure 72](#) shows the inductor DCR current-sensing network as an example of a 3-phase voltage regulator. The principles described can be applied to any of the three outputs.

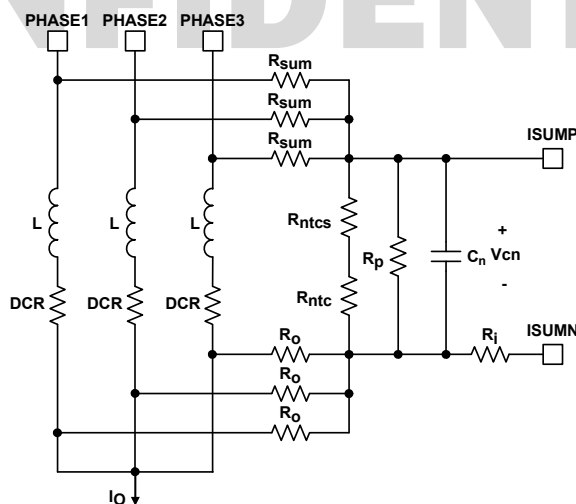


Figure 72. DCR Current-Sensing Network

7.5 Inductor DCR Current-Sensing Network

Referencing [Figure 72](#), an inductor's current flows through the inductor's DCR and creates a voltage drop. Each inductor has two resistors, R_{sum} and R_o , connected to its pads to accurately sense the inductor current by sensing the DCR voltage drop. The R_{sum} and R_o resistors are connected in a summing network as shown and feed the total current information to the NTC network (consisting of R_{ntcs} , R_{ntc} and R_p) and capacitor C_n . R_{ntc} is a Negative Temperature Coefficient (NTC) thermistor that compensates for the change in inductor DCR due to ambient temperature changes and due to power dissipation in the inductor.

The inductor output-side pads are electrically shorted in the schematic but have some parasitic impedance in the actual board layout, which is why one cannot simply short them together for the current-sensing summing network. It is recommended to use 1Ω~10Ω R_o to create quality signals. Because the R_o value is much smaller than the rest of the current sensing circuit, the following analysis will ignore it for simplicity.

The summed inductor current information is applied to the capacitor C_n . [Equations 19](#) through [23](#) describe the frequency-domain relationship between inductor total current $I_o(s)$ and C_n voltage $V_{Cn}(s)$:

$$(EQ. 19) \quad V_{Cn}(s) = \left(\frac{R_{ntcnet}}{R_{ntcnet} + \frac{R_{sum}}{N}} \times \frac{DCR}{N} \right) \times I_o(s) \times A_{cs}(s)$$

$$(EQ. 20) \quad R_{ntcnet} = \frac{(R_{ntcs} + R_{ntc}) \times R_p}{R_{ntcs} + R_{ntc} + R_p}$$

$$(EQ. 21) \quad A_{cs}(s) = \frac{1 + \frac{s}{\omega_L}}{1 + \frac{s}{\omega_{sns}}}$$

$$(EQ. 22) \quad \omega_L = \frac{DCR}{L}$$

$$(EQ. 23) \quad \omega_{sns} = \frac{1}{\frac{R_{ntcnet} \times \frac{R_{sum}}{N}}{R_{ntcnet} + \frac{R_{sum}}{N}} \times C_n}$$

where N is the number of phases.

The inductor DCR value increases as the inductor temperature increases, due to the positive temperature coefficient of the copper windings. If uncompensated, this will cause the estimate of inductor current to increase with temperature. The resistance of a colocated NTC thermistor, R_{ntc} , decreases as its temperature increases, compensating for the increase in DCR. Proper selection of the R_{sum} , R_{ntcs} , R_p , and R_{ntc} parameters ensures that V_{Cn} represents the inductor total DC current over the temperature range of interest.

Many sets of parameters can properly temperature compensate the DCR change. Because the NTC network and the R_{sum} resistors form a voltage divider, V_{cn} is always a fraction of the inductor DCR voltage. It is recommended to have a high ratio of V_{cn} to the inductor DCR voltage, so the current sense circuit has a higher signal level to work with.

A typical set of parameters that provide good temperature compensation are: $R_{sum} = 3.65k\Omega$, $R_p = 11k\Omega$, $R_{ntcs} = 2.61k\Omega$, and $R_{ntc} = 10k\Omega$ (ERT-J1VR103J). The NTC network parameters may need to be fine-tuned on actual boards. One can apply full load DC current and record the output voltage reading immediately, then record the output voltage reading again when the board has reached the thermal steady state. A good NTC network can limit the output voltage drift to within 2mV. It is recommended to follow the Intersil evaluation board layout and current-sensing network parameters to minimize engineering time.

$V_{Cn}(s)$ response must track $I_o(s)$ over a broad range of frequencies for the controller to achieve good transient response. Transfer function $A_{cs}(s)$ ([Equation 24](#)) has unity gain at DC, a pole ω_{sns} , and a zero ω_L . To obtain unity gain at all frequencies, set ω_L equal to ω_{sns} and solve for C_n .

$$(EQ. 24) \quad C_n = \frac{L}{\frac{R_{ntcnet} \times \frac{R_{sum}}{N}}{R_{ntcnet} + \frac{R_{sum}}{N}} \times DCR}$$

For example, given $N = 3$, $R_{sum} = 3.65k\Omega$, $R_p = 11k\Omega$, $R_{ntcs} = 2.61k\Omega$, $R_{ntc} = 10k\Omega$, $DCR = 0.9m\Omega$, and $L = 0.36\mu H$, [Equation 24](#) gives $C_n = 0.397\mu F$.

When the load current I_{core} has a step change, the output voltage V_{CORE} also has a step change, determined by the DC load line resistance (the resistor-programmable output voltage droop value, or source resistance, of the regulator). Assuming the loop compensator design is correct, [Figure 80](#) (see [“Verification of Inductor-DCR Current Sense Pole-Zero Matching” on page 49](#)) shows the expected load transient response waveforms for the correctly chosen value of C_n . If the C_n value is too large or too small, $V_{\text{Cn}}(s)$ will not accurately represent the real-time $I_o(s)$ and the load line transient response will deviate from the ideal. If C_n is too small, V_{CORE} will droop excessively (undershoot) upon abrupt load insertion before recovering to the intended DC value, which can create a system failure. Similarly, there is excessive overshoot during load decreases, which can hurt the CPU reliability. If C_n is too large, the V_{CORE} load line response to load changes will lag.

With the proper selection of C_n , assume that $A_{\text{cs}}(s) = 1$. With this assumption, [Equation 24](#) is recast as [Equation 25](#):

$$(EQ. 25) \quad \frac{V_{\text{Cn}}}{I_o} = \left(\frac{R_{\text{ntcnet}}}{R_{\text{ntcnet}} + \frac{R_{\text{sum}}}{N}} \times \frac{\text{DCR}}{N} \right)$$

The value of DCR and R_{ntcnet} are both temperature dependent. However, with a properly designed inductor temperature compensation network, one can also assume the room temperature inductor DCR value and the room temperature value of R_{ntcnet} in subsequent calculations, because any temperature variation in one value is, ideally, exactly compensated by a variation in the other value. [Equation 25](#) is evaluated, using room temperature resistance values, to obtain a constant value of the ratio V_{Cn}/I_o , in units of resistance, for a given DCR current sense network design. This constant value, designated ρ_o , assumed to be independent of temperature, is required to complete the regulator design.

[Equation 26](#) applies to the DCR current sense circuit of [Figure 72 on page 38](#).

$$(EQ. 26) \quad \rho_o = \left(\frac{R_{\text{ntcnet}}}{R_{\text{ntcnet}} + \frac{R_{\text{sum}}}{N}} \times \frac{\text{DCR}}{N} \right) \Bigg|_{\text{RoomTemp}}$$

7.5.1 Resistor Current-Sensing Network

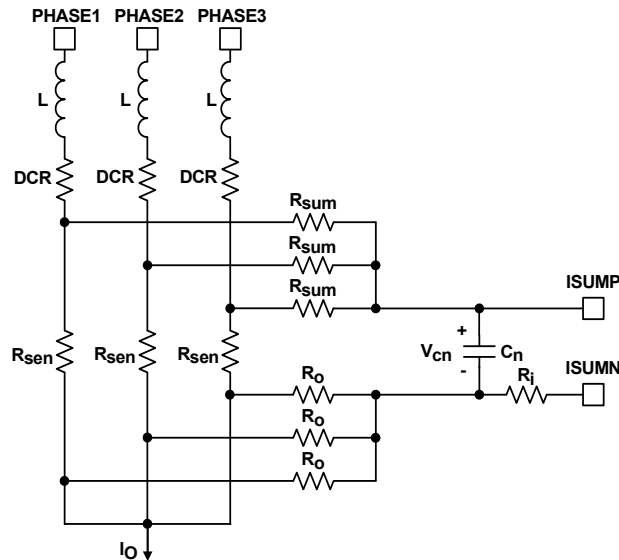


Figure 73. Resistor Current-Sensing Network

Figure 73 shows the resistor current-sensing network for the example of a 3-phase regulator. Each inductor has a series current-sensing resistor R_{sen} . R_{sum} and R_o are connected to the R_{sen} pads to accurately capture the inductor current information. The R_{sum} and R_o resistors are connected to capacitor C_n . R_{sum} and C_n form a filter for noise attenuation. Equations 27 through 29 give the $V_{Cn}(s)$ expression:

$$(EQ. 27) \quad V_{Cn}(s) = \frac{R_{sen}}{N} \times I_o(s) \times A_{Rsen}(s)$$

$$(EQ. 28) \quad A_{Rsen}(s) = \frac{1}{1 + \frac{s}{\omega_{Rsen}}}$$

$$(EQ. 29) \quad \omega_{Rsen} = \frac{1}{\frac{R_{sum}}{N} \times C_n}$$

Transfer function $A_{Rsen}(s)$ always has unity gain at DC. Current-sensing resistor R_{sen} values will not have significant variation over temperature, so there is no need for the NTC network.

The recommended values are $R_{sum} = 1k\Omega$ and $C_n = 5600pF$.

As with the DCR current sense network, Equation 29 is recast as Equation 30:

$$(EQ. 30) \quad \frac{V_{Cn}}{I_o} = \frac{R_{sen}}{N}$$

This equation is evaluated to obtain a constant value of the ratio V_{Cn}/I_o , in Ohm units, for a given sense resistor current sense network design. This constant value is designated ρ_o in Equation 31.

$$(EQ. 31) \quad \rho_o = \frac{R_{sen}}{N}$$

Equation 31 applies to the resistor current sense circuit of Figure 73 on page 41. As with the DCR sense design, this constant value is required to complete the regulator design.

7.5.2 Programming of Output Overcurrent Protection, I_{droop} , and IMON

The final step in designing the current sense network is the selection of resistor R_i of [Figures 72](#) or [73](#). This resistor determines the ratio of the controller's internal representation of output current (I_{droop} , also called the “droop current”) to the actual output current, that is, to the sum of all the measured inductor currents. This internal representation is itself a current that is used (a) to compare to the overcurrent protection threshold, (b) to source the I_{droop} current to the FB pin to provide the programmable load-dependent output voltage “droop” or output DC load line, and (c) to drive the IMON pin external resistor to produce a voltage to represent the output current. This is measured and written to the IOUT register, readable from the SVID bus.

Begin by selecting the maximum current that the regulator is designed to provide. This is the value of $I_{\text{CC(MAX)}}$ programmed with the programming pin resistance to ground for each VR output. Select the appropriate R_{PROG1} to program the lowest available value of $I_{\text{CC(MAX)}}$ that exceeds the expected maximum load. The Overcurrent Protection (OCP) threshold I_{OCP} must exceed this value. I_{OCP} is typically chosen to be 20% to 25% greater than $I_{\text{CC(MAX)}}$. I_{OCP} will determine the value of R_i .

Using VR B as the example, refer to [Table 2 on page 31](#). The value of OCP threshold for either phase configuration (1- or 2-phase) and any power state (PS0-PS3) is the threshold value of I_{droop} that will trigger the output overcurrent protection. Notice that the OCP threshold value of the PS0 row of any phase configuration is 60 μA . R_i should be chosen such that I_{droop} is 60 μA when the regulator output current is equal to the chosen value of output I_{OCP} , as follows.

The mechanism by which R_i determines I_{droop} is illustrated in [Figure 74](#).

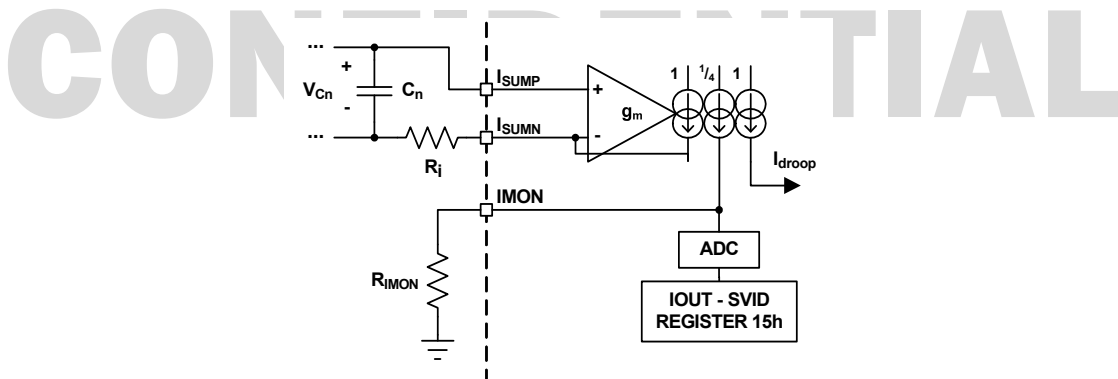


Figure 74. Droop Illustration

The ISUM transconductance amplifier produces the current that drops the voltage V_{Cn} across R_i , to make $V_{\text{ISUMN}} = V_{\text{ISUMP}}$. This current is mirrored 1:1 to produce I_{droop} and 4:1 to produce I_{IMON} . I_{droop} is compared directly to the OCP threshold, always 60 μA in PS0, so R_i must be chosen to obtain the desired I_{OCP} using [Equation 32](#).

$$(EQ. 32) \quad R_i = \rho_o \times \frac{I_{\text{OCP}}}{60\mu\text{A}}$$

where ρ_o is the constant value determined in [Equation 26](#) or [31](#).

For a given value of output current, I_o , I_{droop} will have the value shown in [Equation 33](#):

$$(EQ. 33) \quad I_{\text{droop}} = \frac{\rho_o}{R_i} \times I_o$$

I_{droop} is also used to program the slope of the output DC load line. The DC load line slope is the programmable regulator output resistance. Programming of the DC load line is explained in [“Programming the DC Load Line”](#).

The I_{OUT} register (SVID Register 15h) reports an 8-bit unsigned number indicative of the IMON pin voltage, scaled such that its value is 00h when $V_{IMON} = 0V$ and FFh when $V_{IMON} = 1.214V$. With R_i determined, R_{IMON} is chosen such that $V_{IMON} = 1.214V$ when the regulator load current is equal to $I_{CC(MAX)}$, the maximum current value programmed by R_{PROG2} . Select R_{IMON} using [Equation 34](#):

$$(EQ. 34) \quad R_{IMON} = 1.214V \times \left(\rho_o \times \frac{I_{CC(MAX)}}{R_i \times 4} \right)^{-1}$$

where again ρ_o is the constant value determined in [Equation 26](#) or [31](#). A capacitor should be added in parallel with R_{IMON} to filter the IMON pin voltage and to set the I_{OUT} register response time constant.

7.5.3 Programming the DC Load Line

The DC load line is the effective DC series resistance of the voltage regulator output. The output series resistance causes the output voltage to “droop” below the selected regulation voltage by a voltage equal to the load current multiplied by the output resistance. The linear relationship of the output voltage drop to load current is called the load line and is expressed in units of resistance. It is designated R_{LL} . [Figure 75 on page 43](#) shows the equivalent circuit of a voltage regulator (VR) with the droop function. An ideal VR is equivalent to a voltage source ($V = V_{ID}$) and output impedance $Z_{out}(s)$. If $Z_{out}(s)$ is equal to the load line slope R_{LL} (constant output impedance independent of frequency), V_O will have a step response when I_O has a step change.

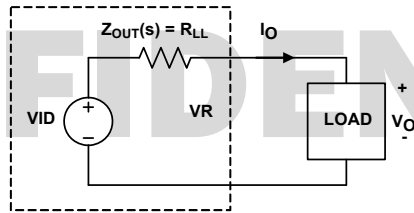


Figure 75. Voltage Regulator Equivalent Circuit

The ISL95859C provides programmable DC load line resistance. A typical desired value of the DC load line for Intel IMVP8 applications is $R_{LL} = 2m\Omega$.

The programmable DC load line mechanism is an integral part of the regulator’s output voltage feedback compensator. This is illustrated in the feedback circuit and recommended compensation network shown in [Figure 76](#).

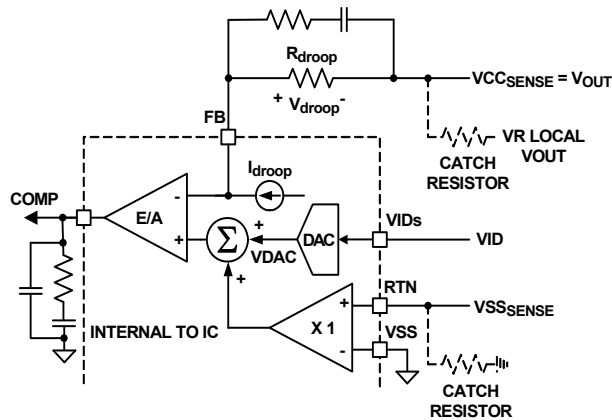


Figure 76. Differential Voltage Sensing and Load Line Implementation

The ISL95859C implements the DC load line by injecting a current, I_{droop} , which is proportional to the regulator output current I_{OUT} , into the voltage feedback node (the FB pin). The scaling of I_{droop} with respect to

I_{OUT} was selected in [“Programming of Output Overcurrent Protection, \$I_{droop}\$, and IMON” on page 42](#) to obtain the desired output I_{OCP} threshold. The droop voltage is the voltage drop across the resistance, called R_{droop} , between the FB pin and the output voltage due to I_{droop} . (R_{droop} is the only DC path between V_{OUT} and the FB pin.) R_{droop} is selected to implement the desired DC load line resistance R_{LL} . The FB pin voltage is thus raised above V_{OUT} by the droop voltage, requiring the regulator to reduce V_{OUT} to make V_{FB} equal to the voltage regulator reference voltage applied to the error amplifier noninverting input.

R_{droop} is a component of the voltage regulator stability compensation network. The regulator stability and dynamic response is determined independently of the value of R_{droop} , because the loop integral gain is set with the COMP-to-FB capacitance and the series RC in parallel with R_{droop} will dominate the compensator response at and well below the open loop crossover frequency. Because R_{droop} plays a singular role in determining the DC load line, it is chosen solely for that purpose.

For a desired R_{LL} , the output voltage reduction, V_{droop} , due to an output load current, I_o , is as shown in [Equation 35](#).

$$(EQ. 35) \quad V_{droop} = R_{LL} \times I_o$$

The value of V_{droop} obtained from the ISL95859C controller is the droop current, I_{droop} , multiplied by the droop resistor, R_{droop} . Using [Equation 33](#), this value is as shown in [Equation 36](#).

$$(EQ. 36) \quad V_{droop} = I_{droop} \times R_{droop} = \frac{p_o}{R_i} \times I_o \times R_{droop}$$

Equate these two expressions for V_{droop} and solve for R_{droop} to obtain the value in [Equation 37](#).

$$(EQ. 37) \quad R_{droop} = \frac{R_i \times R_{LL}}{p_o}$$

7.5.4 Phase DC Voltage and Current Balancing

To equally distribute power dissipation between the active phases of a VR, the controller provides a means to reduce the deviation of the DC component (approximately the product of the duty cycle and V_{VIN}) of each phase voltage from the average of all phases' DC voltages. The controller achieves phase node DC voltage balance by continually trimming the modulator slave circuits to match the $ISEN_n$ pin voltages. The connection of these pins to their respective phase nodes is depicted in [Figure 77](#) for the inductor DCR current sense method, for the example of a three phase VR. The DC voltage and current balancing methods described in this section apply also to current sensing using discrete sense resistors.

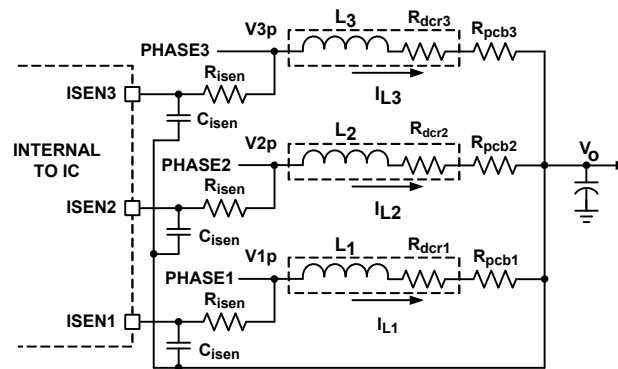


Figure 77. Duty Cycle Balancing Circuit

The phase nodes have high amplitude square-wave voltage waveforms, for which the DC component is indicative of each phase's relative contribution to the output. R_{isen} and C_{isen} form low-pass filters to remove the

switching ripple of the phase node voltages, such that the voltages at the ISEN_n pins approximately indicate each phase's DC voltage component and thus the relative contribution of each phase to the output current. The controller gradually and continually trims the R3 modulator slave circuits. Thus, adjusting the relative duty cycle of each phase reduces the phase node DC voltage differences, as indicated by each V_{ISEN_n}. This adjustment occurs slowly compared to the dynamic response of the multiphase modulator to output voltage commands, load transients, power state changes and other system perturbations.

It is recommended to use a large R_{isen}C_{isen} time constant, such that the ISEN_n voltages have small ripple and are representative of the average or steady-state contribution of each phase to the output. Recommended values are R_{isen} = 10kΩ and C_{isen} = 0.22μF.

Ideally, balancing the phase nodes' average (DC) voltages will also balance the output current provided by each phase and the power dissipated in each phase's components. This is the case if the current sense elements of each phase are identical (DCR of the inductors, or discrete current sense resistors and the associated current sense networks) and if parasitic resistances of the circuit board traces from the sense connections to the common output voltage node are identical. [Figure 77](#) shows the printed circuit trace resistances from each phase to the common output node. If these trace resistances are all equal, then the ideal of phase current balance is achieved with this design. This balance assumes the inductors and other current sense components are identical, comparing each phase to the others, a true assumption within the published tolerance of component parameters.

[Figure 77](#) includes the trace-resistance from each inductor to a single common output node, but not from the MOSFET switches to the inductor. This is correct assuming that each R_{isen} connection (V1p, V2p and V3p) is routed directly to its respective inductor phase-node-side pad in order to eliminate the effect of phase node parasitic PCB resistance from the switching elements to the inductor. [Equations 38](#) through [40](#) give the ISEN pin voltages:

$$(EQ. 38) \quad V_{ISEN1} = (R_{dcr1} + R_{pcb1}) \times I_{L1} + V_o$$

$$(EQ. 39) \quad V_{ISEN2} = (R_{dcr2} + R_{pcb2}) \times I_{L2} + V_o$$

$$(EQ. 40) \quad V_{ISEN3} = (R_{dcr3} + R_{pcb3}) \times I_{L3} + V_o$$

where R_{dcr1}, R_{dcr2}, and R_{dcr3} are the respective inductor DCRs; R_{pcb1}, R_{pcb2}, and R_{pcb3} are the respective parasitic PCB resistances between the inductor output-side pad and the output voltage rail; and I_{L1}, I_{L2}, and I_{L3} are inductor average currents.

The phase balance controller will adjust the phase pulse-width relative to the other phases to make V_{ISEN1} = V_{ISEN2} = V_{ISEN3}, thus obtaining I_{L1} = I_{L2} = I_{L3} if R_{dcr1} = R_{dcr2} = R_{dcr3} and R_{pcb1} = R_{pcb2} = R_{pcb3}.

Because using the same components for L1, L2, and L3 will typically provide a good match of R_{dcr1}, R_{dcr2}, and R_{dcr3}, board layout will determine R_{pcb1}, R_{pcb2}, and R_{pcb3} and thus the matching of current per phase. It is recommended to have symmetrical layout for the power delivery path between each inductor and the output voltage rail, such that R_{pcb1} = R_{pcb2} = R_{pcb3}.

While careful symmetrical layout of the circuit board can achieve very good matching of these trace resistances, such layout is often difficult to achieve in practice. If trace resistances differ, then exact matching the phases' DC voltages will result in the *imbalance* of the phase currents. A modification of this circuit (to couple the signals of all the phases in the ISEN_n networks) can correct the current imbalance due to unequal trace resistances to the output.

For the example case of a 3-phase configuration, [Figure 78 on page 46](#) shows the phase balancing circuit with the recommended trace-resistance imbalance correction. As before, V1p, V2p, and V3p should be routed to their respective inductor phase-node-side pads in order to eliminate the effect of phase node parasitic PCB resistance from the switching elements to each inductor. The sensing traces for V1n, V2n, and V3n should be routed to the

V_{OUT} output-side inductor pads so they sense the voltage due only to the voltage drop across the inductor DCR and not due to the PCB trace resistance.

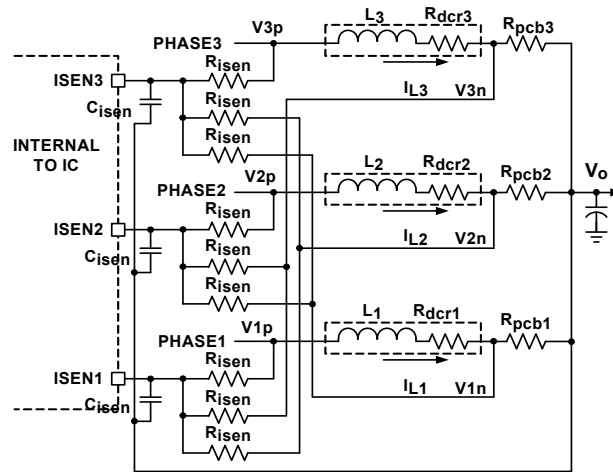


Figure 78. Differential Sensing Current Balancing Circuit

Each ISEN pin sees the average voltage of three sources: its own phase inductor phase-node pad and the other two phases inductor output-side pads. [Equations 41](#) through [43](#) give the ISEN pin voltages:

$$(EQ. 41) \quad V_{ISEN1} = \frac{(V_{1p} + V_{2n} + V_{3n})}{3}$$

$$(EQ. 42) \quad V_{ISEN2} = \frac{(V_{1n} + V_{2p} + V_{3n})}{3}$$

$$(EQ. 43) \quad V_{ISEN3} = \frac{(V_{1n} + V_{2n} + V_{3p})}{3}$$

The controller will make $V_{ISEN1} = V_{ISEN2} = V_{ISEN3}$, resulting in the equalities shown in [Equations 44](#) and [45](#):

$$(EQ. 44) \quad V_{1p} + V_{2n} + V_{3n} = V_{1n} + V_{2p} + V_{3n}$$

$$(EQ. 45) \quad V_{1n} + V_{2p} + V_{3n} = V_{1n} + V_{2n} + V_{3p}$$

Simplifying [Equation 44](#) gives [Equation 46](#):

$$(EQ. 46) \quad V_{1p} - V_{1n} = V_{2p} - V_{2n}$$

and simplifying [Equation 45](#) gives [Equation 47](#):

$$(EQ. 47) \quad V_{2p} - V_{2n} = V_{3p} - V_{3n}$$

Combining [Equations 46](#) and [47](#) gives [Equation 48](#):

$$(EQ. 48) \quad V_{1p} - V_{1n} = V_{2p} - V_{2n} = V_{3p} - V_{3n}$$

which produces the desired result in [Equation 49](#):

$$(EQ. 49) \quad R_{dcr1} \times I_{L1} = R_{dcr2} \times I_{L2} = R_{dcr3} \times I_{L3}$$

Current balancing ($I_{L1} = I_{L2} = I_{L3}$) is achieved independently of any mismatch of R_{pcb1} , R_{pcb2} , and R_{pcb3} to within the tolerance of the resistance of the current sense elements. Note that with the cross coupling of [Figure 79](#), the phase balancing circuit no longer equalizes the average voltage of the phase nodes, but rather equalizes the DC components of the voltage drops across the current sense elements.

Small absolute differences in PCB trace resistance from the inductors to the common output node can result in significant phase current imbalance. It is strongly recommended that the resistor pads and connections for the cross-coupling current balancing method be included in any PCB layout. The decision to include the additional $N \times (N-1)$ trace-resistance correcting resistors can then be deferred until the extent of the current imbalance is measured on a functioning circuit. Considerations for making this decision are described in [“Phase Current Balancing” on page 51](#).

With the ISEN n phase balancing mechanism (with cross coupling resistors if needed, or without if not needed), the R3™ modulator achieves excellent current balancing during both steady state and transient operation. [Figure 79](#) shows current balancing performance of an evaluation board with load transient of 12A/51A at different rep rates. The inductor currents follow the load current dynamic change with the output capacitors supplying the difference. The inductor currents can track the load current well at low rep rate, but cannot track the load when the rep rate gets into the 100kHz range, which is outside of the control loop bandwidth. Regardless, the controller achieves excellent current *balancing* in all cases.

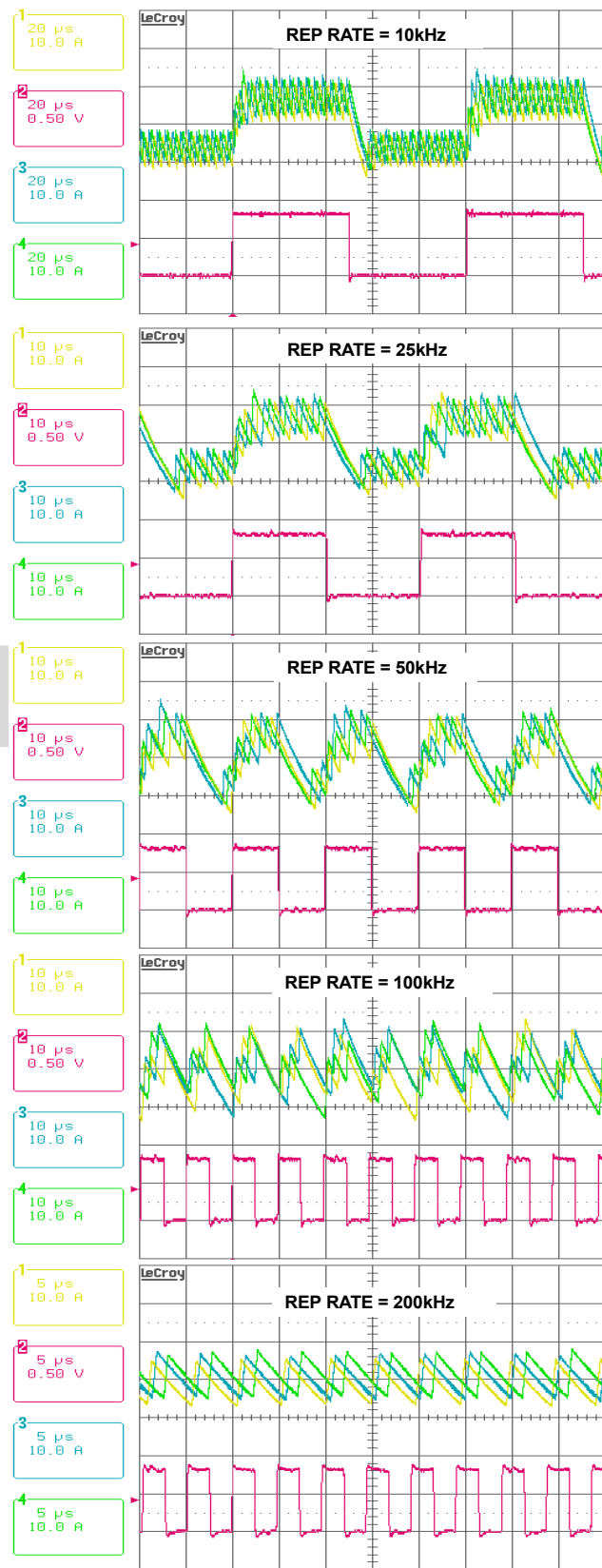


Figure 79. Current Balancing During Dynamic Operation. CH1: I_{L1} , CH2: I_{LOAD} , CH3: I_{L2} , CH4: I_{L3}

7.6 Current Sense Circuit Adjustments

When a voltage regulator (VR) is designed and a functional prototype has been assembled, adjustments may be necessary to correct for non-ideal components or assembly and printed circuit board parasitic effects. These are effects that are usually not known until the design has been realized. The following adjustments should be considered when refining a product design.

7.6.1 Verification of Inductor-DCR Current Sense Pole-Zero Matching

Recall that if the inductor DCR is used as the phase current sense element, it is necessary to select the capacitor C_n such that the current sense transfer function pole at ω_{sns} matches the zero at ω_L . The ideal response to a load step, with DC load line (“droop”) enabled, is shown in [Figure 80](#).

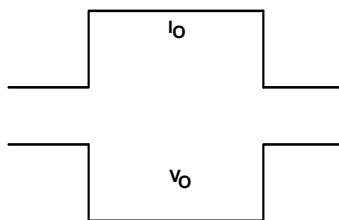


Figure 80. Desired Load Transient Response Waveforms

[Figure 81](#) shows the load step transient response when C_n is too large. V_{CORE} droop response (rising or falling) lags in settling to its final value.

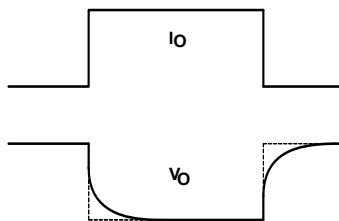


Figure 81. Load Transient Response When C_n is too Large

[Figure 82](#) shows the load step response when C_n is too small. V_{CORE} response is underdamped and overshoots before settling to its final voltage.

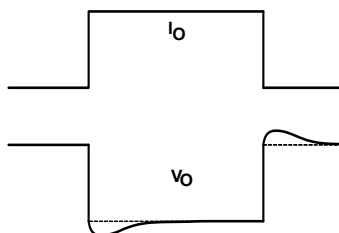


Figure 82. Load Transient Response When C_n is too Small

When the regulator design is complete, the measured load step response is compared to [Figures 80](#) through [82](#). C_n should be adjusted if necessary to obtain the behavior of [Figure 80](#).

7.6.2 Current Sense Sensitivity Error

The current sense, IMON and DC load line (droop) network component values should be designed according to the instructions in [“Programming of Output Overcurrent Protection, Idroop, and IMON” on page 42](#) and [“Programming the DC Load Line” on page 43](#). This will ensure the correct *ratio* of V_{IMON} to I_{droop} (which determines R_{LL}) for the chosen system design parameters, for which no adjustment should be required. However, testing of the resulting circuit may reveal a measurement *sensitivity* error factor, which should effect V_{IMON} and I_{droop} equally. This error may be seen as a too-large R_{LL} value (droop voltage per load current) and as a too-large IMON voltage for a given load current. A single component modification will correct both errors.

The current sense resistance value per phase (either a discrete sense resistor, or the inductor DCR) is typically very small, on the order of $1m\Omega$. The solder connections used in the assembly of such sense elements may contribute significant resistance to these sense elements, resulting in a larger load-dependent voltage drop than due to the sense element alone. Thus, the sensed output current value is greater than intended for a given load current. If this is the case, then the value of R_i (the ISUMN pin resistor) should be increased by the factor of the sensitivity error. For example, if the current sense value is 3% larger than intended, then R_i should be increased by 3%. Changing R_i will change the sensitivity (with respect to I_{OUT}) of V_{IMON} and I_{droop} by the same factor, thus simultaneously correcting the IMON voltage error and the load line resistance, while preserving the intended ratio between the two parameters.

Note that the assembly procedure for installing the current sense elements (sense resistors or inductors) can have a significant impact on the effective total resistance of each sense element. It is important that any adjustments to R_i be performed on circuits that have been assembled with the same procedures that will be used in mass production. The current measurement sensitivity error should be determined on a sufficient number of samples to avoid adjusting sensitivity to correct what may be a component-tolerance outlier.

7.6.3 DCR Current Sense OFFSET Error

When using the inductor DCR current sensing, nonlinearity of the R_{SUM} resistors can induce a small positive offset in the ISUMP voltage and thus, in the IMON pin current (viewed as a positive offset in the ICC register value) and also in the droop current (viewed as an output voltage negative offset). The offset error occurs as follows: for each inductor, the instantaneous voltage across its R_{SUM} resistor is approximately $V_{RSUM} = V_{PHASE} - V_{VOUT}$. During that phase's on time, $V_{PHASE} = V_{VIN}$, giving $V_{RSUM-ON} = V_{VIN} - V_{VOUT}$. During the off time, $V_{PHASE} = 0V$ and so $V_{RSUM-OFF} = -V_{VOUT}$. For the example of $V_{VOUT} = 1.8V$ and $V_{VIN} = 12V$, $V_{RSUM-ON} = 10.2V$ and $V_{RSUM-OFF} = -1.8V$, a sign-dependent magnitude difference exceeding 8V. Inexpensive thick film resistors can have a voltage nonlinearity of 25ppm/volt or more, with the device resistance decreasing with increasing voltage. Because of this R_{SUM} resistor nonlinearity, each R_{SUM} 's (positive) current into the common ISUMP node (during its on-time) is biased slightly greater than the nominal V/R value expected. Each R_{SUM} 's (negative) current (during its off-time) will also be biased negatively due to the resistor nonlinearity, but less so because the R_{SUM} voltage magnitude is always much less during the off-time than during the on-time. This nonlinearity bias current polarity mismatch causes a small positive offset error in V_{ISUMP} . Note that this offset error will not occur if using discrete resistors as current sense elements.

The exact magnitude of this offset error is difficult to predict. It depends on an attribute of the sense resistors that is typically not specified or controlled and so not reliably quantified. It also varies with the input voltage and the output voltage. If battery powered, the input voltage can vary significantly. The output voltage is subject to the VID setting and to a lesser extent on the droop voltage. A further complication is that the nonlinearity offset changes with the number of active phases. For a 3-phase configuration in PS0, three R_{SUM} resistors are subjected to the high difference in on-time compared to off-time voltage magnitudes. But in PS1, one or two phases are disabled (based on the PROG2 setting) with the respective PHASE nodes approximately following the output. Thus, V_{RSUM} for the disabled phases is approximately zero for the entire switching cycle, reducing the offset error by 1/3 to 2/3. In PS2, only one phase is active and two phases are disabled, leaving only a third of the PS0 offset error.

The most direct solution to the phenomenon of current sense offset due to resistor nonlinearity is to use highly linear summing resistors, such as thin film resistors. But the magnitude of the offset error typically does not

warrant the considerably greater expense of doing so. Instead, a correcting fixed offset is introduced to the current sense network.

For the example case described, with each thick film $R_{SUM} = 3.65k\Omega$ and an $I_{CC(MAX)}$ setting of 100A, the current sense offset error in PS0 typically represents less than 1% of full scale and is always positive. It has been found empirically that a $10M\Omega$ pull-down resistor from the ISUMP node to ground provides a good correcting offset compromise slightly undercorrecting in PS0 and slightly overcorrecting in PS2, but meeting processor vendor specification tolerances with adequate margin in all cases. For other applications, a suitable compromise pull-down resistor is determined empirically by testing over the full range of expected operating conditions and power states. It is recommended that this resistor be included in any VR design layout to allow population of the pull-down resistor if required. Because of the high value of resistance, two smaller valued resistors in series may be preferred, to reduce the environmental sensitivity of high resistance value devices.

7.6.4 Phase Current Balancing

Phase current imbalance should be measured on a functioning circuit. First, verify the correct assembly of the current balancing mechanism by measuring, on a stable operating regulator, the voltage difference between the ISEN1 pin and the remaining ISEN n pins (of all the operational phases) with various static loads applied. Whether using the simple circuit of [Figure 77 on page 44](#) or the PCB trace resistance compensating circuit of [Figure 77](#), the voltage difference between any pair of the ISEN n pins should be very small, usually less than 1mV. If not, there may be an assembly error.

Then, again with various static loads applied, measure the voltage directly across each active sense element (sense resistor or inductor). Any discrepancy in the phase sense element voltages beyond what is attributed to the sense element resistance tolerance must be due to PCB trace resistance deviations. Install the cross-coupling resistors shown in [Figure 83](#) and again compare the sense element voltages. Now the sense element voltages should be the same among the phases in all cases (to within the tolerance of the cross coupling resistors) and the phase current balance is within the parametric tolerance of the sense element resistance, independently of the PCB trace resistance differences.

The decision to populate the cross-coupling phase sense resistors will depend upon the magnitude and system tolerance of the uncorrected imbalance current.

7.6.5 Load Step Ringback

[Figure 83](#) shows the output voltage ringback problem during load transient response with DC load line ("droop") enabled. The load current I_O has a fast step change, but the inductor current I_L cannot accurately follow. Instead, I_L responds in first order system fashion due to the nature of current loop. The ESR and ESL effect of the output capacitors makes the output voltage V_O dip quickly upon load current change. However, the controller regulates V_O according to the droop current I_{droop} , which is a real-time representation of I_L .

Therefore it pulls V_O back to the level dictated by I_L , causing the ringback problem. This phenomenon is not observed when the output capacitor bank has very low ESR and ESL, such as if using only ceramic capacitors.

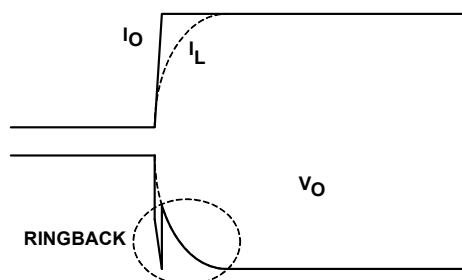


Figure 83. Output Voltage Ringback Problem

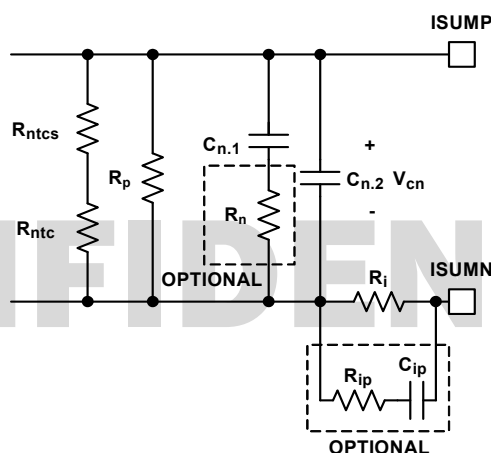


Figure 84. Optional Circuits for Ringback Reduction

Figure 84 shows two optional circuits for reduction of the ringback.

C_n is the capacitor used to match the inductor time constant. It often takes the paralleling of multiple capacitors to get the desired value. Figure 84 on page 52 shows that two capacitors $C_{n.1}$ and $C_{n.2}$ are in parallel. Resistor R_n is an optional component to reduce the V_O ringback. At steady state, $C_{n.1} + C_{n.2}$ provides the desired C_n capacitance. At the beginning of I_O change, the effective capacitance is less because R_n increases the impedance of the $C_{n.1}$ branch. As Figure 82 on page 49 shows, V_O tends to dip when C_n is too small and this effect will reduce the V_O ringback. This effect is more pronounced when $C_{n.1}$ is much larger than $C_{n.2}$. It is also more pronounced when R_n is bigger. However, the presence of R_n increases the ripple of the V_n signal if $C_{n.2}$ is too small. It is recommended to keep $C_{n.2}$ greater than 2200pF. The R_n value is usually a few ohms. $C_{n.1}$, $C_{n.2}$, and R_n values should be determined through tuning the load transient response waveforms directly on the target system circuit board.

R_{ip} and C_{ip} form an R-C branch in parallel with R_i , providing a lower impedance path than R_i at the beginning of I_{OUT} change. R_{ip} and C_{ip} do not have any effect at steady state. Through proper selection of R_{ip} and C_{ip} values, I_{droop} can resemble I_{OUT} rather than I_L and V_O will not ring back. The recommended value for R_{ip} is 100Ω. C_{ip} should be determined by observing the load transient response waveforms in a physical circuit. The recommended range for C_{ip} is 100pF~2000pF. However, it should be noted that the R_{ip} - C_{ip} branch can distort the I_{droop} waveform. Instead of being triangular as the real inductor current, I_{droop} may have sharp spikes, which may adversely affect I_{droop} average value detection and therefore may affect OCP accuracy.

7.7 Voltage Regulation

7.7.1 Compensator

Intersil provides a Microsoft Excel-based spreadsheet to help design the compensator and the current sensing network for each output of the ISL95859C. The spreadsheet helps in designing each VR to achieve constant output impedance as a stable system. Visit www.intersil.com/en/support to request the spreadsheet for the ISL95859C.

A VR with active droop function is a dual-loop system consisting of a voltage loop and a droop loop, which is a current loop. However, neither loop alone is sufficient to describe the entire system. The spreadsheet shows two loop gain transfer functions, $T1(s)$ and $T2(s)$, that describe the entire system. [Figure 85](#) conceptually shows $T1(s)$ measurement setup and [Figure 86](#) conceptually shows $T2(s)$ measurement setup. The VR senses the inductor current, multiplies it by a gain of the load line slope, then adds it on top of the sensed output voltage and feeds it to the compensator. $T1(s)$ is measured after the summing node and $T2(s)$ is measured in the voltage loop before the summing node. The spreadsheet gives both $T1(s)$ and $T2(s)$ plots. However, only $T2(s)$ is actually measured on an ISL95859C regulator.

$T1(s)$ is the total loop gain of the voltage loop and the droop loop. It always has a higher crossover frequency than $T2(s)$ and has more impact on system stability.

$T2(s)$ is the voltage loop gain with closed droop loop. It has more impact on output voltage response.

Design the compensator to get stable $T1(s)$ and $T2(s)$ with sufficient phase margin and output impedance equal or smaller than the load line slope.

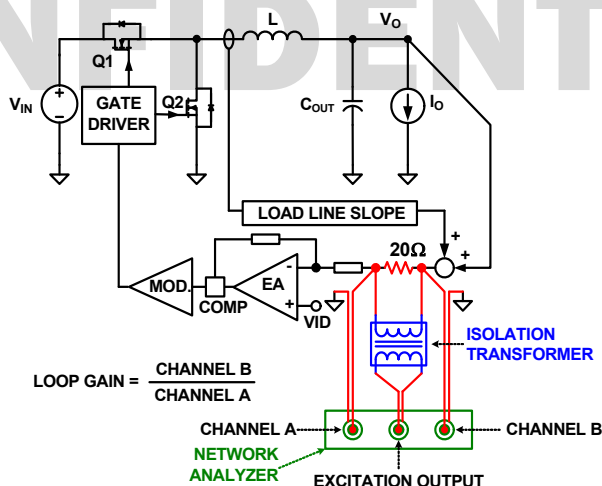


Figure 85. Loop Gain $T1(s)$ Measurement Setup

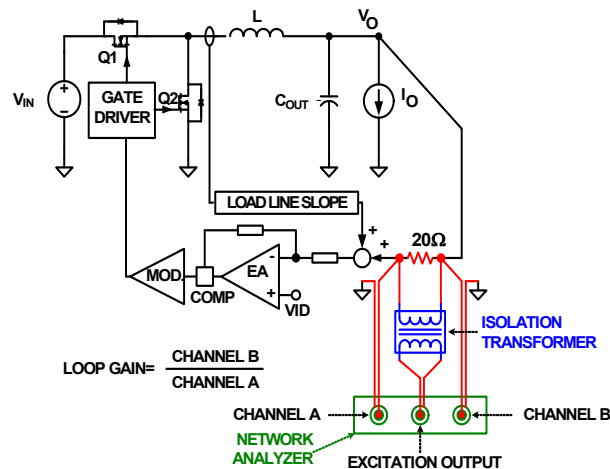


Figure 86. Loop Gain T2(S) Measurement Setup

7.7.2 Start-up Timing

With the controller's VCC voltage above the POR threshold, the start-up sequence begins when VR_ENABLE exceeds the logic high threshold. [Figure 87](#) shows the typical start-up timing for the System Agent (SA) rail of the controller if VRC is configured as the SA rail. The SA rail must soft-start to a V_{BOOT} voltage of 1.05V. The other three potential address options (IA, GT, or GTUS) all V_{BOOT} to 0V per IMVP8 specifications.

The VR_READY signal is asserted high when the controller is initialized and able to receive SVID commands, within 704μs after VR_ENABLE is asserted high as reported by SVID register index 2Dh. VR_READY remains high until either VR_ENABLE is deasserted, or until a fault is detected on any of the VRs. VR_READY also indicates when VRC (if configured as the SA rail) begins incrementally stepping its DAC from 0V to V_{BOOT} at a rate equivalent to a SetVID_slow command (for a precharged output, the DAC begins incrementally stepping from the output's initial voltage). At the end of the SA rail DAC ramp to V_{BOOT}, ALERT# is asserted low, as it would for any SetVID command completion.

Similar behavior occurs if VR_ENABLE is tied directly to V_{CC}. The start-up sequence begins after both V_{CC} and V_{IN} voltages exceed their respective POR rising thresholds.

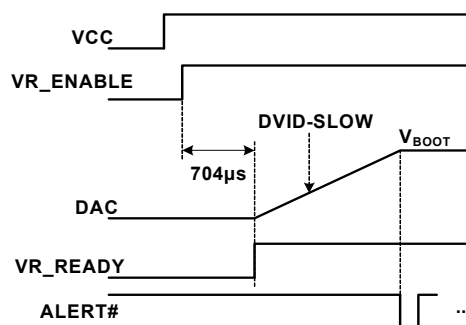


Figure 87. SA Soft-Start Waveforms

7.7.3 Voltage Regulation

After the start-up sequence, the controller regulates the three output voltages to the value set by the VID information per [Table 6 on page 55](#). The controller will control the no load output voltages to an accuracy of ±0.5% over the VID voltage range. A differential amplifier allows voltage sensing for precise voltage regulation at the microprocessor die.

This mechanism is illustrated in [Figure 76 on page 43](#). V_{CC_SENSE} and V_{SS_SENSE} are the remote voltage sensing signals from the processor die. A unity gain differential amplifier senses the V_{SS_SENSE} voltage and adds it to the DAC output. Note how the illustrated DC load line mechanism (the “droop” mechanism, described in [“Programming the DC Load Line” on page 43](#)), introduces a load-dependent reduction in the output voltage, (denoted V_{CC_SENSE}), below the VID value output by the DAC. The error amplifier regulates the inverting and the noninverting input voltages to be equal, as shown in [Equation 50](#):

$$(EQ. 50) \quad V_{CC_SENSE} + V_{droop} = V_{DAC} + V_{SS_SENSE}$$

Rewriting [Equation 50](#) and substituting [Equation 36](#) gives [Equation 51](#):

$$(EQ. 51) \quad V_{CC_SENSE} - V_{SS_SENSE} = V_{DAC} - R_{droop} \times I_{droop}$$

[Equation 51](#) is the ideal relationship required for load line implementation.

The V_{CC_SENSE} and V_{SS_SENSE} signals are sensed at the processor die. The feedback is open circuit in the absence of the processor. As shown in [Figure 76 on page 43](#), it is recommended to add a “catch” resistor to feed the VR local output voltage back to the compensator and add another “catch” resistor to connect the VR local output ground to the RTN pin. These resistors, typically 10Ω~100Ω, will provide voltage feedback if the system is powered up without a processor installed.

The maximum VID (output voltage command) value supported is 1.52V. Any VID command (or sum of VID command and VID offset) above 2.3V is ignored.

Table 6. VID Table

VID								HEX		V _O (V)
7	6	5	4	3	2	1	0			
0	0	0	0	0	0	0	0	0	0	0.00000
0	0	0	0	0	0	0	1	0	1	0.25000
0	0	0	0	0	0	1	0	0	2	0.25500
0	0	0	0	0	0	1	1	0	3	0.26000
0	0	0	0	0	1	0	0	0	4	0.26500
0	0	0	0	0	1	0	1	0	5	0.27000
0	0	0	0	0	1	1	0	0	6	0.27500
0	0	0	0	0	1	1	1	0	7	0.28000
0	0	0	0	1	0	0	0	0	8	0.28500
0	0	0	0	1	0	0	1	0	9	0.29000
0	0	0	0	1	0	1	0	0	A	0.29500
0	0	0	0	1	0	1	1	0	B	0.30000
0	0	0	0	1	1	0	0	0	C	0.30500

Table 6. VID Table (Continued)

VID								HEX		V _O (V)
7	6	5	4	3	2	1	0			
0	0	0	0	1	1	0	1	0	D	0.31000
0	0	0	0	1	1	1	0	0	E	0.31500
0	0	0	0	1	1	1	1	0	F	0.32000
0	0	0	1	0	0	0	0	1	0	0.32500
0	0	0	1	0	0	0	1	1	1	0.33000
0	0	0	1	0	0	1	0	1	2	0.33500
0	0	0	1	0	0	1	1	1	3	0.34000
0	0	0	1	0	1	0	0	1	4	0.34500
0	0	0	1	0	1	0	1	1	5	0.35000
0	0	0	1	0	1	1	0	1	6	0.35500
0	0	0	1	0	1	1	1	1	7	0.36000
0	0	0	1	1	0	0	0	1	8	0.36500
0	0	0	1	1	0	0	1	1	9	0.37000
0	0	0	1	1	0	1	0	1	A	0.37500
0	0	0	1	1	0	1	1	1	B	0.38000
0	0	0	1	1	1	0	0	1	C	0.38500
0	0	0	1	1	1	0	1	1	D	0.39000
0	0	0	1	1	1	1	0	1	E	0.39500
0	0	0	1	1	1	1	1	1	F	0.40000
0	0	1	0	0	0	0	0	2	0	0.40500
0	0	1	0	0	0	0	1	2	1	0.41000
0	0	1	0	0	0	1	0	2	2	0.41500
0	0	1	0	0	0	1	1	2	3	0.42000
0	0	1	0	0	1	0	0	2	4	0.42500
0	0	1	0	0	1	0	1	2	5	0.43000
0	0	1	0	0	1	1	0	2	6	0.43500
0	0	1	0	0	1	1	1	2	7	0.44000
0	0	1	0	1	0	0	0	2	8	0.44500
0	0	1	0	1	0	0	1	2	9	0.45000
0	0	1	0	1	0	1	0	2	A	0.45500
0	0	1	0	1	0	1	1	2	B	0.46000
0	0	1	0	1	1	0	0	2	C	0.46500
0	0	1	0	1	1	0	1	2	D	0.47000
0	0	1	0	1	1	1	0	2	E	0.47500
0	0	1	0	1	1	1	1	2	F	0.48000
0	0	1	1	0	0	0	0	3	0	0.48500
0	0	1	1	0	0	0	1	3	1	0.49000

Table 6. VID Table (Continued)

VID								HEX		V _O (V)
7	6	5	4	3	2	1	0			
0	0	1	1	0	0	1	0	3	2	0.49500
0	0	1	1	0	0	1	1	3	3	0.50000
0	0	1	1	0	1	0	0	3	4	0.50500
0	0	1	1	0	1	0	1	3	5	0.51000
0	0	1	1	0	1	1	0	3	6	0.51500
0	0	1	1	0	1	1	1	3	7	0.52000
0	0	1	1	1	0	0	0	3	8	0.52500
0	0	1	1	1	0	0	1	3	9	0.53000
0	0	1	1	1	0	1	0	3	A	0.53500
0	0	1	1	1	0	1	1	3	B	0.54000
0	0	1	1	1	1	0	0	3	C	0.54500
0	0	1	1	1	1	0	1	3	D	0.55000
0	0	1	1	1	1	1	0	3	E	0.55500
0	0	1	1	1	1	1	1	3	F	0.56000
0	1	0	0	0	0	0	0	4	0	0.56500
0	1	0	0	0	0	0	1	4	1	0.57000
0	1	0	0	0	0	1	0	4	2	0.57500
0	1	0	0	0	0	1	1	4	3	0.58000
0	1	0	0	0	1	0	0	4	4	0.58500
0	1	0	0	0	1	0	1	4	5	0.59000
0	1	0	0	0	1	1	0	4	6	0.59500
0	1	0	0	0	1	1	1	4	7	0.60000
0	1	0	0	1	0	0	0	4	8	0.60500
0	1	0	0	1	0	0	1	4	9	0.61000
0	1	0	0	1	0	1	0	4	A	0.61500
0	1	0	0	1	0	1	1	4	B	0.62000
0	1	0	0	1	1	0	0	4	C	0.62500
0	1	0	0	1	1	0	1	4	D	0.63000
0	1	0	0	1	1	1	0	4	E	0.63500
0	1	0	0	1	1	1	1	4	F	0.64000
0	1	0	1	0	0	0	0	5	0	0.64500
0	1	0	1	0	0	0	1	5	1	0.65000
0	1	0	1	0	0	1	0	5	2	0.65500
0	1	0	1	0	0	1	1	5	3	0.66000
0	1	0	1	0	1	0	0	5	4	0.66500
0	1	0	1	0	1	0	1	5	5	0.67000
0	1	0	1	0	1	1	0	5	6	0.67500

Table 6. VID Table (Continued)

VID								HEX		V _O (V)
7	6	5	4	3	2	1	0			
0	1	0	1	0	1	1	1	5	7	0.68000
0	1	0	1	1	0	0	0	5	8	0.68500
0	1	0	1	1	0	0	1	5	9	0.69000
0	1	0	1	1	0	1	0	5	A	0.69500
0	1	0	1	1	0	1	1	5	B	0.70000
0	1	0	1	1	1	0	0	5	C	0.70500
0	1	0	1	1	1	0	1	5	D	0.71000
0	1	0	1	1	1	1	0	5	E	0.71500
0	1	0	1	1	1	1	1	5	F	0.72000
0	1	1	0	0	0	0	0	6	0	0.72500
0	1	1	0	0	0	0	1	6	1	0.73000
0	1	1	0	0	0	1	0	6	2	0.73500
0	1	1	0	0	0	1	1	6	3	0.74000
0	1	1	0	0	1	0	0	6	4	0.74500
0	1	1	0	0	1	0	1	6	5	0.75000
0	1	1	0	0	1	1	0	6	6	0.75500
0	1	1	0	0	1	1	1	6	7	0.76000
0	1	1	0	1	0	0	0	6	8	0.76500
0	1	1	0	1	0	0	1	6	9	0.77000
0	1	1	0	1	0	1	0	6	A	0.77500
0	1	1	0	1	0	1	1	6	B	0.78000
0	1	1	0	1	1	0	0	6	C	0.78500
0	1	1	0	1	1	0	1	6	D	0.79000
0	1	1	0	1	1	1	0	6	E	0.79500
0	1	1	0	1	1	1	1	6	F	0.80000
0	1	1	1	0	0	0	0	7	0	0.80500
0	1	1	1	0	0	0	1	7	1	0.81000
0	1	1	1	0	0	1	0	7	2	0.81500
0	1	1	1	0	0	1	1	7	3	0.82000
0	1	1	1	0	1	0	0	7	4	0.82500
0	1	1	1	0	1	0	1	7	5	0.83000
0	1	1	1	0	1	1	0	7	6	0.83500
0	1	1	1	0	1	1	1	7	7	0.84000
0	1	1	1	1	0	0	0	7	8	0.84500
0	1	1	1	1	0	0	1	7	9	0.85000
0	1	1	1	1	0	1	0	7	A	0.85500
0	1	1	1	1	0	1	1	7	B	0.86000

Table 6. VID Table (Continued)

VID								HEX		V _O (V)
7	6	5	4	3	2	1	0			
0	1	1	1	1	1	0	0	7	C	0.86500
0	1	1	1	1	1	0	1	7	D	0.87000
0	1	1	1	1	1	1	0	7	E	0.87500
0	1	1	1	1	1	1	1	7	F	0.88000
1	0	0	0	0	0	0	0	8	0	0.88500
1	0	0	0	0	0	0	1	8	1	0.89000
1	0	0	0	0	0	1	0	8	2	0.89500
1	0	0	0	0	0	1	1	8	3	0.90000
1	0	0	0	0	1	0	0	8	4	0.90500
1	0	0	0	0	1	0	1	8	5	0.91000
1	0	0	0	0	1	1	0	8	6	0.91500
1	0	0	0	0	1	1	1	8	7	0.92000
1	0	0	0	1	0	0	0	8	8	0.92500
1	0	0	0	1	0	0	1	8	9	0.93000
1	0	0	0	1	0	1	0	8	A	0.93500
1	0	0	0	1	0	1	1	8	B	0.94000
1	0	0	0	1	1	0	0	8	C	0.94500
1	0	0	0	1	1	0	1	8	D	0.95000
1	0	0	0	1	1	1	0	8	E	0.95500
1	0	0	0	1	1	1	1	8	F	0.96000
1	0	0	1	0	0	0	0	9	0	0.96500
1	0	0	1	0	0	0	1	9	1	0.97000
1	0	0	1	0	0	1	0	9	2	0.97500
1	0	0	1	0	0	1	1	9	3	0.98000
1	0	0	1	0	1	0	0	9	4	0.98500
1	0	0	1	0	1	0	1	9	5	0.99000
1	0	0	1	0	1	1	0	9	6	0.99500
1	0	0	1	0	1	1	1	9	7	1.00000
1	0	0	1	1	0	0	0	9	8	1.00500
1	0	0	1	1	0	0	1	9	9	1.01000
1	0	0	1	1	0	1	0	9	A	1.01500
1	0	0	1	1	0	1	1	9	B	1.02000
1	0	0	1	1	1	0	0	9	C	1.02500
1	0	0	1	1	1	0	1	9	D	1.03000
1	0	0	1	1	1	1	0	9	E	1.03500
1	0	0	1	1	1	1	1	9	F	1.04000
1	0	1	0	0	0	0	0	A	0	1.04500

Table 6. VID Table (Continued)

VID								HEX		V _O (V)
7	6	5	4	3	2	1	0			
1	0	1	0	0	0	0	1	A	1	1.05000
1	0	1	0	0	0	1	0	A	2	1.05500
1	0	1	0	0	0	1	1	A	3	1.06000
1	0	1	0	0	1	0	0	A	4	1.06500
1	0	1	0	0	1	0	1	A	5	1.07000
1	0	1	0	0	1	1	0	A	6	1.07500
1	0	1	0	0	1	1	1	A	7	1.08000
1	0	1	0	1	0	0	0	A	8	1.08500
1	0	1	0	1	0	0	1	A	9	1.09000
1	0	1	0	1	0	1	0	A	A	1.09500
1	0	1	0	1	0	1	1	A	B	1.10000
1	0	1	0	1	1	0	0	A	C	1.10500
1	0	1	0	1	1	0	1	A	D	1.11000
1	0	1	0	1	1	1	0	A	E	1.11500
1	0	1	0	1	1	1	1	A	F	1.12000
1	0	1	1	0	0	0	0	B	0	1.12500
1	0	1	1	0	0	0	1	B	1	1.13000
1	0	1	1	0	0	1	0	B	2	1.13500
1	0	1	1	0	0	1	1	B	3	1.14000
1	0	1	1	0	1	0	0	B	4	1.14500
1	0	1	1	0	1	0	1	B	5	1.15000
1	0	1	1	0	1	1	0	B	6	1.15500
1	0	1	1	0	1	1	1	B	7	1.16000
1	0	1	1	1	0	0	0	B	8	1.16500
1	0	1	1	1	0	0	1	B	9	1.17000
1	0	1	1	1	0	1	0	B	A	1.17500
1	0	1	1	1	0	1	1	B	B	1.18000
1	0	1	1	1	1	0	0	B	C	1.18500
1	0	1	1	1	1	0	1	B	D	1.19000
1	0	1	1	1	1	1	0	B	E	1.19500
1	0	1	1	1	1	1	1	B	F	1.20000
1	1	0	0	0	0	0	0	C	0	1.20500
1	1	0	0	0	0	0	1	C	1	1.21000
1	1	0	0	0	0	1	0	C	2	1.21500
1	1	0	0	0	0	1	1	C	3	1.22000
1	1	0	0	0	1	0	0	C	4	1.22500
1	1	0	0	0	1	0	1	C	5	1.23000

Table 6. VID Table (Continued)

VID								HEX		V _O (V)
7	6	5	4	3	2	1	0			
1	1	0	0	0	1	1	0	C	6	1.23500
1	1	0	0	0	1	1	1	C	7	1.24000
1	1	0	0	1	0	0	0	C	8	1.24500
1	1	0	0	1	0	0	1	C	9	1.25000
1	1	0	0	1	0	1	0	C	A	1.25500
1	1	0	0	1	0	1	1	C	B	1.26000
1	1	0	0	1	1	0	0	C	C	1.26500
1	1	0	0	1	1	0	1	C	D	1.27000
1	1	0	0	1	1	1	0	C	E	1.27500
1	1	0	0	1	1	1	1	C	F	1.28000
1	1	0	1	0	0	0	0	D	0	1.28500
1	1	0	1	0	0	0	1	D	1	1.29000
1	1	0	1	0	0	1	0	D	2	1.29500
1	1	0	1	0	0	1	1	D	3	1.30000
1	1	0	1	0	1	0	0	D	4	1.30500
1	1	0	1	0	1	0	1	D	5	1.31000
1	1	0	1	0	1	1	0	D	6	1.31500
1	1	0	1	0	1	1	1	D	7	1.32000
1	1	0	1	1	0	0	0	D	8	1.32500
1	1	0	1	1	0	0	1	D	9	1.33000
1	1	0	1	1	0	1	0	D	A	1.33500
1	1	0	1	1	0	1	1	D	B	1.34000
1	1	0	1	1	1	0	0	D	C	1.34500
1	1	0	1	1	1	0	1	D	D	1.35000
1	1	0	1	1	1	1	0	D	E	1.35500
1	1	0	1	1	1	1	1	D	F	1.36000
1	1	1	0	0	0	0	0	E	0	1.36500
1	1	1	0	0	0	0	1	E	1	1.37000
1	1	1	0	0	0	1	0	E	2	1.37500
1	1	1	0	0	0	1	1	E	3	1.38000
1	1	1	0	0	1	0	0	E	4	1.38500
1	1	1	0	0	1	0	1	E	5	1.39000
1	1	1	0	0	1	1	0	E	6	1.39500
1	1	1	0	0	1	1	1	E	7	1.40000
1	1	1	0	1	0	0	0	E	8	1.40500
1	1	1	0	1	0	0	1	E	9	1.41000
1	1	1	0	1	0	1	0	E	A	1.41500

Table 6. VID Table (Continued)

VID								HEX		V _O (V)
7	6	5	4	3	2	1	0			
1	1	1	0	1	0	1	1	E	B	1.42000
1	1	1	0	1	1	0	0	E	C	1.42500
1	1	1	0	1	1	0	1	E	D	1.43000
1	1	1	0	1	1	1	0	E	E	1.43500
1	1	1	0	1	1	1	1	E	F	1.44000
1	1	1	1	0	0	0	0	F	0	1.44500
1	1	1	1	0	0	0	1	F	1	1.45000
1	1	1	1	0	0	1	0	F	2	1.45500
1	1	1	1	0	0	1	1	F	3	1.46000
1	1	1	1	0	1	0	0	F	4	1.46500
1	1	1	1	0	1	0	1	F	5	1.47000
1	1	1	1	0	1	1	0	F	6	1.47500
1	1	1	1	0	1	1	1	F	7	1.48000
1	1	1	1	1	0	0	0	F	8	1.48500
1	1	1	1	1	0	0	1	F	9	1.49000
1	1	1	1	1	0	1	0	F	A	1.49500
1	1	1	1	1	0	1	1	F	B	1.50000
1	1	1	1	1	1	0	0	F	C	1.50500
1	1	1	1	1	1	0	1	F	D	1.51000
1	1	1	1	1	1	1	0	F	E	1.51500
1	1	1	1	1	1	1	1	F	F	1.52000

7.7.4 Dynamic VID Operation

The ISL95859C receives VID commands from the Serial VID (SVID) port. It responds to VID changes by slewing to the new voltage at a slew rate indicated in the SetVID command. There are three SetVID slew rates: SetVID_fast, SetVID_slow, and SetVID_decay.

The SetVID_fast command prompts the controller to enter CCM and to actively drive the output voltage to the new VID value at the programmed fast slew rate.

The SetVID_slow command prompts the controller to enter CCM and to actively drive the output voltage to the new VID value at the programmed slow slew rate ($\frac{1}{4}$ of the fast slew rate).

The SetVID_decay command prompts the controller to enter power state PS2, with DEM. The output voltage will decay down to the new VID value at a slew rate determined by the load. If the voltage decay rate is too fast, the controller will limit the voltage slew rate to the programmed fast slew rate.

ALERT# is asserted (low) upon completion of all non-zero VID transitions.

Figure 88 shows a SetVID_decay pre-emptive response, which occurs whenever a new VID command is received before completion of a previous SetVID_decay command.

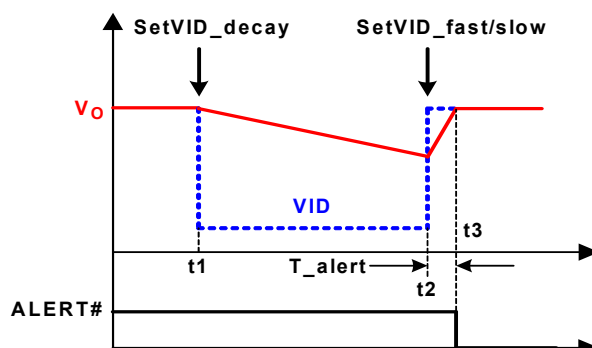


Figure 88. SetVID Decay Pre-Emptive Behavior

The example scenario in Figure 88 shows that the controller receives a SetVID_decay command at t1. The VR enters DEM and the output voltage V_O decays slowly. At t2, before V_O reaches the intended VID target of the SetVID_decay command, the controller receives a SetVID_fast (or SetVID_slow) command to go to a voltage higher than the actual V_O . The controller will pre-empt the decay to the lower voltage and slew V_O to the new target voltage at the slew rate specified by the SetVID command. At t3, V_O reaches the new target voltage and the controller asserts the ALERT# signal.

7.7.5 Slew Rate Compensation Circuit for VID Transition

In executing a SetVID command, the VID DAC steps through the VID table to the destination voltage at the specified step rate. For example, for a SetVID_fast command the DAC will step a minimum of 6 ticks (30mV minimum) per $1\mu\text{s}$, for an output voltage slew rate of at least $30\text{mV}/\mu\text{s}$. For a SetVID_slow command, the DAC step rate is a minimum of 3 ticks per $1\mu\text{s}$, commanding output voltage slew rate of at least $15\text{mV}/\mu\text{s}$. The actual slew rate is indicated in the Electrical Specifications table in page 13.

Figure 89 on page 64 shows the waveforms of VID transition.

During VID transition, the output capacitor is being charged and discharged, causing $C_{\text{out}} \times dV_{\text{CORE}}/dt$ current on the inductor. The controller senses the inductor current increase during the rising VID transition (as the $I_{\text{droop_vid}}$ waveform shows) and will droop the output voltage V_{CORE} accordingly, adding damping to the V_{CORE} slew response. Similar behavior occurs during the falling VID transition. To improve V_{CORE} VID slew response, one can add the $R_{\text{vid}}\text{-}C_{\text{vid}}$ branch, whose current I_{vid} compensates for $I_{\text{droop_vid}}$. Choose the R, C values from the reference design as a starting point, then adjust the actual values on the board to get the best performance.

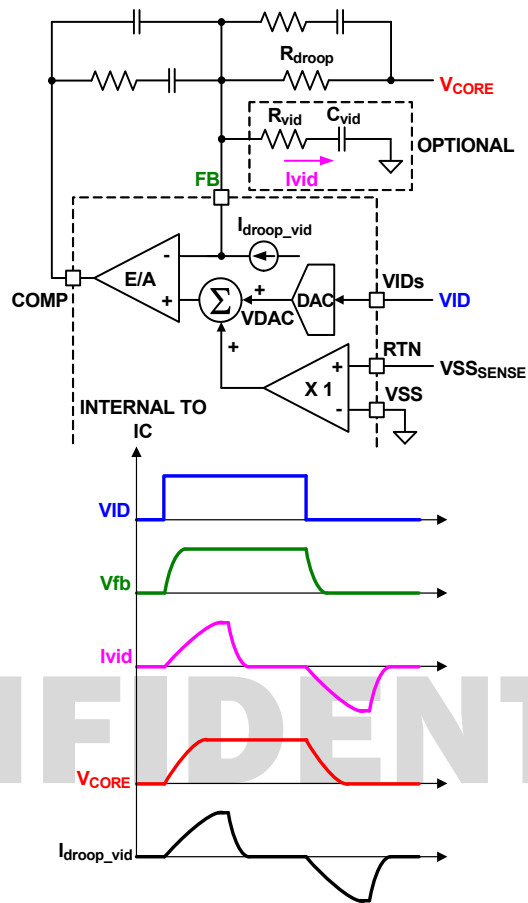


Figure 89. Slew Rate Compensation Circuit for VID Transition

8. Fault Protection

The ISL95859C provides overcurrent, current-balance, and overvoltage fault protection on each VR output. The controller also provides over-temperature protection on VR A and VR B outputs.

The controller determines Overcurrent Protection (OCP) by comparing the average value of the droop current I_{droop} with an internal current source threshold listed in [Tables 1, 2, or 3](#) depending on the output. It declares OCP when I_{droop} is above the threshold for 120 μ s.

For the multiphase output VR B, the controller monitors the two ISEN pin voltages whenever both phases are operating to determine current-balance protection. If the difference of one ISEN pin voltage and the average ISENs pin voltage is greater than 9mV (for at most 4ms), the controller will declare a phase imbalance fault and latch off.

The controller takes the same actions for all of the above fault protections: deassertion of VR_READY and turn-off of all the high-side and low-side power MOSFETs. Any residual inductor current will decay through the MOSFET body diodes.

The controller will detect an Overvoltage Protection (OVP) fault if the voltage of the ISUMN pin (approximately the output voltage) exceeds the OVP threshold, which is the VID set value plus 300mV. When this happens, the controller will immediately declare an OV fault, deassert VR_READY, and take action through the PWM signals to turn on the low-side power MOSFETs of the effected rail. The low-side power MOSFETs remain on until the output voltage is pulled down below the VID set value. If the output voltage rises above the OVP threshold voltage again, the protection process is repeated. This behavior provides the maximum amount of protection against shorted high-side power MOSFETs while preventing the output to ringing below ground.

The overvoltage fault threshold is 2.45V whenever any output voltage ramps up from 0V during soft-start. The overvoltage fault threshold reverts to VID + 300mV after the output voltage settles its commanded voltage.

A fault on any ISL95859C voltage regulator output will shut down all three outputs. All the above fault conditions are reset by bringing VR_ENABLE low or by bringing V_{CC} or V_{IN} below their respective POR thresholds. When VR_ENABLE and V_{CC} (or V_{IN}) return to their high operating levels, the controller will restart as described in [“Start-up Timing” on page 54.](#)

[Table 7](#) summarizes the fault protections.

Table 7. Fault Protection Summary

Fault Type	Fault Duration Before Protection	Protection Action	Fault Reset
Overcurrent	120 μ s	PWM tri-state, VR_READY latched low	VR_ENABLE toggle or VCC or VIN toggle
Phase Current Unbalance (VR B Only)	4ms		
Overvoltage: V _{OUT} > VID + 300mV	Immediate	VR_READY latched low. Actively pulls the output voltage to below the VID value, then tri-states	
2.45V overvoltage threshold during output voltage ramp up from 0V during soft-start			

If at least one rail is not in PS4, then the POR circuitry is still active. If VDD is brought below and back above the POR thresholds, the controller will initiate a soft-start of all outputs. The controller is reset and no longer in PS4. When all outputs are commanded into PS4 and in a low quiescent state, the POR circuitry is not functional. The controller will not detect VDD until an SVID command moves it out of the PS4 state. VDD must remain at +5V while the IC is in PS4.

8.1 VR_HOT#/ALERT# Behavior

The controller drives a 10 μ A current source out of the NTC pin. The current source flows through an NTC resistor network connected from the NTC pin to GND and creates a voltage that is monitored by the controller. The NTC thermistor is placed at a thermal point on the motherboard that is the hottest point for the output stage. Typically this will result in the NTC thermistor being located next to the MOSFETs of Channel 1 of the associated VR output.

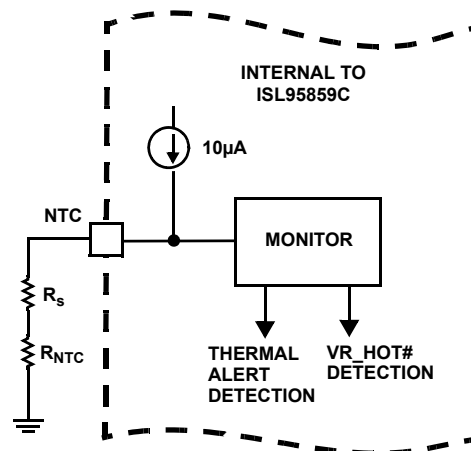


Figure 90. NTC Circuitry

The NTC pin voltage will drop as board temperature rises and the thermistor resistance changes with the thermal increase at the point monitored. When the NTC pin voltage drops below the thermal alert trip threshold, (see the Electrical Specifications table on [page 12](#)), the controller sets the status register and asserts the ALERT# signal. The CPU reads the status register to know that alert assertion has occurred and the controller clears ALERT#. If the system temperature continues to rise and NTC pin voltage continues to fall, it will pass through the VR_HOT# trip threshold and the controller will assert the VR_HOT# signal. The CPU reduces power consumption and the system temperature gradually drops. As the NTC pin voltage rises through the VR_HOT# reset threshold, the controller deasserts VR_HOT#. If the system temperature continues to drop and the NTC pin voltage rises above the thermal alert reset threshold, the controller changes the status register and asserts ALERT# for the CPU read the cleared status register.

To disable the NTC function, connect the NTC pin to VCC using a pull-up resistor.

9. Serial VID (SVID) Supported Data and Configuration Registers

The ISL95859C is compliant with the Intel IMVP8 SVID protocol. To ensure proper CPU operation, refer to related Intel documents for SVID bus design and layout guidelines; each platform requires different pull-up impedance on the SVID bus, while impedance matching and spacing among DATA, CLK, and ALERT# signals must be followed. Common mistakes include insufficient spacing among signals and improper pull-up impedance.

The controller supports the following data and configuration registers, accessible from the SVID interface.

Table 8. Supported Data and Configuration Registers

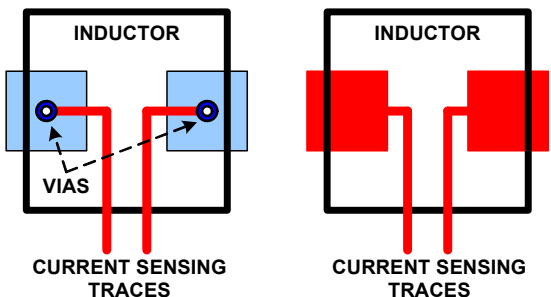
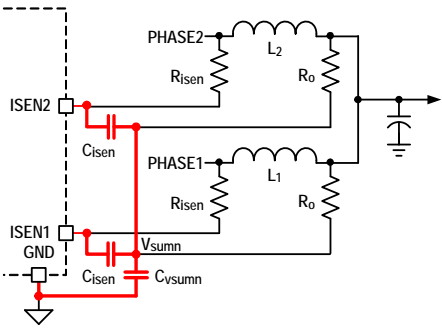
Index	Register Name	Read/Write	Description	Default Value
00h	Vendor ID	R	Uniquely identifies the VR vendor. Intel assigns this number.	12h
01h	Product ID	R	Uniquely identifies the VR product. Intersil assigns this number.	57h
02h	Product Revision	R	Uniquely identifies the revision of the VR control IC. Intersil assigns this data.	03h
05h	Protocol ID	R	Identifies which revision of the SVID protocol the controller supports.	05h
06h	Capability	R	Identifies the SVID VR capabilities and which of the optional telemetry registers are supported.	81h
10h-11h	Status	R	Four separate status registers for reading each active rail.	00h
15h	Output Current	R	Three separate data registers showing the digitalized value of the output current read by the rail selection.	
1Bh	Input Power	R/W	Data register showing system input power information. This register can only be read by the power domain through slave address 0Dh.	
1Ch	Status2_lastread	R/W	Single register that can be read by all rails.	00h
21h	I _{CCMAX}	R	Data register containing the I _{CCMAX} for each rail the platform supports. Set at start-up by PROG resistors and phase configuration.	
24h	Fast Slew Rate	R	Slew rate normal. The fastest slew rate the platform VR can sustain. Binary format in mV/μs (1Eh = 30mV/μs). Single register read back for rail selection.	
25h	Slow Slew Rate	R	Default is 2x slower than normal. Binary format in mV/μs (10h = 16mV/μs). Can be configured by register 2Ah. Three separate registers read by rail selection.	Set by fast slew rate and Register 2Ah
26h	V _{BOOT}	R	For normal run conditions the V _{BOOT} for IA, GT, and GTUS is 0V and is 1.05V for SA. Three separate registers read for rail selection.	
2Ah	Slow Slew Rate Selector	R/W	Three separate registers read/written based on rail selection. xxxx_0001 = 1/2 of fast slew rate xxxx_001x = 1/4 of fast slew rate xxxx_01xx = 1/8 of fast slew rate xxxx_1xxx = 1/16 of fast slew rate	01h
2Bh	PS4 Exit Latency	R	Reports 88μs	7Bh
2Ch	PS3 Exit Latency	R	Reports 4μs	38h
2Dh	Enable to VR_READY Latency	R	Reports 704μs	ABh
30h	V _{OUT} Max	R/W	This register is programmed by the master and sets the maximum VID the VR will support. If a higher VID code is received, the VR will respond with a "not supported" acknowledge.	FFh
31h	VID Setting	R/W	Three separate data registers containing currently programmed VID voltages based on rail selection. VID data format.	
32h	Power State	R/W	Three separate registers containing the current programmed power states based on rail selection.	00h
33h	Voltage Offset	R/W	Three separate registers, which set offset in VID steps added to the VID setting for voltage margining.	00h
34h	Multi VR Config	R/W	Data register that configures multiple VRs behavior on the same SVID bus.	01h

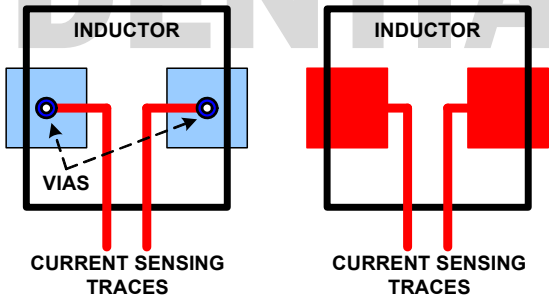
Table 8. Supported Data and Configuration Registers (Continued)

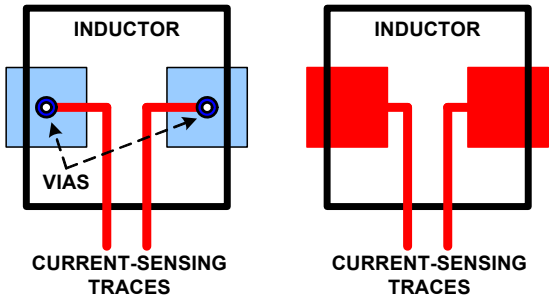
Index	Register Name	Read/Write	Description	Default Value
35h	SetRegADR	R/W	Serial data bus communication address.	00h
42h	IVID1-VID	R/W	R/W register to set the VID value that when the DAC is below this value and above IVID1_VID and Alert# for VRsettled is asserted, the power state is forced to PS1. The processor will change this value as necessary.	00h
43h	IVID1-I	R/W	Three separate R/W registers to set the max current that corresponds to IVID1-VID.	14h
44h	IVID2-VID	R/W	R/W register to set the VID value that when the DAC is below this value and above IVID2_VID and Alert# for VRsettled is asserted, the power state is forced to PS2. The processor will change this value as necessary.	00h
45h	IVID2-I	R/W	R/W register to set the max current that corresponds to IVID2-VID.	14h
46h	IVID3-VID	R/W	R/W register to set the VID value that when the DAC is below this value and above IVID3_VID and Alert# for VRsettled is asserted, the power state is forced to PS2. The processor will change this value as necessary.	00h
47h	IVID3-I	R/W	R/W register to set the max current that corresponds to IVID3-VID.	05h

CONFIDENTIAL

10. Layout Guidelines

Pin Number	Pin Name	Layout Guidelines
BOTTOM PAD		Connect this ground pad to the ground plane through a low impedance path. Use of at least 6 vias to connect to ground planes in PCB internal layers. This is also the primary conduction path for heat removal. Best performance is obtained with an uninterrupted ground plane under the ISL95859C and all associated components and signal sources and signal paths and extending from the controller to the load. Do not attempt to isolate signal and power grounds.
1	PSYS	Analog input from the battery charger, which needs to be routed away from noisy signals.
2	IMON_B	Current monitor resistor and capacitor should be placed near the pin. Route noisy signals away from this connection.
3	NTC_B	The NTC thermistor needs to be placed close to the thermal source for VR B for monitoring and determination of thermal throttling indication to CPU. Place it at the hottest spot of the VR B regulator. Route noisy signals away from this connection.
4	COMP_B	Place the compensation components in close proximity to the pin of the controller.
5	FB_B	Place feedback components in close proximity to the controller.
6	RTN_B	Place the RTN filter in close proximity of the controller for good decoupling.
7	ISUMP_B	Place the current sense components in close proximity of the controller pins.
8	ISUMN_B	Place capacitor C_n very close to the controller pins. Place the inductor temperature sensing NTC thermistor next to the inductor of Phase 1. Each phase of the power stage sends a pair of VSUMP and VSUMN signals to the controller. Route these two signal traces in parallel to the controller. The trace width is recommended to be >20 mil. IMPORTANT: Sense the inductor current by routing the sensing circuit to the inductor pads. Route the ISUMPN and ISENn resistor traces to the phase-side pad of each inductor. The ISUMNn network R_O resistor traces should be routed to the V_{OUT} -side pad of each inductor. If possible, route the traces on a different layer from the inductor pad layer and use vias to connect the traces to the center of the pads. If no via is allowed on the pad, consider routing the traces into the pads from the inside of the inductor. The following figures show the two preferred ways of routing current sensing traces.
		 <p style="text-align: center;">CURRENT SENSING TRACES</p>
9	ISEN1_B	Each ISEN pin has a capacitor (C_{isen}) decoupling it to V_{sumn} , then through another capacitor (C_{vsumn}) to GND.
10	ISEN2_B	Place the C_{isen} capacitors as close as possible to the controller and keep the following loops small: 1. Any ISEN pin to another ISEN pin 2. Any ISEN pin to GND The red traces in the following figure show the loops that need to be minimized.
		
11	FCCM_B	Driver control signal which needs to be routed away from noisy signals.

Pin Number	Pin Name	Layout Guidelines
12	PWM1_B	PWM output to MOSFET driver/Powerstage which needs to be routed away from noisy signals.
13	PWM2_B	
14	IMON_A	Current monitor resistor and capacitor should be placed near the pin. Route noisy signals away from this connection.
15	NTC_A	The NTC thermistor needs to be placed close to the thermal source for VR A for monitoring and determination of thermal throttling indication to CPU. Recommend placing it at the hottest spot of the VR A regulator. Route noisy signals away from this connection.
16	COMP_A	Place the compensation components in close proximity to the pin of the controller.
17	FB_A	Place feedback components in close proximity to the controller.
18	RTN_A	Place the RTN filter in close proximity of the controller for good decoupling.
19	ISUMP_A	Place the current sense components in close proximity of the controller pins.
20	ISUMN_A	<p>Place capacitor C_n very close to the controller pins.</p> <p>Place the inductor temperature sensing NTC thermistor next to the inductor of Phase 1.</p> <p>Each phase of the power stage sends a pair of VSUMP and VSUMN signals to the controller. Route these two signal traces in parallel to the controller. The trace width is recommended to be >20 mil.</p> <p>IMPORTANT: Sense the inductor current by routing the sensing circuit to the inductor pads. Route the ISUMPn and ISENn resistor traces to the phase-side pad of each inductor. The ISUMNn network R_O resistor traces should be routed to the V_{OUT}-side pad of each inductor. If possible, route the traces on a different layer from the inductor pad layer and use vias to connect the traces to the center of the pads. If no via is allowed on the pad, consider routing the traces into the pads from the inside of the inductor. The following drawings show the two preferred ways of routing current sensing traces.</p> <div style="text-align: center;">  <p>The left diagram shows an inductor with two pads. Each pad has a via connected to a current sensing trace. The right diagram shows an inductor with two pads. Each pad has a current sensing trace connected to the pad.</p> </div>
21	FCCM_A	Driver control signal, which needs to be routed away from noisy signals.
22	PWM_A	PWM output to MOSFET driver/Powerstage which needs to be routed away from noisy signals.
23	IMON_C	Current monitor resistor and capacitor should be placed near the pin. Route noisy signals away from this connection.
24	COMP_C	Place the compensation components in close proximity to the pin of the controller.
25	FB_C	Place feedback components in close proximity to the controller.
26	RTN_C	Place the RTN filter in close proximity of the controller for good decoupling.

Pin Number	Pin Name	Layout Guidelines
27	ISUMP_C	Place the current sense components in close proximity of the controller pins.
28	ISUMN_C	<p>Place capacitor C_n very close to the controller pins.</p> <p>Place the inductor temperature sensing NTC thermistor next to the inductor of Phase 1.</p> <p>Each phase of the power stage sends a pair of VSUMP and VSUMN signals to the controller. Route these two signal traces in parallel to the controller. The trace width is recommended to be >20 mil.</p> <p>IMPORTANT: Sense the inductor current by routing the sensing circuit to the inductor pads. Route the ISUMPN and ISENN resistor traces to the phase-side pad of each inductor. The ISUMNN network R_O resistor traces should be routed to the V_{OUT}-side pad of each inductor. If possible, route the traces on a different layer from the inductor pad layer and use vias to connect the traces to the center of the pads. If no via is allowed on the pad, consider routing the traces into the pads from the inside of the inductor. The following drawings show the two preferred ways of routing current sensing traces.</p> <div style="text-align: center;">  <p style="text-align: center;">CURRENT-SENSING TRACES</p> </div>
29	FCCM_C	Driver control signal which needs to be routed away from noisy signals.
30	PWM_C	PWM output to MOSFET driver/Powerstage which needs to be routed away from noisy signals.
31	PROG2	No special considerations. Resistor to GND for each should be placed in general proximity to the related pin.
32	PROG1	Routing noisy signals away from these connections is recommended.
33	VIN	The decoupling capacitor of good quality dielectric should be placed next to this pin with a short connection to the GND plane.
34	VCC	The decoupling capacitor of good quality dielectric should be placed next to this pin with a short connection to the GND plane.
35	SDA	Follow Intel recommendations for routing these pins.
36	ALERT#	
37	SCLK	
38	VR_HOT#	
39	VR_READY	No special considerations.
40	VR_ENABLE	

11. Revision History

Date	Revision	Change
Oct 6, 2017	0.00	Initial release

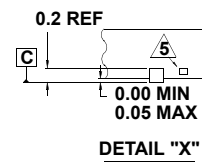
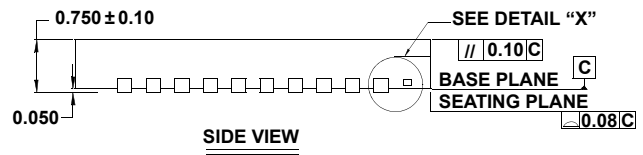
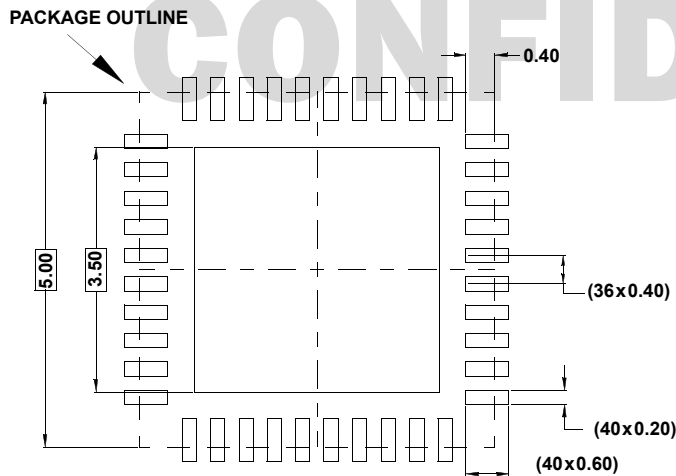
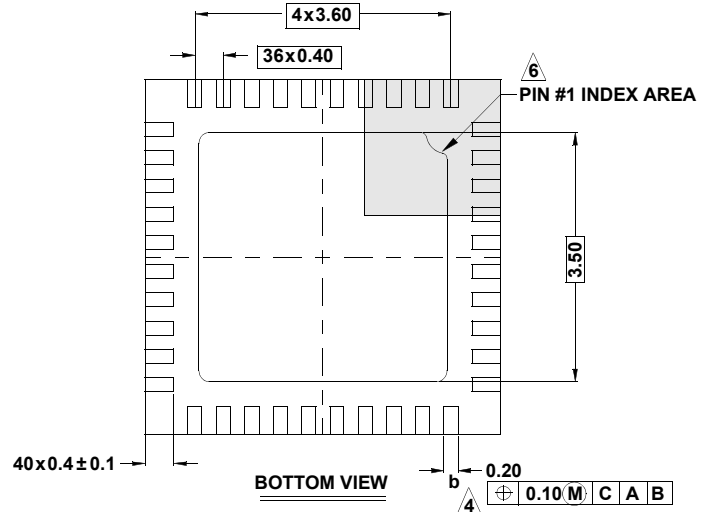
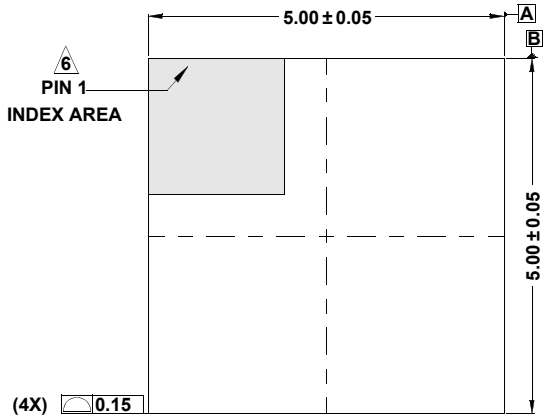
CONFIDENTIAL

12. Package Outline Drawing

L40.5x5

40 LEAD THIN QUAD FLAT NO-LEAD PLASTIC PACKAGE

Rev 2, 7/14

For the most recent package outline drawing, see [L40.5x5](#).

NOTES:

- Dimensions are in millimeters.
Dimensions in () for Reference Only.
- Dimensioning and tolerancing conform to AMSE Y14.5m-1994.
- Unless otherwise specified, tolerance: Decimal ± 0.05
- Dimension b applies to the metallized terminal and is measured between 0.15mm and 0.27mm from the terminal tip.
- Tiebar shown (if present) is a non-functional feature.
- The configuration of the pin #1 identifier is optional, but must be located within the zone indicated. The pin #1 identifier may be either a mold or mark feature.
- JEDEC reference drawing: MO-220WHHE-1

13. About Intersil

Intersil Corporation is a leading provider of innovative power management and precision analog solutions. The company's products address some of the largest markets within the industrial and infrastructure, mobile computing, and high-end consumer markets.

For the most updated datasheet, application notes, related documentation, and related parts, see the respective product information page found at www.intersil.com.

For a listing of definitions and abbreviations of common terms used in our documents, visit: www.intersil.com/glossary.

You can report errors or suggestions for improving this datasheet by visiting www.intersil.com/ask.

Reliability reports are also available from our website at www.intersil.com/support.

CONFIDENTIAL

© Copyright Intersil Americas LLC 2017. All Rights Reserved.

All trademarks and registered trademarks are the property of their respective owners.

For additional products, see www.intersil.com/en/products.html

Intersil products are manufactured, assembled and tested utilizing ISO9001 quality systems as noted in the quality certifications found at www.intersil.com/en/support/qualandrelability.html

Intersil products are sold by description only. Intersil may modify the circuit design and/or specifications of products at any time without notice, provided that such modification does not, in Intersil's sole judgment, affect the form, fit or function of the product. Accordingly, the reader is cautioned to verify that datasheets are current before placing orders. Information furnished by Intersil is believed to be accurate and reliable. However, no responsibility is assumed by Intersil or its subsidiaries for its use; nor for any infringements of patents or other rights of third parties which may result from its use. No license is granted by implication or otherwise under any patent or patent rights of Intersil or its subsidiaries.

For information regarding Intersil Corporation and its products, see www.intersil.com

EN - For pricing and availability in your local country please visit one of the below links:

DE - Informationen zu Preisen und Verfügbarkeit in Ihrem Land erhalten Sie über die unten aufgeführten Links:

FR - Pour connaître les tarifs et la disponibilité dans votre pays, cliquez sur l'un des liens suivants:

[ISL95829CHRTZ](#)

[ISL95829CIRTZ](#)

EN

This Datasheet is presented by
the manufacturer

DE

Dieses Datenblatt wird vom
Hersteller bereitgestellt

FR

Cette fiche technique est
présentée par le fabricant